American Journal of Analytical Chemistry

ISSN: 2156-8251 Vol. 1, No. 2, August 2010

www.scirp.org/journal/ajac

Scientific Research

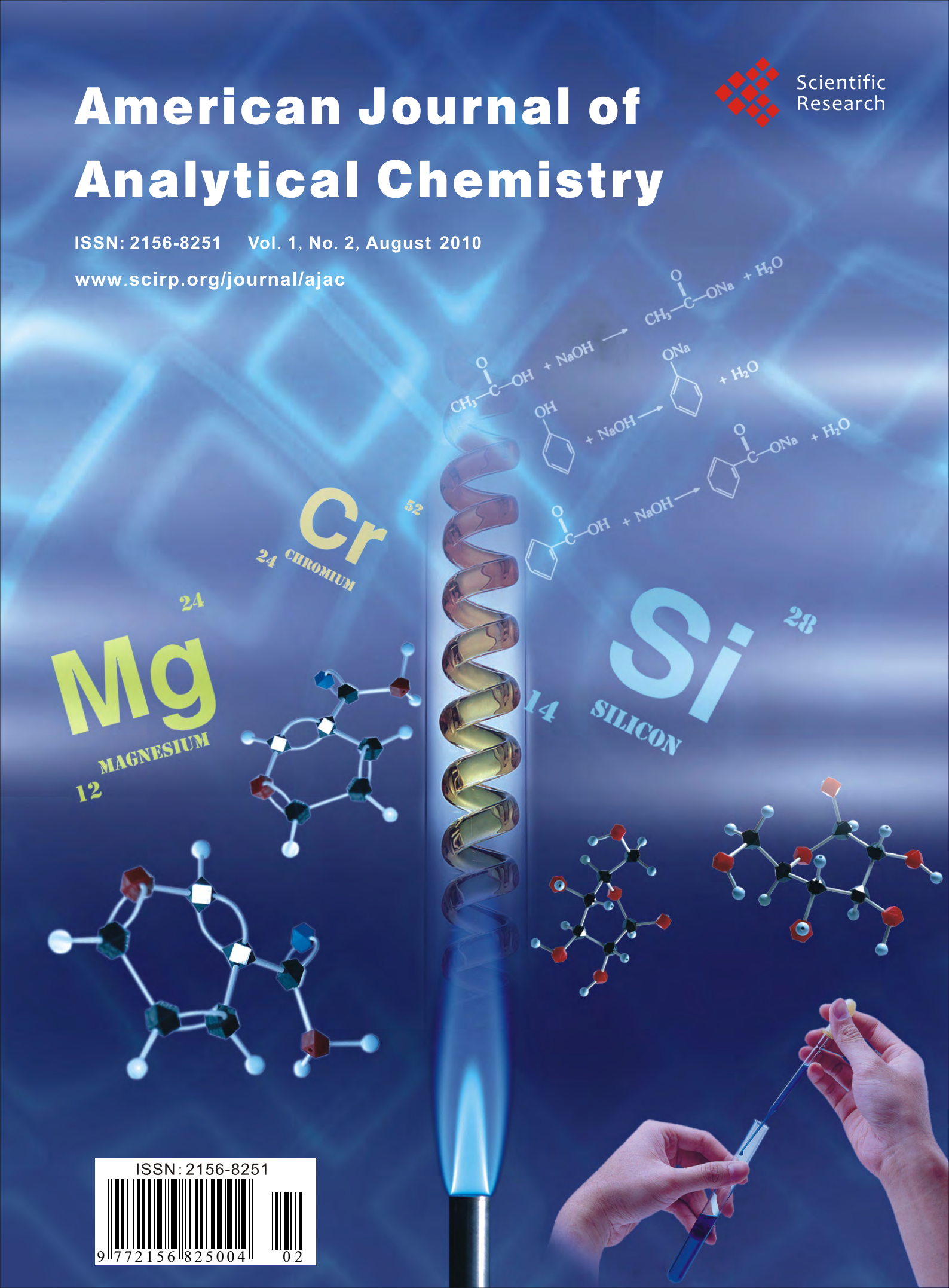

ISSN: 2156-8251

Journal Editorial Board

ISSN Print: 2156-8251 ISSN Online: 2156-8278

http://www.scirp.org/journal/ajac/

Editorial Board

Editorial Assistant

Guest Reviewers

American Journal of Analytical Chemistry, **2010, 2, 41-94**
Published Online August 2010 in SciRes (http://www.SciRP.org/journal/ajac/)

TABLE OF CONTENTS

Volume 1 Number 2 August 2010

American Journal of Analytical Chemistry (AJAC)

Journal Information

SUBSCRIPTIONS

The American Journal of Analytical Chemistry (Online at Scientific Research Publishing, www.SciRP.org) is published quarterly by Scientific Research Publishing, Inc., USA.

Subscription rates:

Print: $50 per issue.
To subscribe, please contact Journals Subscriptions Department, E-mail: sub@scirp.org

SERVICES

Advertisements
Advertisement Sales Department, E-mail: service@scirp.org

Reprints (minimum quantity 100 copies)
Reprints Co-ordinator, Scientific Research Publishing, Inc., USA.
E-mail: sub@scirp.org

COPYRIGHT

PRODUCTION INFORMATION

For manuscripts that have been accepted for publication, please contact:
E-mail: ajac@scirp.org

American Journal of Analytical Chemistry, **2010, 2, 41-46**
doi:10.4236/ajac.2010.12006 Published Online August 2010 (http://www.SciRP.org/journal/ajac)

Amperometric Determination of Serum Cholesterol with Pencil Graphite Rod

Nidhi Chauhan, Jagriti Narang, Chandra S. Pundir*
Department of Biochemistry, Maharshi Dayanand University, Rohtak, India
E-mail: *pundircs@rediffmail.com*
Received March 14, 2010; *revised July* 14, 2010; *accepted July* 20, 2010

Abstract

A cholesterol oxidase from S*treptomycin sp.* was immobilized onto pencil graphite rod and employed for amperometric determination of serum cholesterol. The method has the advantage over earlier amperometric methods that it requires low potential to generate electrons from H_2O_2, which does not allow ionization of serum substances. The optimum working conditions of amperometric determination were pH 6.8, 25˚C and 30 s. The current measured was in proportion to cholesterol concentration ranging from 1.29×10^{-3} to 10.33×10^{-3} M. Minimum detection limit of the method was 0.09×10^{-3} M. Mean analytical recovery of added cholesterol (100 mg/dl and 200 mg/dl) in serum was 85.0% & 90.0% respectively. Within batch and between batch coefficients of variations were 1.59% & 4.15% respectively. A good correlation (r = 0.99) was obtained between serum cholesterol values by standard enzymic colorimetric method and the present method. No interference by metabolites was observed in the method. The enzyme electrode was reused 200 times over a period of 25 days, when stored at 4˚C.

Keywords: Cholesterol, Cholesterol Oxidase, Pencil Graphite, Enzyme Electrode, Serum, Amperometric Biosensor

1. Introduction

Cholesterol an important steroid in human body plays a vital role as a precursor to various hormones. Cholesterol determination in blood is known to be clinically important for diagnosis of various diseases like cardiac disorders, atherosclerosis, nephritis, diabetes mellitus, myxodema, obstructive jaundice and cerebral thrombosis [1]. Among various methods available for cholesterol determination, biosensors are comparatively simpler, rapid, sensitive and specific [2-6]. Various amperometric cholesterol biosensors have been reported, employing cholesterol esterase, cholesterol oxidase and peroxidase immobilized onto nylon mesh over a platinum electrode [7], octyl-agarose gel activated with cyanogen bromide and placed in a reactor [8], pyrrole membrane through electropolymerization and coupled with FIA for H_2O_2 analysis [9], carbon paste electrode modified with hydroxymethyl ferrocene and hydrogen peroxide [10], poly (2-hydroxyethyl methacrylate) (p(HEMA))/polypyrrole membrane [11], graphite-teflon composite matrix with incorporated potassium ferrocyanide [12], layer of silica sol-gel matrix on the top of Prussian blue-modified glassy carbon electrode [13], photosensitive polymer on ultra-thin dialysis membrane [14], conducing polypyrrole (PPY) films using electrochemical entrapment technique [15], porous silicon [16], poly(vinylferrocenium) film [17]. Due to high electrochemical reactivity, good mechanical rigidity, low cost and ease of modification, renewal and miniaturization, pencil graphite electrode (PGE) received attention of workers for its use in working electrode of biosensor [18]. Furthermore, PGE has a large active electrode surface area and therefore able to detect low concentrations and/or volume of the analyte [19]. The aim of this work was to develop a simple cholesterol biosensor based on PGE bound cholesterol oxidase. The electrode is better in the economic sense and a small amount of material used; hence it seems to be a better electrode than "high tech" electrodes described previously [20].

2. Experimental

4-Amino-phenazone/4-aminoantipyrene, horseradish peroxidase from Sigma Aldrich, USA, Triton X-100, Cholesterol, Cholesterol oxidase from *Streptomycin sp.* (500 units/10mg) from SRL, Mumbai. 'HB' lead pencil was from local market. The kit of enzymic colorimetric

method for cholesterol determination was from Erba Transasia, Daman, India. All other chemicals were of analytical reagent grade.

2.1. Assay of Free Cholesterol Oxidase

Assay of free cholesterol oxidase was carried out in a 15 ml test tube wrapped with black paper according to Allain *et al.* (1974) with modification. The reaction mixture, consisting of 1.8 ml sodium phosphate buffer (0.05 M, pH 7.0) containing 0.4% Triton X-100, 0.1 ml of cholesterol solution (10mM) and 0.1 ml of cholesterol oxidase solution (13 Units) incubated for 5 min at 37˚C. Color reagent (1.0 ml) was added and kept at 37˚C for 10 min to develop the colour. A_{520} was read and the content of H_2O_2 was extrapolated from standard curve between H_2O_2 concentration and A_{520}. Color reagent consisted 50 mg 4-aminophenazone, 100 mg phenol and 1 mg horseradish peroxidase per 100 ml 0.4 M sodium phosphate buffer (pH 7.0). It was stored in amber colored bottle at 4˚C & prepared fresh after one weak. One enzyme unit is defined as the amount of enzyme required to generate 1.0 nmol of H_2O_2 per min per ml.

2.2. Immobilization of Enzyme onto Pencil Graphite Rod

The wooden cover of a lead pencil was removed from its both the ends with a sharp blade upto 2 cm height. The one end of pencil graphite rod (0.15 diameter and 2 cm long) was dipped into 60% HCl at room temperature for 24 h and then washed thoroughly with 0.05 M sodium phosphate buffer (pH 7.4). It was dipped again into 70% HNO_3. After keeping it for 24h at room temperature, the pencil rod was washed thoroughly with the same buffer and then put into 0.2% enzyme solution. After keeping it at 4˚C for 8h, the rod was taken off and washed thoroughly with the reaction buffer & tested for cholesterol oxidase activity. The residual enzyme solution was tested for activity and protein by Lowry method. The pencil graphite rod containing immobilized enzyme acted as working electrode (PGE).

2.3. Construction and Response Measurement of Amperometric Cholesterol Biosensor

An amperometric cholesterol biosensor was constructed by connecting pencil graphite electrode (PGE) as working electrode, silver/silver chloride (Ag/AgCl) as reference electrode and Cu wire as auxiliary electrode through electrometer/high resistance meter (Keithley 6517A, Japan). To test the activity of this biosensor, the electrode system was immersed into 1.8 ml 0.02 M sodium phosphate solution pH 7.0 and 0.2 ml of cholesterol (12.9 mM) and polarized at a potential in the range 0-0.4 V versus Ag/AgCl. The current was maximum at 0.1 V. Hence in the subsequent amperometric studies; the sensor was polarized at 0.1 V to generate current. The electrochemical reactions involved in response meas- urement are given in **Figure 1**.

2.4. Optimization of Cholesterol Biosensor

The optimal working conditions of cholesterol biosensor were studied in terms of the current (mA) generated. To study optimum pH, the pH of reaction buffer was varied in the range pH 6.2 to pH 7.8 using the 0.02 M sodium phosphate buffer. Similarly for optimum temperature, the reaction mixture was incubated at temperature ranging from 20 to 50˚C at an interval of 5˚C. Time course was studied by incubating reaction mixture for different time ranging from 5 to 40 s at an interval of 5 s. To study effect of substrate concentration, the concentrations of cholesterol was varied from 1.29 to 12.9 mM. K_m (Michaelis Menten constant) and I_{max} (maximum current) were calculated from L.B. plot.

2.5. Electrochemical Determination of Cholesterol in Serum

Blood samples (1.0 ml each) from apparently healthy male and female (10 each) and diseased persons (suffering from coronary heart diseases, hypertension and atherosclerosis) were collected from local Pt BD Sharma Post Graduate Institute of Medical Sciences, Rohtak, and centrifuged at 5000 rpm for 5 min and their supernatant (serum) was collected. Cholesterol content in serum was determined by the present biosensor in the similar manner as described for its response measurement, under its optimal working conditions except that cholesterol was replaced by serum. The current (mA) was measured and the amount of cholesterol in serum extrapolated from standard curve between cholesterol concentrations and current (in mA) prepared under optimal working conditions (**Figure 2**).

2.6. Evaluation of Cholesterol Biosensor

The biosensor was evaluated by studying analytical re-

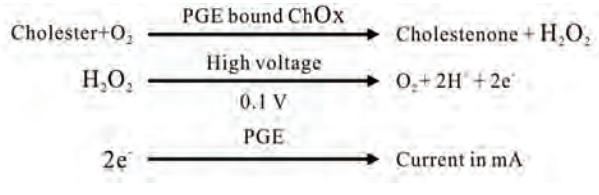

Figure 1. Chemical reactions involved in generation of electron in amperometric cholesterol biosensor based on pencil graphite electrode (PGE) bound cholesterol oxidase (ChOx).

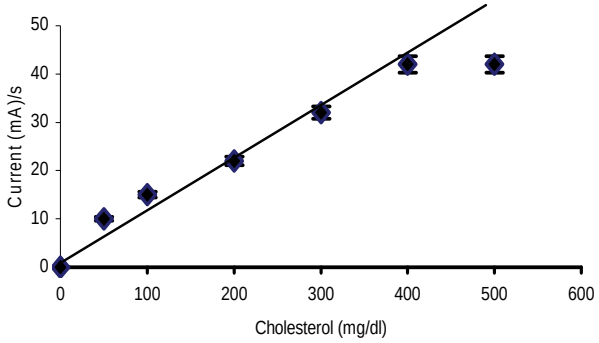

Figure 2. Standard curve of cholesterol by biosensor based on pencil graphite rod bound cholesterol oxidase.

covery, precision and correlation. The effect of various metals and metabolites found in blood, such as uric acid, cholesterol, ascorbic acid, bilirubin, glucose, pyruate and glutathione were studied at their physiological concentration.

3. Results and Discussions

3.1. Immobilization of Cholesterol Oxidase onto PG Rod and Construction of Amperometric Cholesterol Biosensor

Commercial cholesterol oxidase from Streptomyces species was immobilized on PGE through chemisorption (**Figure 3**). The HCl treatment of PGE forms a monolayer which helps in electrostatic interaction of negatively charged cholesterol oxidase at pH 7.0. Nevertheless treatment of graphite with HNO_3 makes it highly porous to provide the large surface area for adsorption or chemical reaction [21]. The chemisorption is better than physisorption for immobilization of enzyme which is characterized by weak Van der Wall forces. A method is described for construction of amperometric cholesterol biosensor based on this PGE bound with cholesterol oxidase. The biosensor showed optimum response at low voltage *i.e.* 0.1 V had advantage that it does not allow the ionization of number of serum substances which get ionized at high voltage and interfere in current measurement [9].

3.2. Optimization of Cholesterol Biosensor

The optimum response for pencil graphite electrode was at pH 6.8 (**Figure 4**), which is comparable to earlier reports pH 7.0 [8,9,15,24] and pH 7.5 [22].The PGE showed optimum response at 40˚C (**Figure 5**), which is higher than that of free enzyme in presence of free cholesterol esterase and peroxidase (30˚C). The increase in optimum temperature might be due to change in conformation of enzyme after immobilization or due to steric hindrance. PGE response was increased from 5 to 30 s after which it became stable (**Figure 6**). Therefore in all subsequent assays, the electrometer reading was recorded at 30 s. A hyperbolic relationship was observed between electrode response (current in mA/s) and cholesterol concentration up to a final concentration of 12.9×10^{-3} M, which is similar to earlier cholesterol biosensor , but higher than 1×10^{-3} M to 8×10^{-3} M for cholesterol ester [15], and 8×10^{-3} M for cholesterol [22]. Lineweaver-Burk plot between the reciprocals of cholesterol concentration and response of PGE working electrode was linear. K_m (Michaelis constant) for cholesterol was 7.38×10^{-3} M (**Figure 7**) which is lower than that for earlier cholesterol biosensor (21.2×10^{-3} M) [23] and 19.6×10^{-3} M [9]. This might be due to the hydrophobic forces of pencil graphite, which facilitate the cholesterol binding with the graphite bound enzyme. I_{max} was 62.5 mA/s.

3.3. Evaluation of Cholesterol Biosensor

3.3.1. Linearity

A linear relationship was obtained between cholesterol concentrations ranging from 1.29×10^{-3} M to 10.3×10^{-3} M and current (mA) measured (**Figure 2**).

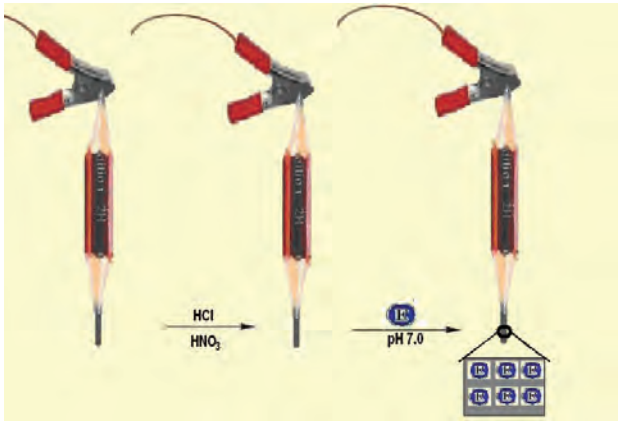

Figure 3. Chemisorption immobilization of cholesterol oxidase onto pencil graphite rod.

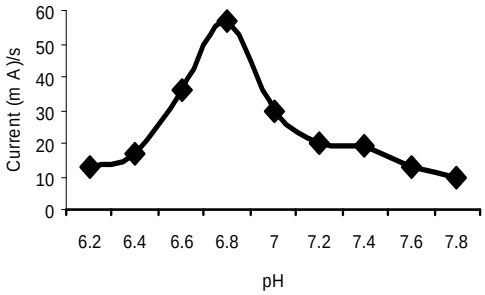

Figure 4. Effect of pH on the response of cholesterol biosensor based on pencil graphite rod bound cholesterol oxidase. Standard assay conditions were used except for the pH that was varied from pH 6.2-7.8.

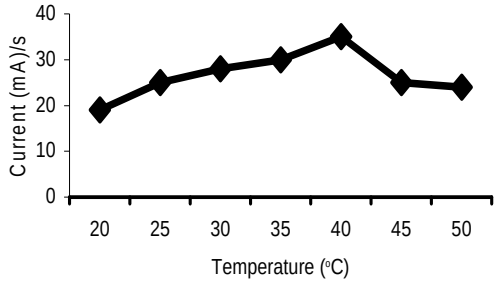

Figure 5. Effect of incubation temperature on the response of cholesterol biosensor based on pencil graphite rod bound cholesterol oxidase. Standard assay conditions were used except for the incubation temperature which was varied from 15-45˚C.

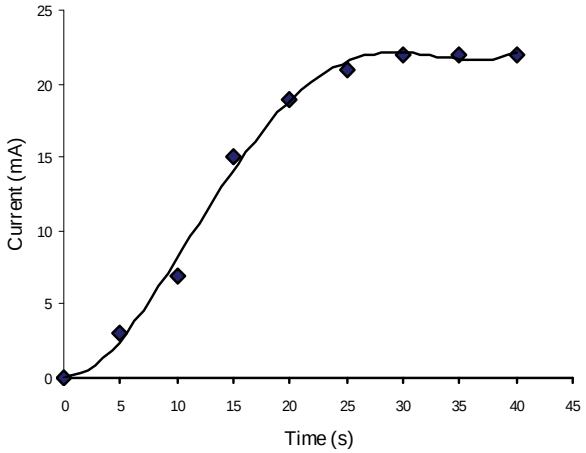

Figure 6. Effect of time of incubation on the response of cholesterol biosensor based on pencil graphite bound cholesterol oxidase.

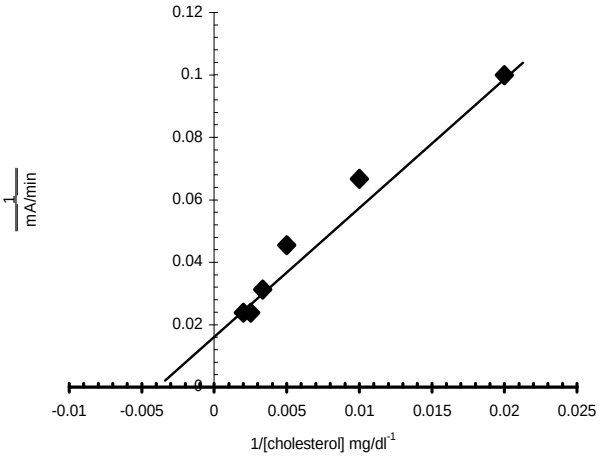

Figure 7. A Lineweaver-Burk plot for cholesterol biosensor based on cholesterol oxidase immobilized onto pencil graphite rod.

3.3.2. Minimum Detection Limit

The minimum detection limit of the present amperometric biosensor was 0.09×10^{-3} M, which is almost 3 times lower than paleographic method employing soluble enzymes (0.32×10^{-3} M) [24], but higher than those methods employing silica gel bound enzyme (0.003×10^{-3} M) [25] and amperometric cholesterol biosensor (0.064×10^{-3} M) [9].

3.3.3. Analytical Recovery

In order to check the accuracy of the method, the analytical recovery of added cholesterol in the serum samples was determined. The mean analytical recovery of added cholesterol (100 mg/dl and 200 mg/dl) in serum was 85% (100 mg/dl) and 90% (200 mg/dl) (**Table 1**), which is comparable with colorimetric method employing alkyl amine glass bound enzyme (95-102%) [26], amperometric method (95-101% recovery) [7], enzymic fluorometric method (103-104 %) for added cholesterol concentration of 150 mg/dl and 50 mg/dl [26].

3.3.4. Precision

To check the reproducibility and reliability of the methods, the cholesterol content of the sample in one run (Within batch) and after storage at -20˚C for one week (Between batch) were determined. The results showed that the cholesterol value of these determination agreed with each other and within batch and between batch coefficient of variation (CV) were 1.59% & 4.15 % (**Table 2**), which is quite close to earlier reports such as colorimetric, electrochemical method [26] employing alkyl amine glass bound enzyme (1.6% for intrabatch and 3.2% for interbatch), amperometric method using silica gel bound enzyme (< 1.5% for all samples) [7] and flow injection method employing controlled pore glass bound cholesterol esterase and cholesterol oxidase (within day < 1.0 and between day < 2.5%) [27], measuring cholesterol after precipitation with phosphotugstic acid/$MgCl_2$ (within day 5.0 % and between day 8.2%) [28] and amperometric detection of cholesterol (within day 2%–between day 4%) [9]. The low coefficient of variation values indicated the accuracy, reproducibility and reliability of the method.

3.3.5. Accuracy

In order to know the accuracy of present method, the level of cholesterol in 10 serum samples was determined by standard enzymic colorimetric method with modification and compared with those obtained by present method. The serum cholesterol values obtained by standard enzymes colorimetric method (x) agreed with the present biosensor (y) with a good correlation (r = 0.99) (**Figure 8**).

3.3.6. Effect of metal ions and metal salts

The effect of some metal salts such as KCl, $MgCl_2$, NaCl, $CaSO_4$, $CuSO_4$, $ZnSO_4$, $CaCl_2{\cdot}2H_2O$ and $MgSO_4{\cdot}7H_2O$,

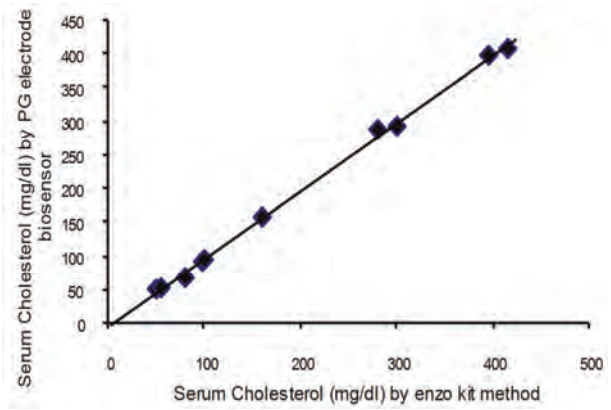

Figure 8. Correlation between serum cholesterol value as determined by enzo kit method employing free enzymes (x axis) and present biosensor method (y-axis) based on pencil graphite rod bound cholesterol oxidase.

Table 1. Analytical recovery of added cholesterol in serum by biosensor based on pencil graphite electrode.

Cholesterol added (mg/dl)	Cholesterol found (mg/dl)	% Recovery
Nil	150	-
100	235	85
200	330	90

Serum cholesterol was measured by cholesterol biosensor as described in text. It was measured again after adding cholesterol into serum at 100 mg/dl & 200 mg/dl. % Recovery was calculated. Values are mean of six serum samples.

Table 2. Precision measurement of serum cholesterol by a cholesterol biosensor based on pencil graphite electrode (PGE).

Total number of samples (n = 6)	Mean Cholesterol (mg/dl)	% CV
6 (within assay)	54.25	1.59
6 (between assay)Ψ	54.2	4.15

Cholesterol was measured in six serum samples six times on the same day (Within assay) and after one week storage at -20°C (Between assays) by cholesterol biosensor based on pencil graphite rod bound cholesterol oxidase. % Coefficient of variation (CV) was calculated.

each at a final concentration of 1.0 mM was tested on the response of the working electrode. Only Mg^{2+} caused slight stimulation, while rest metals had practically no effect.

3.3.7. Effect of Serum Metabolites

To study interference by serum metabolites glucose, uric acid, ascorbic acid, acetone and bilirubin were added into the reaction mixture at their normal physiological concentration before addition of cholesterol. The results showed that there was practically no interference in presence of these metabolites. Earlier uric acid and ascorbic acid, at 0.6 V caused significant increase in the value of current [29], which were attributed to the fact that at high potentials for both uric acid & ascorbic acid got oxidized contributing to oxidation current. Some interference of endogenous electro reactive species like uric acid, glucose had been reported when their concentration was higher than their normal physiological concentrations [15].

3.4. Storage Stability and Reusability

The PG electrode lost 50% of its initial activity after its regular use for 200 times over a period of 25 days, when stored in 0.05 M sodium phosphate buffer, pH 7.0 at 4˚C.

4. Conclusions

A method is described for immobilization of cholesterol oxidase onto pencil graphite (PG) rod and its use in construction of a simple amperometric cholesterol biosensor. The biosensor had an advantage that it worked at low potential and thus had no interference by serum substances. The sensor was evaluated.

5. References

[1] S. Hirany, D. Li and I. Jialal, "A More Valid Measurement of Low Density Lipoprotein Cholesterol in Diabetic Patients", *American Journal of Medicine*, Vol. 102, No. 1, 1997, pp. 48-53.

[2] C. C. Allain, L.S. Poon, C. S. G. Chan, W. Richmond and P.C. Fu, "Enzymatic Determination of Serum Total Cholesterol," *Clinical Chemistry*, Vol. 20, No. 4, 1974, pp. 470-475.

[3] H. Osman and Kwee Yap, "Comparative Sensivity of Cholesterol Analysis Using GC, HPLC and Spectrophotometric Methods," *Malaysian Journal of Food Science*, Vol. 10, No. 2, 2006, pp. 205-210.

[4] D. L. Witte, D. A. Barrett and D. A. Wycoff, "Evaluation of an Enzymatic Procedure for Determination of Serum Cholesterol with the Abbott ABA-100," *Clinical Chemistry*, Vol. 20, No. 10, 1974, pp. 1282-1286.

[5] I. Karubeet, K. Hera, H. Matsuoka and S. Suzuki, "Amperometric Determination of Total Cholesterol in Serum with Use of Immobilized Cholesteriol Esterase and Cholesterol Oxidase," *Analytical Chimica Acta*, Vol. 139, No. 10, 1982, pp. 127-132.

[6] B. Shahnaz, S. Tada, T. Kajikawa, T. Ishida and K. Kawanishi, "Automated Fluimetric Determination of Cellular Cholesterol," *Annals of Clinical Biochemistry*, Vol. 35, No. 6, 1998, p. 665.

[7] M. J. Tabata and T. Murachi, "Automated Analysis of Total Cholesterol in Serum Using Coimmobilized Cholesterol Ester Hydrolase and Cholesterol Oxidase," *Journal of Applied Biochemistry*, Vol. 3, 1981, pp. 84-92.

[8] Suman and C. S. Pundir, "Co-immobilization of Cholesterol Esterase, Cholesterol Oxidase & Peroxidase onto Alkylamine Glass Beads for Measurement of Total Cho-

lesterol in Serum," *Current Applied Physics*, Vol. 3, No. 2-3, 2003, pp. 129-133.

[9] V. Hooda, A. Gahlautb, H. Kumar and C. S. Pundir, "Biosensor Based on Enzyme Coupled PVC Reaction Cell for Electrochemical Measurement of Serum Total Cholesterol," *Sensor and Actuator B*, Vol. 136, No. 1, 2009, pp. 235-241.

[10] L. Braco, J. A. Daros and M. de la. Guardia, "Enzymatic Flow Injection Analysis in Nonaqueous Media," *Analytical Chemistry*, Vol. 64, No. 2-3, 1992, pp. 129-133.

[11] B. Sean, P. Narine, D. Singh and A. Guiseppi-Elie, "Amperometric with in Determination of Cholesterol in Serum Using A Biosensor of Cholesterol Oxidase Contained Polypyrol-Hydrogel Membrane," *Analytical Chimica Acta*, Vol. 448, No. 1-2, 2001, pp. 27-36.

[12] P. Nuria, Gloria Ruiz, A. Julio Reviejo and Jose M. Pingarron, "Graphite Teflon Composite Bienzyme Electrodes for the Determination of Cholesterol in Reversed Micelles: Application to Food Samples," *Analytical Chemistry*, Vol. 5, No. 6, 2001, pp. 1190-1195.

[13] L. Jianping, T. Peng and Y. Peng, "Cholesterol Biosensor Based on Entrapment of Cholesterol Oxidase in a Silicic Sol-Gel Matrix at a Prussian Blue Modified," *Electroanalysis*, Vol. 15, No. 12, 2003, pp. 1031-1033.

[14] H. Endo, M. Masashi, T. Mio, R. Huifeng, H. Tetushito, U. Naoto and M. Kohji, "Enzyme Sensor System for Determination of Total Cholesterol in Fish Plasma," *Fisheries Science*, Vol. 69, No. 6, 2003, pp. 1194-1199.

[15] S. Singh, A. Chaubey and B. D. Mahlotra, "Amperometric Cholesterol Biosensor Based on Immobilized Cholesterol Esterase and Cholesterol Oxidase on Conducting Polypyrol Films," *Analytical Chimica Acta*, Vol. 502, No. 2, pp. 229-234, 2004.

[16] M. J. Song, D. H. Yun, J. H. Jin, N. K. Min and S. Hong, "Comparison of effective working electrode area on planar and porous silicon substrates for cholesterol biosensor," Japanese Journal of Applied Physics, Vol. 45, No. 9A, 2006, pp. 7197-7202.

[17] Ö. B. Cem, Ö. Haluk, Celebi, S. Serda and Y. Atilla, "Amperometric Enzyme Electrode for Free Cholesterol Determination Prepared with Cholesterol Oxidase Immobilized in Poly(Vinylferrocenium) Film," *Enzyme Microbial Technology*, Vol. 40, No. 2, 2007, pp. 262-265.

[18] W. Gao, J. Song and N. Wu, "Voltametric Behaviour and Square-Wave Voltametric Determination of Trepibutone at a Pencil Graphite Electrode," *Journal of Electroanalytical Chemistry*, Vol. 576, No. 1, 2005, pp. 1-7.

[19] M. D. Vestergaard, K. Kerman and E. Tamiya, "An Electrochemical Approach for Detecting Copper-Chelating Properties of Flavonoids Using Disposable Pencil Graphite Electrodes: Possible Implications in Copper-Mediated Illnesses," *Analytical Chimica Acta*, Vol. 538, No. 1-2, 2005, pp. 273-281.

[20] A. M. Bond, J. Peter, Mahon, J. G. Schiewe and V. Vicente-Beckett, "An Inexpensive and Renewable Pencil Electrode for Use in Field Based Stripping Voltammetry," *Analytical Chimica Acta*, Vol. 345, No. 1-2, 1997, pp. 67- 74.

[21] B Erable, N. Duteanu, S. M. Kumar, Y. Feng, M. M. Ghangrekar and K. Scott, "Nitric Acid Activation of Graphite Granules to Increase the Performance of the Non-Catalyzed Oxygen Reduction Reaction (ORR) for MFC Applications," *Electrochemistry Communication*, Vol. 11, No. 7, 2009, pp. 1547-1549.

[22] J. C. Vidal, J. Espuelas and J. R. Castillo, "Amperometric Cholesterol Biosensor Based on *In Situ* Reconstituted Cholesterol Oxidase on an Immobilized Monolayer of Flavin Adenine Dinucleotide Cofactor," *Analytical Biochemistry*, Vol. 333, No. 1, 2004, pp. 88-98.

[23] A. Kumar, R. R. Pandey and B. Brantley, "Tetraethylorthosilicate Film Modified with Protein to Fabricate Cholesterol Biosensor," *Talanta*, Vol. 69, No. 3, 2006, pp. 700-705.

[24] A. Noma and K. Nakayama, "Polarographic Method for Rapid Micro Determination of Cholesterol with Cholesterol Esterase and Cholesterol Oxidase," *Clinical Chemistry*, Vol. 22, No. 3, 1976, pp. 336-40.

[25] T. Yao, M. Sato, Y. Kobayashi and T. Wasa, "Amperometric Assays of Total and Free Cholesterol in Serum by the Combined Use of Immobilized Cholesterol Esterase and Cholesterol Oxidase Reactors and Peroxidase Electrode in Flow Injection System," *Analytical Biochemistry*, Vol. 149, 1985, pp. 387-391.

[26] H. S. Huang, S. S. Kuan and G. G. Guiblault, "Amperometric Determination of Total Cholesterol in Serum, with Use of Immobilized Cholesterol Ester Hydrolase and Cholesterol Oxidase," *Clinical Chemistry*, Vol. 23, No. 1, 1977, pp. 671-676.

[27] R. J. Fernandez, M. M. D. L. De Castro and M. Valcarcel, "Determination of Total Cholesterol in Serum by Flow Injection Analysis with Immobilized Enzyme," *Clinical Chimica Acta*, Vol. 31, No. 2, 1987, pp. 97-104.

[28] C. Heuck, I. Erbe and D. Mathias, "Cholesterol Determination in Serum after Fractionation of Lipoproteins by Immunoprecipitation," *Clinical Chemistry*, Vol. 31, No. 1-2, 1985, pp. 252-256.

[29] S. Singh, P. R. Solanki and B. D. Malhotra, "Covalent Immobilization of Cholesterol Esterase and Cholesterol Oxidase on Polyaniline Films for Application to Cholesterol Biosensor," *Analytica Chimica Acta*, Vol. 568, No. 1-2, 2006, pp. 126-132.

American Journal of Analytical Chemistry, **2010, 2, 47-58**
doi:10.4236/ajac.2010.12007 Published Online August 2010 (http://www.SciRP.org/journal/ajac)

A Validated Enantioselective Assay for the Determination of Ibuprofen in Human Plasma Using Ultra Performance Liquid Chromatography with Tandem Mass Spectrometry (UPLC-MS/MS)

András Szeitz[1]*, Andrea Nicole Edginton[2], Henry Tao Peng[3], Bob Cheung[3], Kenneth Wayne Riggs[1]
[1]*Faculty of Pharmaceutical Sciences, The University of British Columbia, Vancouver, Canada*
[2]*School of Pharmacy, University of Waterloo, Waterloo, Canada*
[3]*Defence Research and Development Canada–Toronto, Toronto, Canada*
E-mail: *szeitz@interchange.ubc.ca*
Received April 8, 2010; *revised July* 13, 2010; *accepted July* 20, 2010

Abstract

A modified ultra performance liquid chromatography-tandem mass spectrometry (UPLC-MS/MS) method was developed and validated for the quantitation of ibuprofen enantiomers in human plasma. Ibuprofen and flurbiprofen (internal standard) were extracted from human plasma at acidic pH, using a single-step liquid-liquid extraction with methyl-tert-butyl ether. The enantiomers of ibuprofen and flurbiprofen were derivatized to yield the corresponding diastereomers. Chromatographic separation was achieved using a phenyl column with a run time of 20 min. (*R*)- and (*S*)-ibuprofen were quantitated at the multiple reaction monitoring (MRM) transition of *m/z* 360.2 → 232.1, and (*R*)- and (*S*)-flurbiprofen were monitored at the MRM transition of *m/z* 398.3 → 270.1. The method was validated for accuracy, precision, linearity, range, limit of quantitation (LOQ), limit of detection (LOD), selectivity, absolute recovery, matrix effect, dilution integrity, and evaluation of carry-over. Accuracy for (*R*)-ibuprofen ranged between –11.8% and 11.2%, and for (*S*)-ibuprofen between –8.6% and –0.3%. Precision for (*R*)-ibuprofen was ≤ 11.2%, and for (*S*)-ibuprofen ≤ 7.0%. The calibration curves were weighted ($1/X^2$, n = 7) and were linear with r^2 for (*R*)-ibuprofen ≥ 0.988 and for (*S*)-ibuprofen ≥ 0.990. The range of the method was 50 to 5000 ng/mL with the LOQ of 50 ng/mL, and LOD of 1 ng/mL, for (*R*)- and (*S*)-ibuprofen requiring 100 µL of sample. The method was applied successfully to a pharmacokinetic study with the administration of a single oral dose of ibuprofen capsules to human subjects.

Keywords: Ibuprofen Enantiomers, UPLC-MS/MS, Human Plasma, Method Validation, Pharmacokinetics

1. Introduction

Ibuprofen, a member of the 2-substituted arylpropionic acid (2-APA) family, is a non-steroidal anti-inflammatory drug (NSAID), which is used to treat moderate pain, fever, rheumatic disorders and related inflammatory diseases. Ibuprofen, one of the most popular "profen" drugs, was first marketed in the UK in 1969, and has been commercialized as a racemate drug. In Switzerland and Austria, in addition to the racemate drug, the (*S*)-enantiomer is also sold.

Ibuprofen undergoes chiral inversion *in vitro* [1] and *in vivo*, during metabolism in rats, mouse, rabbits [2-4] and humans [5,6] and shows stereoselective pharmacological effects [7,8] metabolism, pharmacokinetics [9-11] and disposition [12,13]. It has been reported also that ibuprofen is extensively bound to proteins in plasma in humans [11,14,15].

Several methodologies are available for the determination of ibuprofen. These techniques include direct or indirect high performance liquid chromatography (HPLC) methods. In the direct HPLC methods, a chiral stationary phase is used and the enantiomers are analyzed without sample derivatization. Certain direct HPLC methods employ ultra-violet (UV) detection using α_1-acid glycoprotein [16-19], β-cyclodextrin [20], cellulose [21], polysaccharide [22], and amylose derivative [23] chiral sta-

tionary phases (CSPs). A cellulose derivative CSP using radiometric and tandem mass spectrometric (MS/MS) detection [24] and an amylose derivative CSP using MS/MS [25] were also employed for the determination of ibuprofen enantiomers.

The direct HPLC methods have the advantage that the ibuprofen enantiomers can be analyzed without derivatization, however, these assays have poor sensitivity, reproducibility, require a large sample volume [16,18-20] or lack the satisfactory chromatographic baseline separation of the stereoisomer peaks [20,25]. Some direct HPLC methods achieved good sensitivity and use a small sample volume, but due to the non-selective characteristics of the UV detection they require extended analysis time to avoid interferences between the ibuprofen enantiomers and the co-eluting endogenous components from the biological matrix [23]. Further direct HPLC assays employ radiometric and selective mass spectrometric detection, but they are reported for *in vitro* applications, and not for the quantitation of the ibuprofen enantiomers over a concentration range in body fluids [24].

In the indirect HPLC methods, a reverse-phase stationary phase is used and the enantiomers are analyzed after sample derivatization to yield their corresponding diastereomers. The indirect methods have improved sensitivity and are better suited for the analysis of ibuprofen enantiomers in a variety of complex biological matrices. The indirect techniques include HPLC using UV [26,27], fluorescence [28,29], and mass spectrometric detection [30-33]. Gas chromatography-mass spectrometry (GC/MS) methods have been reported as well [2,6,34-36].

While the indirect HPLC methods using UV and fluorescence detection are suitable for the enantioselective determination of (*R*)- and (*S*)-ibuprofen in biological samples, they still lack the satisfactory sensitivity (e.g., limit of quantitation, LOQ $\geq$ 0.1 μg/mL) and use a large sample volume (*i.e.*, 0.5 mL plasma or serum) [26,27, 29], therefore, they may not be used satisfactorily for detailed pharmacokinetic studies over prolonged time periods. GC/MS methods can be stereoselective, but they use a larger sample size for analysis (*i.e.*, 0.8 mL plasma or 1 mL of serum) [34,6], and their sensitivity is insufficient (*i.e.*, 0.25 μg/mL or LOQ 5 μg/mL) [34,35], or they are not stereoselective [35,36]. Several indirect HPLC/MS/MS methods were reported for various *in vitro* [30-32] and *in vivo* [33] analyses of ibuprofen, but these methods are not stereoselective and do not represent significant improvement in comparison to the methodologies reported above.

In the present study, an enantioselective ultra performance liquid chromatography-tandem mass spectrometry (UPLC-MS/MS) method with improved sensitivity is presented for the quantitation of (*R*)- and (*S*)-ibuprofen enantiomers in human plasma using (*R*)- and (*S*)-flurbiprofen as internal standards. The assay was validated and applied successfully to the pharmacokinetic study of orally administered ibuprofen capsules to humans.

2. Experimental

2.1. Chemicals and Standards

(R)-(-)-ibuprofen (purity 98%), and (S)-(+)-ibuprofen (purity 98%), were purchased from Toronto Research Chemicals Inc. (North York, ON, Canada). (S)-(+)-Flurbiprofen (purity 98%), (R)-(-)-Flurbiprofen (purity 97%), internal standards, N-(3-Dimethylaminopropyl)-N'-ethyl-carbodiimide hydrochloride (CDI) (purity >98%), (R)-(+)-1-(1-Naphtyl)-ethylamine ((R)-NEA) (purity > 99%) were purchased from Sigma-Aldrich (St. Louis, MO, USA), and 1-hydroxybenzotriazole (HOBt·H2O) was purchased from AnaSpec, Inc. (San Jose, CA, USA). Methyl-tert-butyl ether, acetonitrile, methanol (HPLC grade) were purchased from Fisher Scientific (Fair Lawn, NY, USA), and dichloromethane (HPLC Grade) was obtained from Acros Organics (Geel, Belgium). Ammonium Acetate (AnalaR grade) was obtained from BDH Inc., (Toronto, ON, Canada), formic acid (puriss. p.a. for mass spectroscopy) was purchased from Fluka (Steinheim, Germany), hydrochloric acid (1.0 N) was purchased from VWR (West Chester, PA, USA). Blank human plasma (Sodium EDTA-treated) was purchased from Bioreclamation, Inc. (Westbury NY, USA). Ultra pure water was prepared in our laboratory using a Milli-Q Synthesis system (Millipore, Billerica, MA, USA). Ibuprofen capsules (Advil^{TM} ibuprofen 400 mg Liquid Filled Capsules, Extra Strength Liqui-Gels, Wyeth Consumer Healthcare Inc., Mississauga, ON, Canada) were obtained from Shoppers Drug Mart, Toronto, ON, Canada.

2.2. Instrumentation and Experimental Conditions

The UPLC-MS/MS system consisted of a Waters Acquity UPLC Binary Solvent Manager and a Waters Acquity UPLC Sample Manager connected to a Waters Quattro Premier XE triple quadrupole mass spectrometer. The mass spectrometer was operated in electrospray positive ionization (ES+) mode, and data were acquired using a MassLynx v. 4.1 software on a Microsoft Windows XP Professional operating platform.

Chromatographic separation was achieved using a Waters Acquity UPLC BEH Phenyl 1.7 μm, 2.1 × 150 mm column maintained at 30˚C, and the autosampler tray temperature was maintained at 10˚C. Solvent a was water containing 10 mM ammonium acetate and 0.1% formic acid, and solvent b was a mixture of 64% acetonitrile/36% methanol containing 10 mM ammonium acetate and 0.1% formic acid. The mobile phase initial conditions were solvent a (35%) and solvent b (65%)

with a flow rate of 0.2 mL/min, which were maintained for 12 min (0-12 min). At 12.1 min, solvent b was increased to 100% and the flow rate was gradually increased to 0.5 mL/min by 14 min (12.1-14 min) and held for 1 min (14-15 min). At 15.1 min, the initial conditions were set and the column was equilibrated for 4.9 min (15.1-20 min). The total run time was 20 min, the injection volume was 15 µL.

Mass spectrometric conditions were as follows: capillary voltage 3 kV, cone voltage 30 V, source temperature 120˚C, desolvation gas temperature 300˚C, desolvation gas flow 1000 L/hour. Diastereomeric amide derivatives of (*R*)- and (*S*)-ibuprofen were quantitated in multiple reaction monitoring (MRM) using the transition of *m/z* 360.2 → 232.1 at collision energy (CE) 10 eV. The dwell time was set to 25 ms. Diastereomeric amide derivatives of (*R*)- and (*S*)-flurbiprofen were monitored in MRM using the transition of *m/z* 398.3 → 270.1 at CE 10 eV. The dwell time was set to 50 ms. To protect the mass spectrometer from contamination from the samples and to reduce the solvent load in the source, the mobile phase flow was diverted to the waste before 7 min and after 12 min during the chromatographic run.

2.3. Preparation of Stock Solutions and Calibration Standards

Two separate master stock solutions of (*R*)-ibuprofen (100 µg/mL), and (*S*)-ibuprofen (100 µg/mL) enantiomers were prepared in methanol. The (*R*)- and (*S*)-ibuprofen master stock solutions were combined in equal parts into a mixed working stock solution of (*R*) and (*S*)-ibuprofen (50 µg/mL, each). The mixed working stock solution was further diluted with water to yield a series of diluted working stock solutions. The series of diluted working stock solutions were used to prepare the calibration standards in human plasma. The calibration standards were prepared by spiking 10 µL aliquots of appropriately diluted working stock solutions into 90 µL aliquots of blank human plasma yielding the final volume of 100 µL calibration standards in human plasma. Calibration standards were prepared freshly on the day of a batch analysis in the concentration range of 50 ng/mL to 5000 ng/mL for (*R*)- and (*S*)-ibuprofen. The solutions were stored at 4˚C until analysis.

The internal standard solutions were prepared as follows. Two separate master stock solutions of (*R*)-flurbiprofen (100 µg/mL), and (*S*)-flurbiprofen (100 µg/mL) enantiomers were prepared in methanol. The (*R*)- and (*S*)-flurbiprofen master stock solutions were combined in equal parts and diluted with water into a mixed working stock solution of (*R*)- and (*S*)-flurbiprofen (10 µg/mL, each). The mixed working stock solution was further diluted with water to yield the diluted working stock solution of (*R*)- and (*S*)-flurbiprofen (100 ng/mL, each). The solutions were stored at 4˚C until analysis.

2.4. Preparation of Quality Control Samples

Quality control (QC) samples were prepared as QC-Low (80 ng/mL), QC-Mid (250 ng/mL), and QC-High (2500 ng/mL) samples in human plasma. A volume of 5 mL of QC samples at each concentration level was prepared. The QC-High samples were prepared by spiking appropriate volumes of each of the master stock solutions of (*R*)-ibuprofen (100 µg/mL), and (*S*)-ibuprofen (100 µg/mL) enantiomers in methanol into blank human plasma, and the QC-Mid, and QC-Low samples were prepared by spiking the appropriately diluted mixed working stock solutions of (*R*)- and (*S*)-ibuprofen into blank human plasma. The QC samples were dispensed in equal aliquots (approx. 130 µL) into vials and stored at –80˚C until use. For each batch analysis, fresh aliquots of QC-Low, QC-Mid, and QC-High samples were thawed, analyzed, and then discarded.

2.5. Preparation of Reagent Solutions

Stock solutions of CDI and (*R*)-NEA (1 mg/mL) were prepared in dichloromethane. Stock solution of HOBt Hydrate (1 mg/mL) was prepared in dichloromethane containing 10% acetonitrile. The stock solutions were stored at 4˚C until use.

2.6. Sample Preparation

Human plasma samples were stored at –80˚C until analysis. On the day of sample analysis, the samples were thawed at room temperature and processed with the method. All human plasma samples, with the exception of the 0-min time point samples, were diluted into the range of the calibration curve by mixing 10 µL aliquots of human plasma samples with 90 µL aliquots of blank human plasma yielding a final volume of 100 µL of sample (*i.e.*, 10-fold dilution). In disposable borosilicate glass tubes, to 100 µL of samples, aliquots of 100 µL of the diluted working stock solution of the internal standards ((*R*)- and (*S*)-flurbiprofen, 100 ng/mL, each) were added followed by the addition of 200 µL of 1 N HCl solution. The samples were vortex-mixed for at least 15 seconds, and 3.0 mL of methyl-tert-butyl ether was added to the tubes. The samples were vortex-mixed for at least 45 seconds, and the tubes were placed at –80˚C for at least 10 min. The tubes were removed from the –80˚C freezer and the top layers were transferred to a new set of tubes. The organic layer was brought to dryness in a sample evaporator, under nitrogen, at *ca.* 35˚C, and the dried residues were derivatized according to a previously reported procedure [29] with modification. In short, to the dried residues, aliquots of 100 µL of CDI solution (1 mg/mL), 100 µL of HOBt Hydrate solution (1 mg/mL), and 100 µL of (*R*)-NEA solution (1 mg/mL) were added, and the mixtures were kept in a dark environment, at

room temperature, for 2 hours. The samples were then brought to dryness in a sample evaporator, under nitrogen, at *ca*. 35˚C, and the dried residues were reconstituted with 200 µL of acetonitrile/water : 50/50 mixture containing 0.1% formic acid. The samples were analyzed with UPLC-MS/MS.

2.7. Method Validation

The method was validated for accuracy, precision, linearity, range, limit of quantitation (LOQ), limit of detection (LOD), selectivity, absolute recovery, matrix effect, dilution integrity, and evaluation of carry-over in human plasma using 100 µL of sample. Calibration curves included six to seven calibration levels and were prepared on each day of batch analysis with a matrix blank. QC-Low, QC-Mid, and QC-High samples were freshly thawed on each day of batch analysis and 100 µL aliquots were used during the validation process.

2.7.1. Accuracy

Six replicate spiked samples of QC-Low, QC-Mid, and QC-High were prepared in human plasma, and analyzed. Accuracy was expressed as the percentage deviation of the measured (*R*)- and (*S*)-ibuprofen concentration against the added concentration, according to the following formula: %Deviation = [(measured amount/added amount) × 100]-100 with negative %Deviation representing under-estimation, and positive %Deviation representing over-estimation of the true value. The acceptance criteria for accuracy were %Deviation ± 20% for the QC-Low samples, and ± 15% for QC-Mid, and QC-High samples.

For intra-day accuracy, six replicates of QC-Low, QC-Mid, and QC-High samples were prepared and analyzed on the same day. Intra-day accuracy experiments were repeated for three separate days. For inter-day accuracy, six replicates of QC-Low, QC-Mid, and QC-High were prepared and analyzed on three separate days.

2.7.2. Precision

A single spiked sample for QC-Low, QC-Mid, and QC-High (5 mL each) was prepared in human plasma. Six aliquots were removed from each of the QC-Low, QC-Mid, and QC-High samples and analyzed. The relative standard deviation (%RSD) of the (*R*)- and (*S*)-ibuprofen concentrations measured in each QC sample were calculated. The acceptance criteria for precision were %RSD ≤ 20% for the QC-Low samples, and %RSD ≤ 15% for the QC-Mid, and QC-High samples.

For intra-day precision, six aliquots were removed from each of the QC-Low, QC-Mid, and QC-High spiked samples and analyzed on the same day. Intra-day precision experiments were repeated for three separate days. For inter-day precision, six aliquots were removed from each of the QC-Low, QC-Mid, and QC-High spiked samples and analyzed on three separate days.

2.7.3. Linearity and Range

Calibration curves were prepared for each batch analysis in the following concentrations: 50, 100, 200, 300, 400, 1000, 5000 ng/mL in human plasma. Calibration curves were constructed by plotting the concentrations of (*R*)- and (*S*)-ibuprofen on the X-axis, *vs*. the chromatographic peak area ratio of (*R*)- and (*S*)-ibuprofen to (*R*)- and (*S*)-flurbiprofen internals standards on the Y-axis. Linear regression analyses were performed using the calibration curve data. At least six out of seven of the calibration standards were used to construct the calibration curves. Using the y = mx + b equation, the y-intercept (b), slope (m) and correlation coefficient (r) were calculated. The calibration curves were weighted using the weighting factor of $1/X^2$. The acceptance criterion for linearity was the coefficient of determination $r^2 \geq 0.980$ for (*R*)- and (*S*)-ibuprofen after weighting with $1/X^2$. (*R*)- and (*S*)-ibuprofen concentrations were calculated by the MassLynx software using the following formula: x = (y-b)/m, where y = (*R*)- and (*S*)-ibuprofen to IS peak area ratio, b = weighted y-intercept, m = weighted slope. The range of the assay was established as the section of the calibration curve where the curve was linear, *i.e.*, $r^2 \geq 0.980$, the calibration levels were accurate (%Deviation ± 15%) and precise (%RSD ≤ 15%).

2.7.4. Limit of Quantitation and Limit of Detection

To determine LOQ, six replicates of the 50 ng/mL calibration standard were prepared in human plasma and analyzed. The mean response (*i.e.*, signal-to-noise ratio, S/N), accuracy and precision were determined from the samples. The LOQ was determined as the lowest concentration of the calibration curve which met the following acceptance criteria. The mean response of (*R*)- and (*S*)- ibuprofen peaks in the samples was at least 5-times the response compared to the blank sample (the response, S/N, was calculated using MassLynx software). The (*R*)- and (*S*)-ibuprofen peaks were identifiable, discrete, and reproducible, with an accuracy (%Deviation) of ±20% and precision (%RSD) ≤ 20%. To determine LOD, triplicate samples of 1 ng/mL (*R*)- and (*S*)-ibuprofen were prepared in human plasma and analyzed. The mean response was determined from the samples. The LOD was determined as the lowest concentration of (*R*)- and (*S*)-ibuprofen in the samples where the mean response of the (*R*)- and (*S*)-ibuprofen peaks was at least 3-times the response compared to the blank sample.

2.7.5. Selectivity

Selectivity was determined in pooled human plasma samples made from three separate lots spiked at the LOQ level. Triplicate samples were prepared. Blank human plasma samples without (*R*)- and (*S*)-ibuprofen and (*R*)-

and (*S*)-flurbiprofen were also prepared using the pooled human plasma samples made from the three lots. The blank samples were visually compared to the LOQ samples for any significant interference at the retention times of (*R*)- and (*S*)-ibuprofen and (*R*)- and (*S*)-flurbiprofen. The acceptance criteria for selectivity were that the mean response (*i.e.*, S/N) of (*R*)- and (*S*)-ibuprofen in the LOQ samples were at least 5-times the response compared to the blank samples, and there was no significant matrix interference at the retention times of (*R*)- and (*S*)-ibuprofen and (*R*)- and (*S*)-flurbiprofen when the blank samples were compared with the LOQ samples.

2.7.6. Absolute Recovery

Samples of QC-Low, QC-Mid, and QC-High were prepared in human plasma and analyzed. The (*R*)- and (*S*)-ibuprofen peak area counts of the extracted samples were compared to the (*R*)- and (*S*)-ibuprofen peak area counts of directly injected standards of the same concentration. Six determinations per concentration were performed and absolute recovery was calculated according to the following formula: %Absolute recovery = (extracted (*R*)- and (*S*)-ibuprofen peak area counts/unextracted (*R*)- and (*S*)-ibuprofen peak area counts) × 100.

2.7.7. Matrix Effect

Matrix effect, which may cause ionization suppression or enhancement of the analytes, was determined in three blank human plasma lots. Samples of QC-Low, QC-Mid, and QC-High were prepared in human plasma and in water and analyzed. The (*R*)- and (*S*)-ibuprofen peak area counts of the plasma samples were compared to that obtained in samples prepared in water. Samples were analyzed in triplicates and the matrix effect was calculated according to the following formula: %Matrix Effect = peak area counts in plasma—peak area counts in water/ peak area counts in water × 100. Matrix effect was considered negligible if no more than 10% difference in the peak area counts of (*R*)- and (*S*)-ibuprofen was observed in the human plasma samples compared to the samples prepared in water. Negative %matrix effect represented ionization suppression, and positive %matrix effect represented ionization enhancement.

2.7.8. Dilution-Integrity

Six aliquots of QC-High (2500 ng/mL) samples were diluted 10-fold with blank human plasma and analyzed. The acceptance criteria for (*R*)- and (*S*)-ibuprofen were the accuracy (%Deviation) ± 15% from the actual value (250 ng/mL), and precision (%RSD) ≤ 15% from the six determinations.

2.7.9. Evaluation of Carry-over

An aliquot of a QC-Mid sample was prepared and three injections were made, immediately followed by three injections of a blank human plasma sample. Carry-over was expressed as the percentage difference between the mean (*R*)- and (*S*)-ibuprofen or (*R*)- and (*S*)-flurbiprofen peak area counts in blank human plasma samples and the mean (*R*)- and (*S*)-ibuprofen or (*R*)- and (*S*)-flurbiprofen peak area count in the QC-Mid sample. Carry-over was considered negligible if no more than 5% of (*R*)- and (*S*)-ibuprofen or (*R*)- and (*S*)-flurbiprofen was observed in the blank plasma. The percentage carry-over was calculated as follows: %Carry-over = (BL/QC-Mid) × 100, where BL = Mean peak area count in the blank samples (at retention times of (*R*)- and (*S*)-ibuprofen or (*R*)- and (*S*)-flurbiprofen), QC-Mid = Mean (*R*)- and (*S*)-ibuprofen or (*R*)- and (*S*)-flurbiprofen peak area count in the QC-Mid sample.

3. Results and Discussion

The objective of this study was to develop and validate a sensitive and enantioselective UPLC-MS/MS method for the quantitation of the (*R*)- and (*S*)-ibuprofen in human plasma. A method was needed, which had a simple sample preparation step including derivatization, so that the resulting (*R*)- and (*S*)-ibuprofen diastereomers could be analyzed with conventional reverse-phase chromatographic conditions.

3.1. Method Development and Optimization

The present analytical procedure is based upon a previously reported assay [29] with modifications to the method of detection, chromatography and sample preparation as described below.

3.1.1. Mass Spectrometry

The spectrofluorometric detection [29] was replaced with mass spectrometric detection. Mass spectrometry is a much improved detection technique, because it allows for the selective monitoring of the MRM transitions of (*R*)- and (*S*)-ibuprofen and (*R*)- and (*S*)-flurbiprofen, therefore, eliminating any interferences with co-eluting endogenous components from human plasma. In order to monitor (*R*)- and (*S*)-ibuprofen and (*R*)- and (*S*)-flurbiprofen using a non-chiral chromatographic system, the compounds were derivatized as described above to yield the corresponding diastereomeric amides. The amide derivatives contained a nitrogen atom, which could be ionized efficiently using ES + mode. The molecular ions were determined by the direct injection of about 100 µg/mL solutions of the analytes in water/methanol: 50/50 into the mobile phase flow of the same composition in the absence of a chromatographic column. The molecular ions observed for (*R*)- and (*S*)-ibuprofen were *m/z* 360.2, and *m/z* 398.3 for (*R*)- and (*S*)-flurbiprofen. The cone voltage value was optimized with the most intense signal

obtained at a cone voltage of 30 V for each analyte. Source temperature, desolvation temperature, and desolvation gas flow values were optimized for the highest signal and are reported in Subsection 2.2. The product ions of the analytes were determined and representative product ion mass spectra obtained in ES+ for (*R*)- and (*S*)-ibuprofen, and for (*R*)- and (*S*)-flurbiprofen are presented in **Figure 1**. The CE values were optimized to obtain the most abundant signals for the product ions. The proposed fragmentation pattern of the diastereomeric amide derivatives of (*R*)- and (*S*)-ibuprofen, and (*R*)- and (*S*)-flurbiprofen obtained in ES+ is presented in **Figure 2**. MRM transitions were created and (*R*)- and (*S*)-ibuprofen was detected at *m/z* 360.2→ 232.1 (CE 10 eV), and (*R*)-and (*S*)-flurbiprofen at *m/z* 398.3 → 270.1 (CE 10 eV). The dwell time was set to 25 ms for (*R*)-and (*S*)-ibuprofen as this provided sufficient sampling points during the chromatographic peaks to achieve reliable integration and, therefore, reproducible results. The dwell time for (*R*)-and (*S*)-flurbiprofen was set to 50 ms.

3.1.2. Liquid Chromatography

The HPLC system using a conventional C18 column was replaced with a UPLC system using a narrow-bore Acquity UPLC ethylene bridged hybrid (BEH) phenyl column, and the mobile phase system containing a mixture of phosphate buffer and acetonitrile was replaced with a mobile phase system containing a mixture of water, ammonium acetate, formic acid, methanol and acetonitrile.

For our initial studies, an Acquity UPLC BEH C18 1.7 µm, 2.1 × 100 mm column was tested for the separation of (*R*)- and (*S*)-ibuprofen, and (*R*)- and (*S*)-flurbiprofen. The mobile phase composition was solvent a: water with 0.1% formic acid and solvent b: methanol with 0.1% formic acid with the flow rate set at 0.2 mL/min. A series of isocratic chromatographic experiments were performed which are summarized as follows. Ammonium acetate (10 mM) was added to the mobile phase, different mobile phase compositions were tested, methanol was replaced with acetonitrile in solvent b, various solvent b compositions were prepared with different proportions of methanol and acetonitrile mixed in solvent b. While it was found that methanol was a selective solvent for the separation of (*R*)- and (*S*)-ibuprofen and acetonitrile for (*R*)- and (*S*)-flurbiprofen, no baseline separation could be achieved for these compounds with any additional changes made to the chromatographic conditions when the C18 chromatographic column was used.

Based on these findings, the C18 column was replaced with a Waters Acquity UPLC BEH Phenyl 1.7 µm 2.1 × 150 mm column. With the phenyl column, when solvent a was water with 10 mM ammonium acetate and 0.1% formic acid, and solvent b was a mixture of acetonitrile/methanol: 64/36 containing 10 mM ammonium acetate and 0.1% formic acid, and using an isocratic run with a flow rate of 0.2 mL/min, and a mobile phase composition of solvent a/solvent b: 35/65, baseline separation was achieved for (*R*)- and (*S*)-ibuprofen, and (*R*)- and (*S*)-flurbiprofen. The final gradient programming is detailed in Subsection 2.2. With this chromatographic column, mobile phase composition and gradient programming, (*R*)- and (*S*)-flurbiprofen eluted at a retention time of 8.82

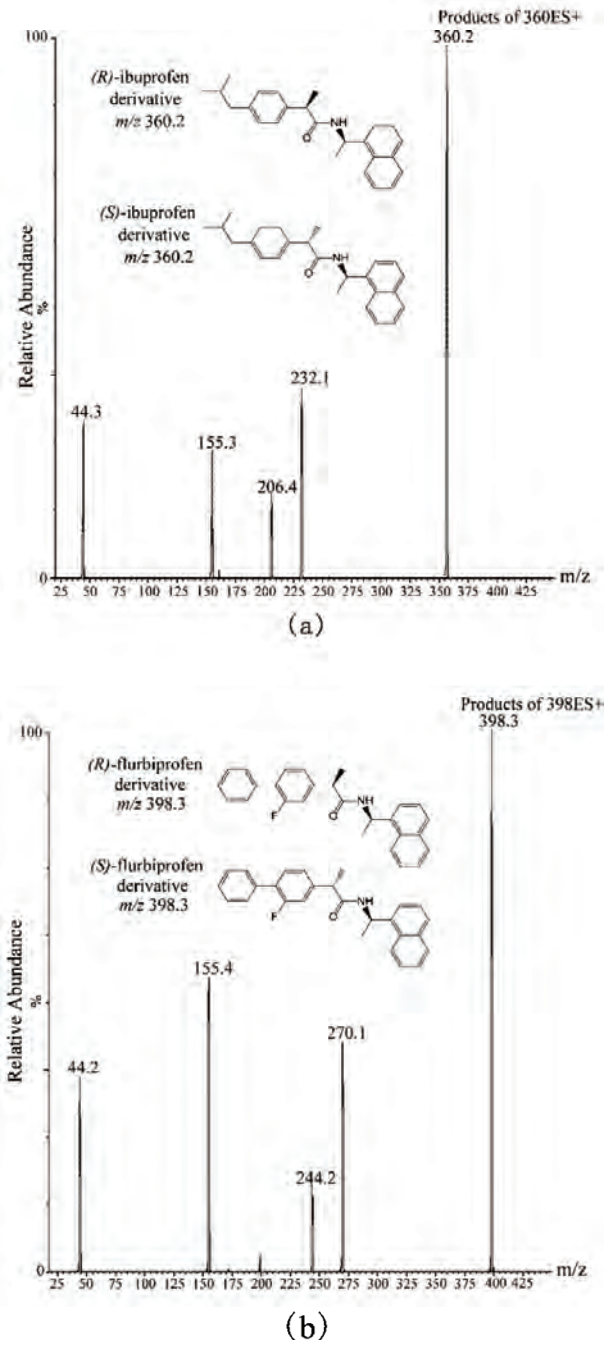

Figure 1. Representative product ion mass spectra of the diastereomeric amide derivatives of (a) *(R)*- and *(S)*-ibuprofen, and (b) *(R)*- and *(S)*-flurbiprofen obtained in ES+ with a collision energy (CE) 10 eV.

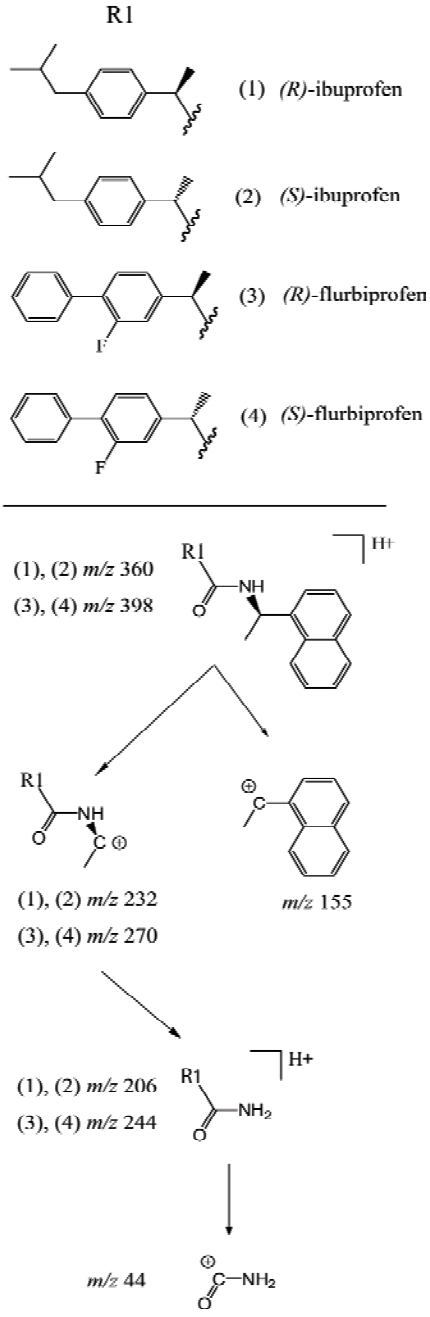

Figure 2. Proposed fragmentation pattern of diastereomeric amide derivatives of (1) *(R)*- and (2) *(S)*-ibuprofen, (3) *(R)*- and (4) *(S)*-flurbiprofen obtained in ES+.

min and 10.03 min, respectively, and (*R*)- and (*S*)-ibuprofen eluted at a retention time 10.12 min and 11.07 min, respectively. A representative chromatogram of the plasma sample taken from a human volunteer 120 min after the oral administration of a 400 mg ibuprofen capsule is presented in **Figure 3**.

3.1.3. Sample Preparation

The sample volume required for analysis was reduced from 0.5 mL [29] to 100 µL, and the sample preparation was simplified. The buffering step with sodium phosphate buffer was removed and the extraction solvent diethylether was replaced with methyl-tert-butyl ether which is less flammable, less toxic and easier to use. The mixing time for sample preparation was reduced, and the transfer of the organic layer was made quicker and more efficient by freezing the bottom aqueous layer in the tubes and decanting the top organic layer into a clean set of tubes. After derivatization, the step of passing the samples through solid-phase extraction silica cartridges was eliminated.

3.2. Method Validation

3.2.1. Accuracy and Precision

The results for accuracy and precision are presented in **Table 1**. Accuracy was expressed as the %Deviation for the QC-Low, QC-Mid and QC-High samples. Intra-day accuracy for (*R*)-ibuprofen ranged between -11.8% and 11.2%, and for (*S*)-ibuprofen between -8.6% and -0.3%. Inter-day accuracy for (*R*)-ibuprofen ranged between –10.4% and 4.5%, and for (*S*)-ibuprofen between –4.8% and –0.6%. Precision was expressed as the %RSD for the QC-Low, QC-Mid and QC-High samples. Intra-day precision for (*R*)-ibuprofen ranged between 2.2% and 10.3%, and for (*S*)-ibuprofen between 1.7% and 7.0%. Inter-day precision for (*R*)-ibuprofen ranged between 5.9% and 11.2%, and for (*S*)-ibuprofen between 4.0% and 4.8%. The method met the acceptance criteria for accuracy of %Deviation ± 20% for the QC-Low samples, and ± 15% for the QC-Mid, and QC-High samples, and for precision of % RSD ≤ 20% for QC-Low samples, and ≤ 15% for the QC-Mid, and QC-High samples. This indicated that the method was accurate and precise over the range of the assay.

3.2.2. Linearity and Range

Linearity of the calibration curve was evaluated in seven batches over the course of the validation. The coefficient of determination (mean ± SD, n = 7) for (*R*)-ibuprofen was $r^2 = 0.995 \pm 0.004$, and for (*S*)-ibuprofen $r^2 = 0.996 \pm 0.004$. The accuracy (%Deviation) of the calibration curve levels for (*R*)-ibuprofen ranged between -12.9% and 5.5%, and for (*S*)-ibuprofen between -4.6% and 3.4%. The precision (%RSD) of the calibration curve levels for (*R*)-ibuprofen ranged between 2.3% and 4.4%, and for (*S*)-ibuprofen between 1.2% and 10.2%. The calibration curve met the acceptance criterion for linearity of $r^2 \geq 0.980$ after weighting with $1/X^2$. The range of the method was established as 50 ng/mL to 5000 ng/mL where the calibration levels met the acceptance criteria of accuracy (%Deviation) ± 15%, and precision (%RSD) ≤ 15%. The results indicated that the calibration curve was linear, accurate, and precise over the range of the method.

Table 1. Accuracy (intra- and inter-day) and precision (intra-and inter-day) for (*R*)- and (*S*)-ibuprofen in human plasma.

	(*R*)-ibuprofen				(*S*)-ibuprofen				
Accuracy	**Intra-Day**			**Inter-Day**	**Accuracy**	**Intra-Day**			**Inter-Day**
QC-Low (80 ng/mL)	Day 1 (n = 5)	Day 2 (n = 6)	Day 3 (n = 6)	Day 1-3 (n = 17)	**QC-Low** (80 ng/mL)	Day 1 (n = 5)	Day 2 (n = 6)	Day 3 (n = 6)	Day 1-3 (n = 17)
Mean (ng/mL)	76.7	82.2	81.1	80.2	Mean (ng/mL)	79.7	79.1	79.6	79.5
SD (ng/mL)	2.38	5.11	3.63	4.38	SD (ng/mL)	4.99	5.21	3.69	4.36
%Deviation	**–4.1**	**2.7**	**1.3**	**0.2**	%Deviation	**–0.3**	**–1.1**	**–0.5**	**–0.6**
QC-Mid (250 ng/mL)					**QC-Mid** (250 ng/mL)				
Mean (ng/mL)	242	261	278	261	Mean (ng/mL)	244	244	249	246
SD (ng/mL)	22.6	10.8	14.5	18.9	SD (ng/mL)	6.72	7.82	8.47	7.62
%Deviation	**–3.4**	**4.4**	**11.2**	**4.5**	%Deviation	**–2.3**	**–2.4**	**–0.5**	**–1.7**
QC-High (2500 ng/mL)					**QC-High** (2500 ng/mL)				
Mean (ng/mL)	2205	2246	2267	2241	Mean (ng/mL)	2428	2285	2433	2379
SD (ng/mL)	18.1	71.0	43.9	54.0	SD (ng/mL)	37.7	98.4	85.7	104
%Deviation	**–11.8**	**–10.2**	**–9.3**	**–10.4**	%Deviation	**–2.9**	**–8.6**	**–2.7**	**–4.8**

	(*R*)-ibuprofen				(*S*)-ibuprofen				
Precision	**Intra-Day**			**Inter-Day**	**Precision**	**Intra-Day**			**Inter-Day**
QC-Low (80 ng/mL)	Day 1 (n = 6)	Day 2 (n = 5)	Day 3 (n = 6)	Day 1-3 (n = 17)	**QC-Low** (80 ng/mL)	Day 1 (n = 6)	Day 2 (n = 5)	Day 3 (n = 6)	Day 1-3 (n = 17)
Mean (ng/mL)	78.6	89.6	96.7	88.2	Mean (ng/mL)	89.5	90.0	89.0	89.4
SD (ng/mL)	4.88	8.29	5.73	9.87	SD (ng/mL)	3.40	6.28	2.36	3.92
%RSD	**6.2**	**9.2**	**5.9**	**11.2**	%RSD	**3.8**	**7.0**	**2.6**	**4.4**
QC-Mid (250 ng/mL)					**QC-Mid** (250 ng/mL)				
Mean (ng/mL)	268	298	274	279	Mean (ng/mL)	271	267	252	263
SD (ng/mL)	9.25	12.5	10.3	16.4	SD (ng/mL)	4.48	5.20	8.58	10.5
%RSD	**3.4**	**4.2**	**3.7**	**5.9**	%RSD	**1.7**	**1.9**	**3.4**	**4.0**
QC-High (2500 ng/mL)					**QC-High** (2500 ng/mL)				
Mean (ng/mL)	1912	2121	2040	2018	Mean (ng/mL)	2219	2121	2074	2139
SD (ng/mL)	81.7	218	44.5	149	SD (ng/mL)	79.6	110	68.4	103
%RSD	**4.3**	**10.3**	**2.2**	**7.4**	%RSD	**3.6**	**5.2**	**3.3**	**4.8**

SD = Standard Deviation; %Deviation = [(measured amount/added amount) × 100]-100 [%]; %RSD = Relative Standard Deviation [%].

3.2.3. Limit of Quantitation, Selectivity, Limit of Detection

LOQ was determined in six replicates of the 50 ng/mL calibration standard. The mean response of the (*R*)- and (*S*)-ibuprofen peaks in the samples was higher than 5-times the response obtained in the blank sample. The accuracy (%Deviation) for (*R*)-ibuprofen ranged between –7.1% and 7.3% and for (*S*)-ibuprofen between –0.4% and 5.2%. The precision (%RSD) for (*R*)-ibuprofen was 5.8% and for (*S*)-ibuprofen 2.0%. Results for the determination of LOQ met the acceptance criteria of the mean response which was at least 5-times the response compared to the blank sample, accuracy (%Deviation) ± 20% and precision % RSD ≤ 20%, and the (*R*)- and (*S*)-ibuprofen peaks were identifiable, discrete, and reproducible. The method was accurate and precise with an established LOQ of 50 ng/mL of (*R*)- and (*S*)-ibuprofen requiring 100 µL of sample. The selectivity of the method was investigated in triplicate samples of pooled human plasma made from three separate lots spiked at LOQ level. Blank human plasma samples from three separate lots were also prepared. The selectivity met the acceptance criteria that the mean response for (*R*)- and (*S*)-ibuprofen was at least 5-times the response compared to the blank samples, and there was no significant interference at the retention times of (*R*)- and (*S*)-ibuprofen and

(*R*)- and (*S*)-flurbiprofen when the blank human plasma samples were compared to the LOQ samples. The results indicated that the method was selective for these analytes. LOD was determined in triplicate samples of 1 ng/mL (*R*)- and (*S*)-ibuprofen prepared in human plasma. The mean response (*i.e.*, S/N) of the (*R*)- and (*S*)-ibuprofen peaks in the samples was higher than 3-times the response obtained in the blank sample. The method had an established LOD of 1 ng/mL of (*R*)- and (*S*)-ibuprofen requiring 100 µL of sample. Representative chromatograms of LOD (1 ng/mL), and blank human plasma samples are presented in **Figure 4**.

3.2.4. Absolute Recovery and Matrix Effect

The mean %Absolute recovery values (n = 6) for (*R*)-ibuprofen for QC-Low, QC-Mid and QC-High were 81.9%, 86.9% and 84.5%, respectively, and for (*S*)-ibuprofen 82.2%, 83.4% and 83.7%, respectively. The results indicated that (*R*)- and (*S*)-ibuprofen were extracted relatively uniformly over the concentration range of the assay. The mean %Matrix effect values (n = 9) for (*R*)-ibuprofen for QC-Low, QC-Mid, and QC-High were 1.3%, 2.2% and –2.5%, respectively, and for (*S*)- ibuprofen 2.1%, –6.2%, and –2.0%, respectively. The results met the acceptance criterion of %Matrix effect of no more than 10%. This indicated that the matrix effect from human plasma contributing to the ionization suppression or enhancement of (*R*)- and (*S*)-ibuprofen was negligible.

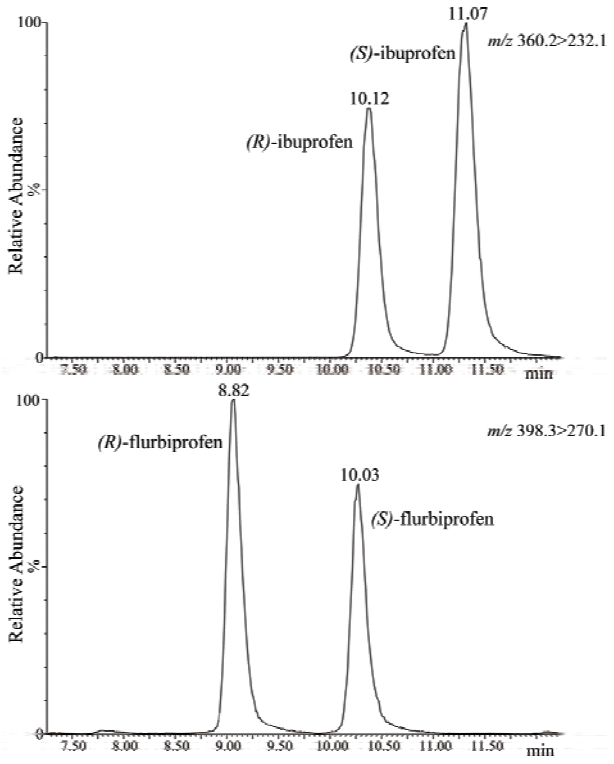

Figure 3. A representative chromatogram of the plasma sample taken from a human volunteer 120 min after the oral administration of a 400 mg ibuprofen capsule. The MRM signal of *m/z* 360.2 → 232.1 for (*R*)- and (*S*)-ibuprofen is on the top, and *m/z* 398.3 → 270.1 for internal standards (*R*)- and (*S*)-flurbiprofen is on the bottom (the measured *(R)*- and (*S*)-ibuprofen concentrations were 803 ng/mL and 1087 ng/mL, respectively).

3.2.5. Dilution Integrity and Evaluation of Carry-over

After the 10-fold dilution of the six aliquot of the QC-High samples, the accuracy (%Deviation, n = 6) for (*R*)-ibuprofen ranged between –5.5% and 4.1%, and for (*S*)-ibuprofen between –7.9% and 5.6%. The precision (%RSD, n = 6) for (*R*)-ibuprofen was 3.7% and for (*S*)-ibuprofen 4.5%. The results met the acceptance criteria of accuracy (%Deviation) ±15% from the actual value (250 ng/mL), and precision (%RSD) ≤ 15%. This indicated that samples exceeding the calibration curve concentrations could be diluted 10-fold to bring them into the range of the assay with accuracy and precision. Carry-over between injections of the QC-Mid and blank plasma samples for (*R*)-ibuprofen was 0.4%, for (*S*)-ibuprofen 1.0%, for (*R*)-flurbiprofen 0.1%, and for (*S*)-flurbiprofen 0.1%; all met the acceptance criteria of no more than 5%.

3.2.6. Pharmacokinetics of (*R*)- and (*S*)-ibuprofen in humans

Healthy human volunteers were involved in a pharmacokinetic study following the administration of a single oral dose of 400 mg ibuprofen capsules. The detailed pharmacokinetic results of this study will be published elsewhere. Here we report the results of four randomly selected subjects to demonstrate the applicability of the developed and validated method to determine the (*R*)- and (*S*)-ibuprofen concentrations in human plasma. Plasma samples were collected at various time intervals up to 300 min following the ibuprofen dose. A representative plasma concentration *vs*. time plot obtained from one subject is presented in **Figure 5**. (*R*)- and (*S*)-ibuprofen concentrations increased during the first 90 min reaching a peak value of 15,026 ng/mL for (*R*)-ibuprofen, and 18,915 ng/mL for (*S*)-ibuprofen. After that time, the drug concentrations decreased gradually and remained above 3100 ng/mL for (*R*)-ibuprofen, and 5800 ng/mL for (*S*)-ibuprofen at the final sampling time of 300 min. Pharmacokinetic analysis of the plasma concentration data obtained from the four subjects was performed using a non-compartmental analysis (PK Solutions 2.0, Montrose, CO, USA). The results were normalized to body weights. The estimated pharmacokinetic parameters for (*R*)-ibuprofen were as follows (mean ± SD, n = 4): terminal elimination half-life ($t_{1/2}$): 83.8 ± 8.62 min, T_{max}: 37.5 ± 8.66 min, C_{max}: 14,076 ± 3160 ng/mL, apparent volume of distribution (V/F): 350 ± 50.4 mL/kg, apparent oral clearance (CL/F): 2.91 ± 0.519 mL/min/kg,

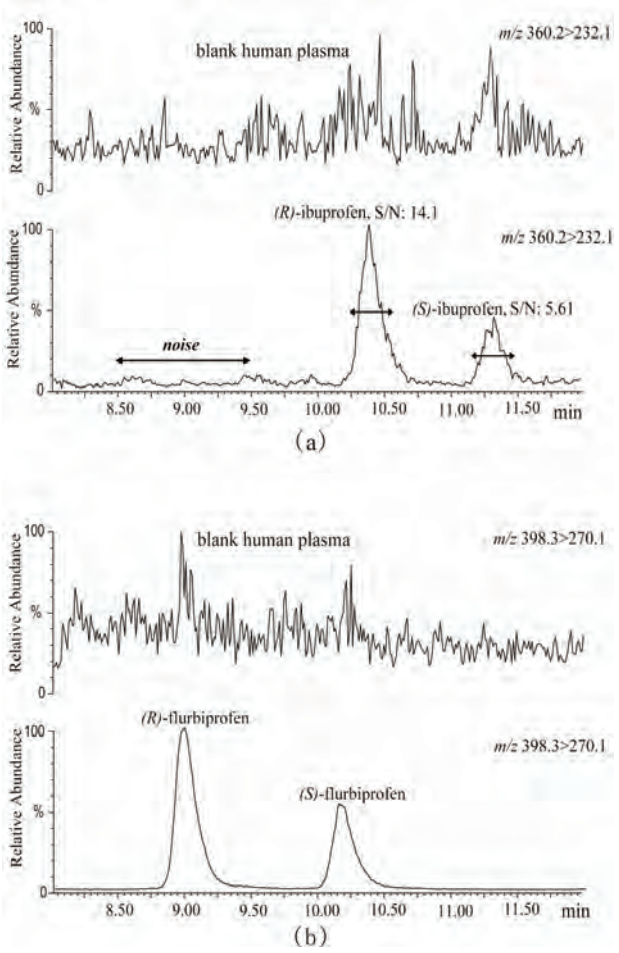

Figure 4. Limit of detection (LOD, 1 ng/mL) and blank human plasma samples. (a) shows the MRM *m/z* 360.2 → 232.1 for (*R*)- and (*S*)-ibuprofen in blank human plasma (top), and in the LOD sample (bottom) (the signal-to-noise [S/N] values are reported on the top of the (*R*)- and (*S*)-ibuprofen peaks). (b) shows the MRM *m/z* 398.3 → 270.1 for (*R*)- and (*S*)-flurbiprofen, internal standard, in blank human plasma (top), and in the LOD sample (bottom).

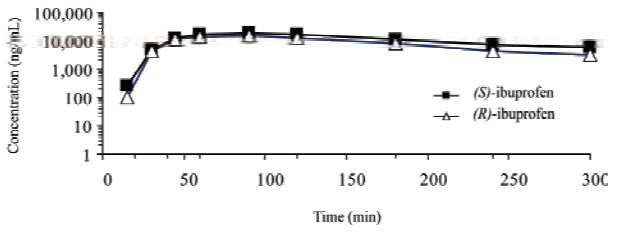

Figure 5. Concentration of (*R*)- and (*S*)-ibuprofen *vs*. time profile obtained from a volunteer following a single oral dose of a 400 mg ibuprofen capsule.

and mean residence time (MRT_{INF}): 142 ± 23.4 min; and for (*S*)-ibuprofen (mean ± SD, n = 4): terminal elimination half-life ($t_{1/2}$): 108 ± 14.6 min, T_{max}: 41.3 ± 7.50 min, C_{max}: 15,779 ± 4720 ng/mL, apparent volume of distribution (V/F): 325 ± 91.1 mL/kg, apparent oral clearance (CL/F): 2.06 ± 0.303 mL/min/kg, and mean residence time (MRT_{INF}): 173 ± 16.1 min.

In summary, the results show that following the oral administration of 400 mg racemic ibuprofen, both enantiomer showed rapid absorption and stereoselective disposition. For (*S*)-ibuprofen, the plasma concentrations peaked at 41.3 min, reached higher levels (*i.e.*, 15,779 ng/mL), had higher terminal elimination half life (108 min), apparent volume of distribution (325 mL/kg), mean residence time (173 min), and lower apparent oral clearance (2.06 mL/min/kg) than those values for (*R*)-ibuprofen (*i.e.*, T_{max}: 37.5 min, C_{max}: 14,076 ng/mL, $t_{1/2}$: 83.8 min, V/F: 350 mL/kg, MRT_{INF}: 142 min, and CL/F: 2.91 mL/min/kg, respectively). These findings are consistent with the data of *in vivo* chiral inversion of (*R*)-ibuprofen to (*S*)-ibuprofen reported in the literature [9-11].

4. Conclusions

An enantioselective modified UPLC-MS/MS method was developed and validated for the quantitation of (*R*)- and (*S*)-ibuprofen enantiomers in human plasma. Compared to previously published assays, sample preparation was simplified without the need of post-derivatization sample clean-up [29], sample volume required for analysis was reduced at least 5-fold [6,25,29], the range of the calibration curve was extended into the three-digit range [23,25,29], baseline separation of (*R*)- and (*S*)-ibuprofen was achieved [20,25] and the sensitivity was increased 2-fold [23-25,29]. The assay was validated with a LOQ of 50 ng/mL, however, the sensitivity of the assay proved to be significantly higher with a LOD of 1 ng/mL. It was not necessary to validate the method at a LOQ less than 50 ng/mL, because of the high concentration of the samples analyzed during this study. However, the LOQ of the present assay can be easily extended to the low ng/mL levels if future studies require a methodology with significantly higher sensitivity. The assay demonstrated good reproducibility and was applied to investigate the pharmacokinetics of ibuprofen enantiomers following oral administration of the racemate drug.

5. Acknowledgements

The authors would like to thank Dr. Cathy Boscarino for her valuable work with the design of the human study; Mrs. Debbie Kerrigan-Brown, Ingrid Smith, Christina Powlesland, and Mr. Kevin Hofer, Robert Limmer, Doug Saunders, Jan Pope for their excellent technical support of the human study. This work was funded by a research contract with Defence Research and Development Canada; contract number W7711-088126.

6. References

[1] R. D. Knihinicki, K. M. Williams and R. O. Day, "Chiral Inversion of 2-Arylpropionic Acid Non-Steroidal Anti-Inflammatory Drugs—I. In Vitro Studies of Ibuprofen and Flurbiprofen," *Biochemical Pharmacology*, Vol. 38, No. 24, December 1989, pp. 4389-4395.

[2] S. M. Sanins, W. J. Adams, D. G. Kaiser, G. W. Halstead, J. Hosley, H. Barnes and T. A. Baillie, "Mechanistic Studies on the Metabolic Chiral Inversion of R-Ibuprofen in the Rat," *Drug Metabolism and Disposition*, Vol. 19, No. 2, March-April 1991, pp. 405-410.

[3] S. Fournel and J. Caldwell, "Metabolic Chiral Inversion of 2-Phenylpropionic Acid in Rat, Mouse and Rabbit," *Biochemical Pharmacology*, Vol. 35, No. 23, December 1986, pp. 4153-4159.

[4] J. Caldwell, A. J. Hull and S. Fournel-Gigleux, "The Metabolic Chiral Inversion and Dispositional Enantioselectivity of the 2-Arylpropionic Acids and their Biological Consequences," *Biochemical Pharmacology*, Vol. 37, No. 1, January 1988, pp. 105-114.

[5] D. G. Kaiser, G. J. Van Giessen, R. J. Reischer and W. J. Wechter, "Isomeric Inversion of Ibuprofen (R)-Enantiomer in Humans," *Journal of Pharmaceutical Sciences*, Vol. 65, No. 2, February 1976, pp. 269-273.

[6] T. A. Baillie, W. J. Adams, D. G. Kaiser, L. S. Olanoff, G. W. Halstead, H. Harpootlian and G. J. Van Giessen, "Mechanistic Studies of the Metabolic Chiral Inversion of (R)-Ibuprofen in Humans," *Journal of Pharmacology and Experimental Therapeutics*, Vol. 249, No. 2, May 1989, pp. 517-523.

[7] S. S. Adams, P. Bresloff and C. G. Mason, "Pharmacological Differences Between Optical Isomers of Ibuprofen: Evidence for Metabolic Inversion of the (–)-Isomer," *Journal of Pharmacy and Pharmacology*, Vol. 28, No. 3, March 1976, pp. 256-257.

[8] A. J. Hutt and J. Caldwell, "The Metabolic Chiral Inversion of 2-Aryl Propionic Acids—A Novel Route with Pharmacological Consequences," *Journal of Pharmacy and Pharmacology*, Vol. 35, No. 11, November 1983, pp. 693-704.

[9] A. J. Hutt and J. Caldwell, "The Importance of Stereochemistry in the Clinical Pharmacokinetics of the 2-Arylpropionic Acid Non-Steroidal Anti-Inflammatory Drugs," *Clinical Pharmacokinetics*, Vol. 9, No. 4, July-August 1984, pp. 371-373.

[10] S. C. Tan, B. K. Patel, S. H. D. Jackson, C. G. Swift, and J. Hutt, "Stereoselectivity of Ibuprofen Metabolism and Pharmacokinetics Following the Administration of the Racemate to Healthy Volunteers," *Xenobiotica*, Vol. 32, No. 8, August 2002, pp. 683-697.

[11] H. Hao, G. Wang and J. Sun, "Enantioselective Pharmacokinetics of Ibuprofen and Involved Mechanisms," *Drug Metabolism Reviews*, Vol. 73, No. 1, January 2005, pp. 215-234.

[12] E. J. Lee, K. Williams, R. Day, G. Graham and D. Champion, "Stereoselective Disposition of Ibuprofen Enantiomers in Man," *British Journal of Clinical Pharmacology*, Vol. 19, No. 5, May 1985, pp. 669-674.

[13] S. C. Tan, B. K. Patel, S. H. Jackson, C. G. Swift and A. J. Hutt, "Influence of Age on the Enantiomeric Disposition of Ibuprofen in Healthy Volunteers," *British Journal of Clinical Pharmacology*, Vol. 55, No. 6, June 2003, pp. 579-587.

[14] G. F. Lockwood, K. S. Albert, G. J. Szpunar and J. G. Wagner, "Pharmacokinetics of Ibuprofen in Man—III: Plasma Protein Binding," *Journal of Pharmacokinetics & Biopharmaceutics*, Vol. 11, No. 5, October 1983, pp. 469-482.

[15] J. K. Paliwal, D. E Smith, S. R Cox, R. R Berardi, V. A. Dunn-Kucharski and G. H. Elta, "Stereoselective, Competitive, and Nonlinear Plasma Protein Binding of Ibuprofen Enantiomers as Determined in Vivo in Healthy Subjects," *Journal of Pharmacokinetics and Biopharmaceutics*, Vol. 21, No. 2, April 1993, pp. 145-161.

[16] J. C. Nielsen, P. Bjerring, L. Arendt-Nielsen and K.-J. Petterson, "A Double-Blind, Placebo Controlled, Crossover Comparison of the Analgesic Effect of Ibuprofen 400 Mg and 800 Mg on Laser-Induced Pain," *British Journal of Clinical Pharmacology*, Vol. 30, No. 5, November 1990, pp. 711-715.

[17] P. Camilleri and C. Dyke, "Effect of ^2H_2O on the Resolution of the Optical Isomers of Ibuprofen on an A_1-Acid Glycoprotein Column," *Journal of Chromatography A*, Vol. 518, June 1990, pp. 277-281.

[18] S. Menzel-Soglowek, G. Geisslinger and K. Brune, "Stereoselective High-Performance Liquid Chromatographic Determination of Ketoprofen, Ibuprofen and Fenoprofen in Plasma Using a Chiral Alpha 1-Acid Glycoprotein Column," *Journal of Chromatography A*, Vol. 532, No. 2, November 1990, pp. 295-303.

[19] K. J. Pettersson and A. Olsson, "Liquid Chromatographic Determination of The Enantiomers of Ibuprofen in Plasma Using a Chiral AGP Column," *Journal of Chromatography A*, Vol. 563, No. 2, February 1991, pp. 414-418.

[20] W. Naidong and J. W. Lee, "Development and Validation of a Liquid Chromatographic Method for the Quantitation of Ibuprofen Enantiomers in Human Plasma," *Journal of Pharmaceutical and Biomedical Analysis*, Vol. 12, No. 4, April 1994, pp. 551-556.

[21] H. Y. Aboul-Enein, A. Van Overbeke, G. Vander Weken, W. Baeyens, H. Oda, P. Deprez and A. De Kruif, "HPLC on Chiralcel OJ-R for Enantiomer Separation and Analysis of Ketoprofen, from Horse Plasma, as the 9-Aminophenanthrene Derivative," *Journal of Pharmacy and Pharmacology*, Vol. 50, No. 3, March 1998, pp. 291-296.

[22] K. Tachibana and A. Ohnishi, "Reversed-Phase Liquid Chromatographic Separation of Enantiomers on Polysaccharide Type Chiral Stationary Phases," *Journal of Chromatography A*, Vol. 906, No. 1-2, January 2001, pp. 127-154.

[23] X. W. Teng, S.W. Wang and N. M. Davies, "Stereospecific High-Performance Liquid Chromatographic Analysis of Ibuprofen in Rat Serum," *Journal of Chromatography B*, Vol. 796, No. 2, November 2003, pp. 225-231.

[24] A. Reddy, M. Hashim, Z. Wang. L. Penn, C. J. Stankovic, D. Burdette, N. Surendran and H. Cai, "A Novel Method for Assessing Inhibition of Ibuprofen Chiral Inversion and its Application in Drug Discovery," *International Journal of Pharmaceutics*, Vol. 335, No. 1-2, April 2007, pp. 63-69.

[25] P. S. Bonato, M. P. Del Lama and R. Carvalho, "Enantioselective Determination of Ibuprofen in Plasma by High-Performance Liquid Chromatography-Electrospray Mass Spectrometry," *Journal of Chromatography B*, Vol. 796, No. 2, November 2003, pp. 413-420.

[26] E. J. D. Lee, K. M. Williams, G. G. Graham, R. O. Day, and G. D. Champion, "Liquid Chromatographic Determination and Plasma Concentration Profile of Optical Isomers of Ibuprofen in Humans," *Journal of Pharmaceutical Sciences*, Vol. 73, No. 11, November 1984, pp. 1542-1544.

[27] R. Mehvar, F. JamaII and F. M. Pasutto, "Liquid-Chromatographic Assay of Ibuprofen Enantiomers in Plasma," *Clinical Chemistry*, Vol. 34, No. 3, March 1988, pp. 493-496.

[28] C. H. Lemko, G. Caille and R. T. Foster, "Stereospecific High-Performance Liquid Chromatographic Assay of Ibuprofen: Improved Sensitivity and Sample Processing Efficiency," *Journal of Chromatography A*, Vol. 619, No. 2, September 1993, pp. 330-335.

[29] S. C. Tan, S. H. D Jackson, C. G Swift and A. J. Hutt, "Enantiospecific Analysis of Ibuprofen by High Performance Liquid Chromatography: Determination of Free and Total Drug Enantiomer Concentrations in Serum and Urine," *Chromatographia*, Vol. 46, No. 1-2, July 1997, pp. 23-32.

[30] M. J. Hilton and K. V. Thomas, "Determination of Selected Human Pharmaceutical Compounds in Effluent and Surface Water Samples by High-Performance Liquid Chromatography-Electrospray Tandem Mass Spectrometry," *Journal of Chromatography A*, Vol. 1015, No. 1-2, October 2003, pp. 129-141.

[31] R. Leverence, M. J. Avery, O. Kavetskaia, H. Bi, C. E. Hop and A. I. Gusev, "Signal Suppression/Enhancement in HPLC-ESI-MS/MS from Concomitant Medications," *Biomedical Chromatography*, Vol. 21, No. 11, November 2007, pp. 1143-1150.

[32] S. Y. Chang, W. Li, S. C. Traeger, B. Wang, D. Cui, H. Zhang, B. Wen and A.D. Rodrigues, "Confirmation that Cytochrome P450 2C8 (CYP2C8) Plays a Minor Role in (S)-(+)- and (R)-(-)-Ibuprofen Hydroxylation in Vitro," *Drug Metabolism and Disposition*, Vol. 36, No. 12, December 2008, pp. 2513-2522.

[33] G. D. Mendes, F. D. Mendes, C. C. Domingues, R. A de Oliveira, M. A. da Silva, L. S. Chen, J. O. Ilha, C. E. Fernandes and G. De Nucci, "Comparative Bioavailability of Three Ibuprofen Formulations in Healthy Human Volunteers," *International Journal of Clinical Pharmacology and Therapeutics*, Vol. 46, No. 6, June 2008, pp. 309-318.

[34] P. Seideman, F. Lohrer, G. G. Graham, M. W. Duncan, K. M. Williams and R. O. Day, "The Stereoselective Disposition of the Enantiomers of Ibuprofen in Blood, Blister and Synovial Fluid," *British Journal of Clinical Pharmacology*, Vol. 38, No. 3, September 1994, pp. 221-227.

[35] B. A. Way, T. R. Wilhite, C. H. Smith and M. Landt, "Measurement of Plasma Ibuprofen by Gas Chromatography-Mass Spectrometry," *Journal of Clinical Laboratory Analysis*, Vol. 11, No. 6, April 1997, pp. 336-339.

[36] Á. Sebők, A. Vasanits-Zsigrai, Gy. Palkó, Gy. Záray and I. Molnár-Perl, "Identification and Quantification of Ibuprofen, Naproxen, Ketoprofen and Diclofenac Present in Waste-Waters, as their Trimethylsilyl Derivatives, by Gas Chromatography Mass Spectrometry," *Talanta*, Vol. 76, No. 3, July 2008, pp. 642-650.

American Journal of Analytical Chemistry, **2010, 2, 59-69**
doi:10.4236/ajac.2010.12008 Published Online August 2010 (http://www.SciRP.org/journal/ajac)

Quantitative Application to a Polypill by the Development of Stability Indicating LC Method for the Simultaneous Estimation of Aspirin, Atorvastatin, Atenolol and Losartan Potassium

Satheesh K. Shetty[1,5]*, Koduru V. Surendranath[1], Pullapanthula Radhakrishnanand[1], Roshan M. Borkar[2],Prashant S. Devrukhakar[2], Johnson Jogul[3], Upendra M. Tripathi[4]

[1]*United States Pharmacopeia-India Private Limited, Research and Development Laboratory, ICICI Knowledge Park, Turkapally, Shameerpet, Hyderabad, India*

[2]*National Institute of Pharmaceutical education and Research* (*NIPER*), *Hyderabad, India*

[3]*Department of Chemistry, St. Kittel Science College, Dharwad, India*

[4]*Startech Labs private Limited, SMR Chambers Madinaguda, Hyderabad, India*

[5]*Department of Chemistry, Jawaharlal Nehru Technological University, Kukatpally, Hyderabad, India*

E-mail: *skshetty*69*@rediffmail.com, sks@usp.org*

Received May 21, 2010; *revised July* 10, 2010; *accepted July* 23, 2010

Abstract

Polypill is a fixed-dose combination (FDC) containing three or more drugs in a single pill with the intention of reducing the number of tablets or capsules that need to be taken. Developing a single analytical method for the estimation of individual drugs in a Polypill is very challenging, due to the formation of drug-drug and drug-excipients interaction impurities. Here an attempt was made to develop a new, sensitive, single stability-indicating HPLC method for the simultaneous quantitative determination of Aspirin (ASP) Atorvastatin (ATV), Atenolol (ATL) and Losartan potassium (LST) in a polypill form in the presence of degradation products. Efficient chromatographic separation was achieved on a C18 stationary phase with simple mobile phase combination of buffer and Acetonitrile. Buffer consists of 0.1% Orthophosphoric acid (pH 2.9), delivered in a gradient mode and quantitation was carried out using ultraviolet detection at 230 nm with a flow rate of 1.0 mL/min. The retention times of Atenolol, Aspirin, Losartan potassium, and Atorvastatin were 3.3, 7.6, 10.7 and 12.9 min respectively. The combination drug product are exposed to thermal, acid/base hydrolytic, humidity and oxidative stress conditions, and the stressed samples were analyzed by proposed method. The method was validated with respect to linearity; the method was linear in the range of 37.5 to 150.0 µg/mL for ASP, 5.0 to 20.0 µg/mL for ATV and 25.0 to 100.0 µg/mL for ATL and LST. Acceptable precision and accuracy were obtained for concentrations over the standard curve ranges. The validated method was successfully applied to the analysis of Starpill tablets constituting all the four drugs; the percentage recoveries obtained were 99.60% for ASP, 99.30% for ATV, 99.41% for ATL and 99.62% for LST.

Keywords: Liquid Chromatography, Polypill, Aspirin, Atorvastatin, Atenolol and Losartan Potassium, Forced Degradation, Validation, Stability Indicating

1. Introduction

A Polypill concept to reduce CVD by more than 80% was firstly given by Wald and Law [1] and has been applied to pharmaceutical preparations [2-6]. Foreseeing the need of different analytical methods for estimation of ingredients of these pills, the ultimate goal of our work was to develop and validate a single high-performance liquid chromatography method selective for the four main components of tablets Starpill. Starpill is a fixed dose combination of Aspirin (ASP), Atorvastatin (ATV), Atenolol (ATL) and Losartan potassium (LST). Each trilayered tablet contains Aspirin 75 mg, Atorvastatin 10 mg, Atenolol 50 mg and Losartan 50 mg. Aspirin (ASP), 2-acetoxybenzoic acid affects platelet aggregation by irreversibly inhibiting prostaglandin cyclooxygenase. This effect lasts for the

life of the platelet and prevents the formation of the platelet aggregating factor thromboxane A2 [7-8]. Atorvastatin (ATV), (3*R*, 5R)-7-[2-(4-fluorophenyl)-3-phenyl -4-(phenylcarbamoyl)-5-(propan-2-yl)-1*H*-pyrrol-1-yl]-3, 5-dihydroxyheptanoic acid is a selective competitive inhibitor of 3-hydroxy-3-methyl-glutarylcoenzyme A (HMG-CoA) reductase enzyme. This enzyme catalyzes the conversion of HMG-CoA to mevalonate, an early and rate limiting step in the synthesis of cholesterol [9]. Atenolol (ATL), (*RS*)-2-{4-[2-hydroxy-3-(propan-2-ylamino) propoxy]phenyl} acetamide is a beta1-selective (cardio selective) beta-adrenergic receptor blocking agent without membrane stabilizing or intrinsic sympathomimetic (partial agonist) activities. This preferential effect is not absolute, however, and at higher doses, Atenolol inhibits beta2-adrenoreceptors, chiefly located in the bronchial and vascular musculature [10-11]. Losartan (LST), 2-butyl-4-chloro-1-{[2'-(1*H*-tetrazol-5-yl)biphenyl-4-yl]methyl}-1 *H*-imidazol-5-yl) methanol is an angiotensin II receptor (type AT1) antagonist. Losartan and its principal active metabolite block the vasoconstrictor and aldosterone-secreting effects of angiotensin II by selectively blocking the binding of angiotensin II to the AT 1 receptor found in many tissues, (e.g., vascular smooth muscle, adrenal gland). The active metabolite is 10 to 40 times more potent by weight than Losartan and appears to be a reversible, non-competitive inhibitor of the AT 1 receptor [12-13].

Extensive literature survey did not reveal any simple, sensitive and stability indicating LC method for the simultaneous determination of all the four drugs as a fixed dose combination. Literature survey reveals that a variety of spectrophotometric and chromatographic methods, and a stability indicating LC method, has been reported for determination of ASP and ATV in pharmaceutical preparations in combination with other drugs [14-21]. Spectrophotometer and chromatographic methods have been reported for determination of ATL, in combination with other drugs, in bulk and pharmaceutical preparations [22-23].Also there are some papers for the estimation of LST individually and combination with other drugs [24-27].The present drug stability test guideline Q1A (R2) [28-29] issued by International Conference on Harmonization (ICH) suggests that stress studies should be carried out on a drug to establish its inherent stability characteristics, leading to separation of degradation products and hence supporting the suitability of the proposed analytical procedures.

In the present paper an attempt has been made to develop an accurate, rapid, specific and reproducible method for the estimation of Aspirin (ASP), Atorvastatin (ATV), Atenolol (ATL) and Losartan potassium (LST) in Starpill along with method validation as per ICH norms.

2. Experimental

2.1. Chemicals

Samples of Aspirin (ASP) Atorvastatin (ATV), Atenolol (ATL) and Losartan potassium (LST) were procured from USP India (P) limited, Hyderabad, India (**Figure 1**). Market samples of Starpill (Cipla Ltd Mumbai) tablets were purchased from the retail pharmacy. HPLC grade Acetonitrile, Analytical reagent grade Orthophosphoric acid purchased from Merck, Darmstadt, Germany. High purity water was prepared by using Millipore Milli-Q plus water purification system. The purity of the all drug substances and the chemicals used for the experiment were greater than 99.5% and the purity of the working standards used for the analysis was 99.9%.

2.2. Equipments

The LC system, used for method development, forced degradation studies and method validation was Waters 2695 binary pump plus auto sampler and a 2996 photo diode array detector. The output signal was monitored and processed using Empower software on Pentium computer (Digital equipment Co). Photo stability studies were carried out in a photo stability chamber (Mack Pharmatech, Hyderabad, India). Thermal stability studies were performed in a dry air oven (Mack Pharmatech, Hyderabad, India).Accelerated stability studies were performed in a stability Chamber (Thermo Lab Mumbai).

2.3. Chromatographic Conditions

The chromatographic column used was Inertsil ODS C18 (150 × 4.6) mm with 5 µm particles. The mobile phase A consists of 0.1% Orthophosphoric acid adjusted to pH 2.9 with triethylamine (TEA). The mobile phase B consists of Acetonitrile. Flow rate of the mobile phase was 1.0 mL/min. The HPLC gradient program was set as: (time (min)/% solution B: 0/5, 10/60, 15/80, 17/60, 20/5, 25/5. The column temperature was maintained at 35˚C and the detection was monitored at a wavelength of 230 nm. The injection volume was 10 µL. Buffer: Acetonitrile 80:20; (v/*v*) was used as diluent.

2.4. Preparation of Standard Solutions

A stock solution of ASP, ATV, ATL,and LST standard and sample (7.5 mg/mL of ASP, 1 mg/mL of ATV, 5.0 mg/mL each of ATL and LST) were prepared in diluent. Working solutions 0.075 mg/mL of ASP, 0.01 mg/mL of ATV, 0.05 mg/mL each of ATL and LST were prepared from above stock solution in the diluent for assay determination.

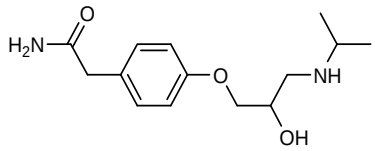

(a) Atenolol (ATL): (*RS*)-2-{4-[2-hydroxy-3-(propan-2-ylamino)propoxy]phenyl}acetamide, M.F: $C_{14}H_{22}N_2O_3$, M.W: 266.336 g/mol.

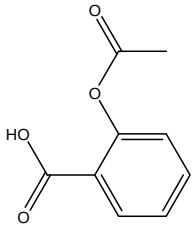

(b) Aspirin (ASP): 2-acetoxybenzoic acid, M.F: $C_9H_8O_4$, M.W: 180.16 g/mol.

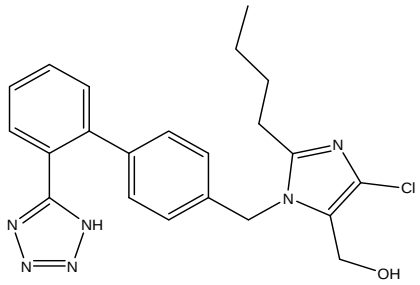

(c) Losartan (LST): 2-butyl-4-chloro-1-{[2'-(1*H*-tetrazol-5-yl)biphenyl-4-yl]methyl}-1*H*-imidazol-5-yl)methanol, M.F: $C_{22}H_{23}ClN_6O$, M.W: 422.91 g/mol.

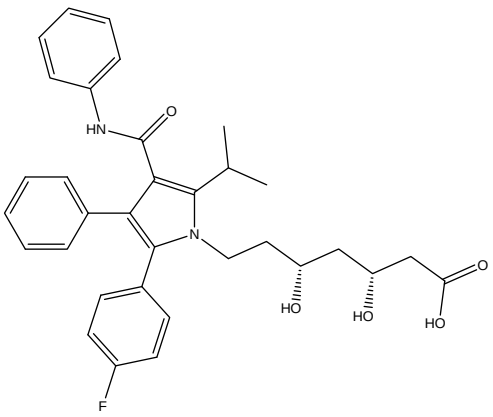

(d) Atorvastatin (ATV): (3*R*,5R)-7-[2-(4-fluorophenyl)-3-phenyl-4-(phenylcabamoyl)-5-(propan-2-yl)-1*H*-pyrrol-1-yl]-3,5-dihydroxyheptanoic acid, M.F: $C_{33}H_{35}FN_2O_5$, M.W: 558.64 g/mol.

Figure 1. Chemical structures and labels of all the drug substances: ATL, ASP, LST and ATV.

2.5. Preparation of Sample Solutions

Twenty tablets were weighed and their average weight was calculated. The tablets were crushed to a homogeneous powder and a quantity equivalent to one tablet (75 mg ASP, 10 mg ATV, 50 mg: ATL and 50 mg LST) was weighed in a 100-mL volumetric flask, extracted in diluents by sonication, and filtered through Whatman no. 41 filter paper. The filtrate (1 mL) was quantitatively transferred to a 10-mL volumetric flask, and solution was diluted to volume with the diluent.

2.6. Preparation of System Suitability Solution

System Suitability Solution was prepared by spiking 0.01 mg/mL of Salicylic acid (SA) to a mixture of all the four drugs at the target test concentration levels (0.075 mg/mL of ASP, 0.01 mg/mL of ATV, 0.05 mg/mL each of ATL and LST).

2.7. Analytical Method Validation

The developed chromatographic method was validated for selectivity, linearity, range, precision, accuracy, sensitivity, robustness and system suitability.

2.7.1. Specificity/Application of Stress (Forced Degradation Study)

Selectivity of the developed method was assessed by performing forced degradation studies. The terms selectivity and specificity are often used interchangeably. Specificity is the ability of the method to measure the analyte response in the presence of its potential impurities. Stress testing of the drug substance can help to identify the likely degradation products, which can in turn help to establish the degradation pathways and the intrinsic stability of the molecule and validate the stability indicating power of the analytical procedures used.

The specificity of the developed LC method for quantification of all the four drugs was determined in the presence of its degradation products. Forced degradation studies were performed on individual as well as mixture of all the four drugs, to provide an indication of stability indicating property and specificity of the proposed method [30-31].

The stress conditions employed for degradation study includes light (carried out as per ICH Q1B), heat (60˚C), acid hydrolysis (0.1N HCl), base hydrolysis (0.1N NaOH), water hydrolysis and oxidation (5% H_2O_2). For acid study period was reflux for 1 h, and oxidation it was at room temperature (RT) for 48 h and for base it was reflux for 2 h. Peak purity of stressed samples was checked by using a 2996 photo diode array detector (PDA) from Waters. The purity angle within the purity threshold limit demonstrates the analyte peak homogeneity.

2.7.2. Precision

System Precision was investigated by injecting the 6 replicates of the sample preparations of the commercial tablet (Starpill).Repeatability (Intra-Day precision) of the assay method was evaluated by carrying out six inde-

pendent assays of the commercial tablets (0.075 mg/mL of ASP, 0.05 mg/mL of ATL and LST, 0.010 mg/mL of ATV test concentration) against qualified reference standard and calculating the % RSD of the assay results.

Intermediate Precision (Inter-Day) was evaluated by carrying out the experiment with a different analyst, different column on different day and estimating the % RSD of the result obtained.

2.7.3. Sensitivity

Sensitivity was determined by establishing the Limit of detection (LOD) and Limit of quantitation (LOQ) for ASP, ATV, ATL, and LST estimated at a signal-to-noise ratio of 3:1 and 10:1 respectively, by injecting a series of dilute solutions with known concentration. The precision study was also carried out at the LOQ level by injecting six individual preparations of ASP, ATV, ATL, and LST, calculated the % RSD for the areas of each drug.

2.7.4. Linearity

Linearity solutions were prepared from stock solution at five concentration levels from 50 to 200% of analyte concentrations (37.5 to 150 µg/mL for ASP, 5.0 to 20 µg/mL for ATV and 25.0 to 100 µg/ml for ATL and LST). The peak area versus concentration data was collected and performed regression analysis by the method of least squares. The Correlation coefficient, Slope & y-intercept values were calculated from the calibration plot obtained.

2.7.5. Accuracy

The accuracy of the method was determined by measuring the recovery of the drugs by the method of standard additions. Known amounts of each drug corresponding to 50,100, and 150% of the target test concentrations (0.075 mg/mL of ASP, 0.01 mg/mL of ATV, 0.05 mg/mL each of ATL and LST) were added to a placebo mixture to determine whether the exccipients present in the formulation led to positive or negative interferences. Each set of additions was repeated three times at each level. Extraction sample preparation procedure is followed and assayed against qualified reference standard. The accuracy was expressed as the percentage of the analytes recovered by the assay.

2.7.6. Robustness

To determine the robustness of the developed method, experimental conditions were deliberately changed and the relative standard deviation for replicate injections of ASP, ATV, ATL and LST peaks and the USP resolution factor between ASP and SA peaks were evaluated. The mobile phase flow rate was 1.0 mL/min. This was changed by 0.1 units to 1.1 and 1.2 mL/min. The effect of column temperature was studied at 40˚C and 30˚C instead of 35˚C. The effect of buffer pH was studied at pH 2.8 and 3.0.

2.7.7. Solution Stability and Mobile Phase Stability

The solution stability of ASP, ATV, ATL and LST was carried out by leaving the test solution in tightly capped volumetric flasks at room temperature for 48 h and assayed at 6 h interval, against the freshly prepared standard solution. The mobile phase stability was carried out by assaying the freshly prepared sample solution against the freshly prepared standard at 6 h interval up to 48 h. The percentage of RSD of assay of ASP, ATV, ATL and LST was calculated for the study period during mobile phase and solution stability experiments.

3. Results and Discussions

3.1. Method Development and Optimization

All the four drug solutions were prepared in diluent at a concentration of 100 µg/mL and scanned in UV-Visible spectrometer; all the drugs were having UV maxima at around 230 nm. Hence detection at 230 nm was selected for method development purpose.

The main analytical challenge during development of a new method was obtaining adequate retention of the polar parent compound, Atenolol (ATL) while maintaining a reasonable elution time for the less-polar Atorvastatin (ATV) and to separate one of the degradation impurity Salicylic acid (SA) from the ASP peak.

To achieve this, Water and Acetonitrile (50:50 v/v) mobile phase, on a C18 stationary phase with a 25 cm length, 4.6 mm ID and 5µm particle size were investigated. Experiments were also performed using the columns of varying lengths from 250 to 100 mm. Different mobile phase compositions containing phosphate buffer and Acetonitrile (50:50-20:80 v/v) were also tried. But was unsuccessful in getting good peak shapes for all the peaks. Although good separation was achieved with 0.1% phosphoric acid: Acetonitrile in the ratio of 50:50 (v/v), Atorvastatin peak symmetry was found to be greater than 2.0. The asymmetry of the Atorvastatin peak was improved by addition of Triethylamine (TEA) and adjusting the mobile phase pH to 2.9 in the aqueous phase. The chromatographic separation with better peak shape was achieved using a mixture of aqueous 0.1% Orthophosphoric acid and Acetonitrile in the ratio of 50:50 (v/v). The columns, 250, 150 and 125 mm × 4.6 mm, 5 µm of varied lengths were tried but 150 × 4.6 mm, 5 µm C18 Column gave reasonable retention for all the peaks. But when degradation samples were injected with these conditions, one of the degradation impurity of ASP namely salicylic acid (SA) was not separated from the ASP Peak. Then method was optimized to separate all the degradants from the main peaks by changing to Gradient mode. Several gradient conditions were tried before optimizing the final gradient programme as: time (min)/% solution B: 0/5, 10/60, 15/80, 17/60, 20/5, 25/5 Effect of

the diluent on the peak shapes was studied. The ATL peak was observed as split in most of the compositions of the buffer and Acetonitrile. Finally Buffer: Acetonitrile (80:20, v/v) was optimized as the diluent to obtain good peak shapes.

The satisfactory chromatographic separation, with good peak shapes were achieved on Inertsil ODS-C18 (150 × 4.6) mm with 5 µm particles, using 0.1 % Orthophosphoric acid (adjusted to pH 2.9 with TEA) as mobile phase A and Acetonitrile as solution B with a flow rate of 1.0 mL/min. The HPLC gradient program was optimized as: (time (min)/% solution B: 0/5, 10/60, 15/80, 17/60, 20/5, 25/5. The column temperature as maintained at 35˚C and the detection was monitored at a wavelength of 230 nm. The injection volume was 10 µL. Buffer: Acetonitrile (80: 20, v/v) was used as diluent. In the optimized gradient conditions ATL, ASP, SA, LST and ATV were well separated with a resolution (Rs) of greater than 2 and the typical retention times of ATL, ASP, SA, LST and ATV were about 3.3, 7.6, 8.1, 10.7 and 12.9 respectively, the typical chromatogram of System suitability shown in **Figure 2**.

Peak purity of stressed samples of all the four drug substances were checked by using 2996 Photo diode array detector of Waters (PDA). The purity angle within the purity threshold limit obtained in all stressed samples demonstrates the analyte peak homogeneity. All stressed samples of the drug product (heat (60˚C), acid hydrolysis (0.1N HCl), base hydrolysis (0.1N NaOH), water hydrolysis and oxidation (5% H2O2)) were analyzed for extended run time of 60 min to check the late eluting degradants.The System suitability results were given in (**Table 1**).

The proposed method is applied for the assay analysis of 3 different batches of the polypills. The assay results obtained were within the specification limit. The assay of polypill is unaffected in the presence of excipients confirming the stability indicating power of the developed method.

3.2. Method Validation

3.2.1. Precision

The percentage RSD values for the assays in precision study were 0.4, 0.8, 0.4, 0.5% (intra-day precision) and 0.5, 0.8, 0.6, 0.7% (inter-day precision) for ASP, ATV, ATL, and LST confirming a good precision and the ruggedness of the method ,The % RSD obtained for the Ruggedness study were as shown in (**Table 2**).

3.2.2. Sensitivity

The limits of detection (LOD) and quantitation (LOQ) were established at signal-to-noise ratios of 3:1 and 10:1, respectively. The LOD and LOQ of ASP, ATV, ATL and LST were determined experimentally by injecting

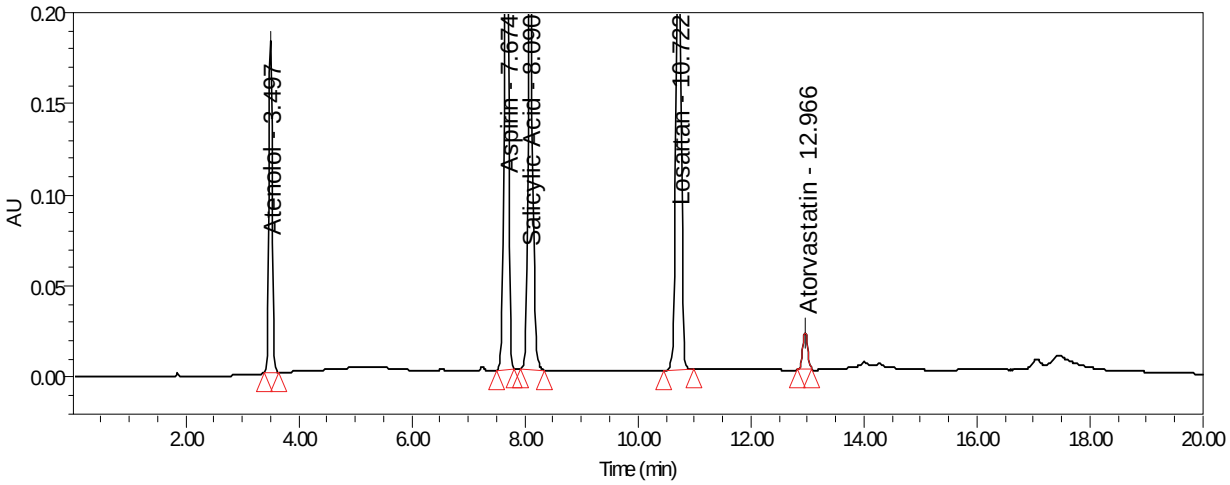

Figure 2. Typical chromatogram of system suitability.

Table 1. System suitability report.

Compound	Retention time	USP Resolution (RS)	USP Tailing factor (T)	No of theoretical plates USP tangent method (N)
Atenolol (ATL)	3.5		1.03	16743
Aspirin (ASP)	7.6	34.1	1.02	53435
Salicylic acid (SA)	8.1	2.8	1.1	46436
Losartan (LST)	10.7	16.6	0.99	76004
Atorvastatin (ATV)	12,9	13.4	0.97	91198

Table 2. Results of intermediate precision.

S. No	Parameter	Variation	% RSD for Assay			
			ASP	ATV	ATL	LST
1	Different System	(a) Waters 2695 Alliance system	0.7%	0.3%	0.5%	0.7%
		(b) Agilent 1100 series VWD system	0.6%	0.8%	0.6%	0.9%
2	Different Column	(a) B.No: 0014	0.4%	0.5%	0.7%	0.6%
		(b)B.No:00118	0.5%	0.4%	0.6%	0.6%
3	Different Analyst	(a) Analyst-1	0.5%	0.9%	0.6%	0.6%
		(b) Analyst-2	0.4%	0.7%	0.6%	0.8%
4	Different Days (Interday precision)	(a) Day-1	0.4%	0.9%	0.3%	0.5%
		(b) Day-2	0.5%	0.8%	0.5%	0.6%
		(c) Day-3	0.6%	0.7%	0.4%	0.4%

each drug six times. The LOD for ASP, ATV, ATL and LST were 0.1, 0.2, 0.15 and 0.02 µg/mL respectively. The LOQ for ASP, ATV, ATL and LST were 0.3, 0.7, 0.4 and 0.06 µg/mL, respectively.

3.2.3. Linearity

The linear ranges were from (37.5 to 150 µg/mL for ASP, 5.0 to 20 µg/mL for ATV and 25.0 to 100 µg/mL for ATL and LST).The correlation coefficient obtained was greater than 0.999. The Slope and the Intercept value obtained from the linear regression graph is as shown in (**Table 3**). The result shows an excellent correlation existed between the peak area and concentration of the analyte in the range 50-200% of analyte concentration.

3.2.4. Accuracy

The percentage recovery of the results obtained is listed in **Table 4**, the results indicate the method enables highly accurate simultaneous determination of the all the four drugs in the polypill combination.

3.2.5. Robustness

Close observation of analysis results for deliberately changed chromatographic conditions (flow rate, column temperature and pH of the mobile phase) revealed that the resolution between closely eluting peaks, namely ASP and SA was always greater than 2.0 and also there was not much effect on the peak shapes, illustrating the robustness of the method (**Table 5**).

3.2.6. Solution Stability and Mobile Phase Stability

The % RSD of assay of Polypill during solution stability and mobile phase stability experiments was within 1.0. No significant changes were observed in the content of ATL, ASP, LST and ATV during the study. The solution stability and mobile phase stability experiments data confirms that sample solutions and mobile phase used during assay determination were stable up to the study period of 48 h.

Table 3. Results of Linearity study for drug substance.

	Atenolol (ATL)	Aspirin (ASP)	Losartan (LST)	Atorvastatin (ATV)
Calibration Equation	Y=8027X-28993	Y=18480X-65531	Y=17299X-38592	Y=1584X-6390
Linearity Range	50-200 %	50-200 %	50-200 %	50-200 %
Regression coefficient	0.999	0.999	0.999	0.999
Slope	8027	18480	17299	1584
Intercept	-28993	-65531	-38592	-6390

Table 4. Results of accuracy study for drug substance.

Analyte	Initial concentration (%)	Added concentration (mg)	Concentration found (mg)	RSD (%)	Recovery (%)
Atenolol (ATL)	50	24.9	24.8	0.23	99.60
	100	50.1	49.8	0.28	99.41
	150	74.8	74.9	0.22	100.13
Aspirin(ASP)	0	0	0		
	50	37.4	37.2	0.36	99.46
	100	75.1	74.8	0.29	99.60
	150	112.3	112.1	0.37	99.82
Losartan(LST)	0	0	0		
	50	25.2	25.1	0.40	99.60
	100	50.1	49.9	0.38	99.62
	150	74.8	74.9	0.34	100.13
Atorvastatin(ATV)	0	0	0		
	50	5.02	5.05	0.40	100.60
	100	10.05	9.98	0.28	99.30
	150	14.85	14.89	0.18	100.27

Table 5. Results of robustness study.

S.No	Parameter	Variation	Resolution (Rs) between ASP and salicylic acid
1	Temperature (± 5˚C of set temperature)	(a) At 30°C (b) At 40°C	2.9 2.7
2	Flow rate (± 20% of the set flow)	(a) At 0.8 mL min-1 (b) At 1.2 mL min-1	2.9 2.8
3	pH Buffer	pH 2.8 pH 3.0	2.9 2.5

3.2.7. Results of Forced Degradation Studies

1) Degradation Behavior

Stress studies on combination of all the four drugs under different stress conditions suggested the following degradation behavior.

2) Degradation in Acidic solution

The combination of all the four drugs was exposed to 0.1 N HCl at 100°C for 1 h. ATL, ASP and ATV showed considerable degradation. The drugs gradually undergone degradation with time in 0.1 N HCl and prominent degradation was observed (**Figure 3(a)**).

3) Degradation in Basic solution

The combination of all the four drugs was exposed to 0.1 N NaOH under reflux for 2 h. ASP and ATV has shown significant sensitivity towards the treatment of 0.1 N NaOH. The drug undergone degradation immediately in 0.1 N NaOH and prominent degradation was observed for ASP with the conversion to SA (**Figure 3(b)**).

4) Oxidative Conditions

The combination of all the four drugs was exposed to 5% hydrogen peroxide at room temperature for 48 h. ASP, LST and ATV has shown significant sensitivity towards the treatment of 5% hydrogen peroxide and the drugs gradually undergone oxidative degradation with time to yield prominent degradation products (**Figure 3(c)**).

5) Photolytic Conditions

When the combination of all the four drugs was exposed to light for an overall illumination of 1.2 million lux hours and an integrated near ultraviolet energy of 200-watt hours/square meter (w/mhr) (in photo stability chamber). Major degradation observed with LST and ATV (**Figure 3(d)**).

6) Thermal Degradation

When the drug product was exposed to dry heat at 60˚C for 8 h, Considerable degradation was observed with ATL and ASP (**Figure 3(e)**).

Accelerated Stability sample:

The stability indicating nature of the method was further confirmed by injecting three month accelerated stability sample and observed that all the degradants were well separated from the main components (**Figure 3(f)**).

Peak purity test results derived from PDA detector, confirmed that the all the four drug components were homogeneous and pure in all the analyzed stress samples. No degradants were observed after 30 min in the extended runtime of 60 min of all the samples.

6) Assay analysis

Assay analysis was performed for different batches of the drug product in tablets (n=3), with the targeted analyte concentrations. The assay results obtained for the three Starpill tablets were, STP/002 (99.7% ATL, 99.8% ASP, 100.25 LST and 99.6% ATV), STP/005 (99.67% ATL, 100.3% ASP, 99.4% LST and 99.8% ATV) and STP/011 (100.1% ATL, 99.9% ASP, 99.7% LST and 100.3% ATV) depicted in (**Table 6**).

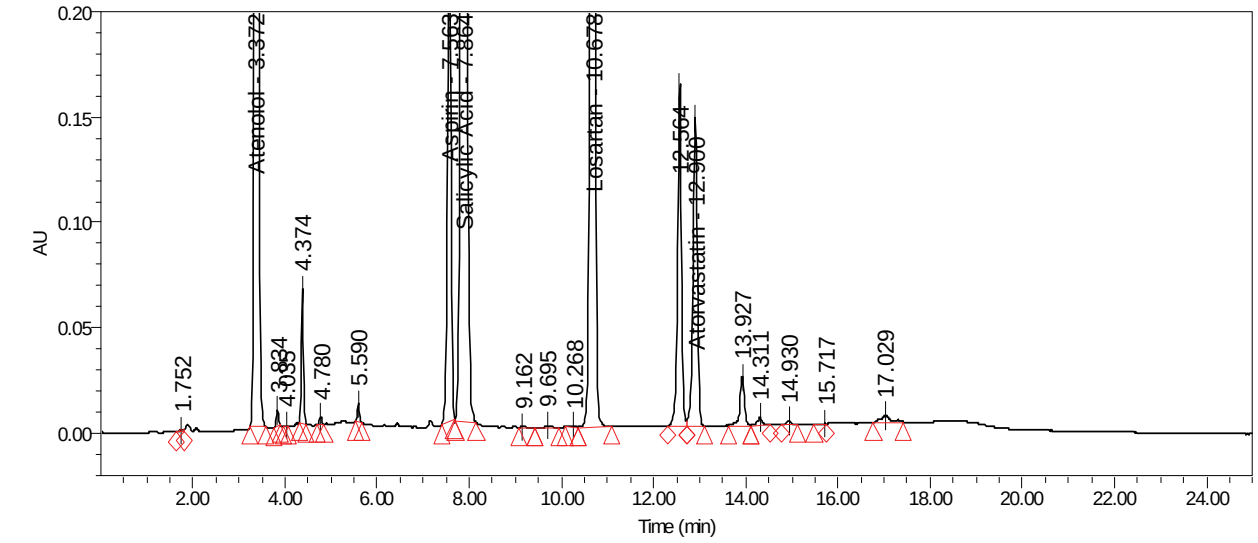

(a)

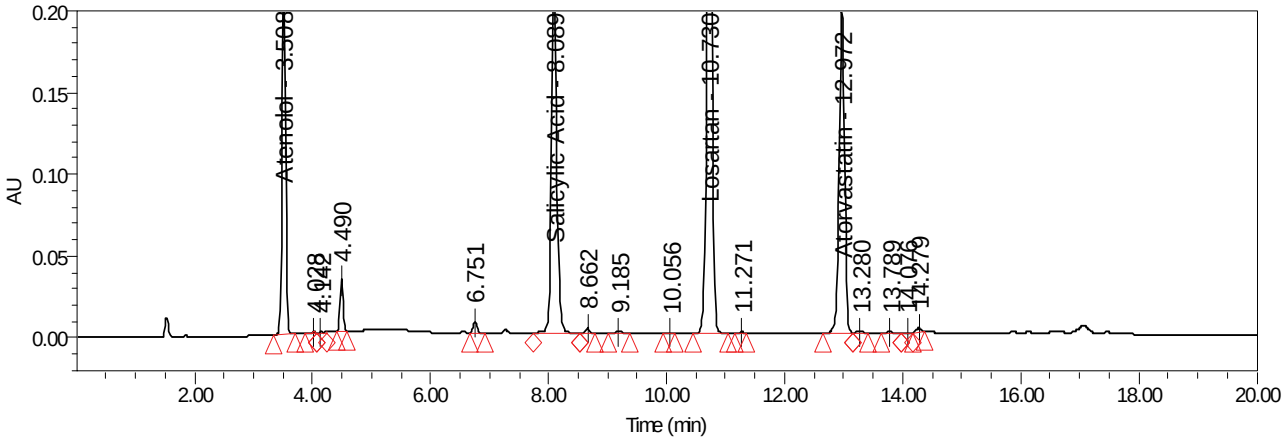

(b)

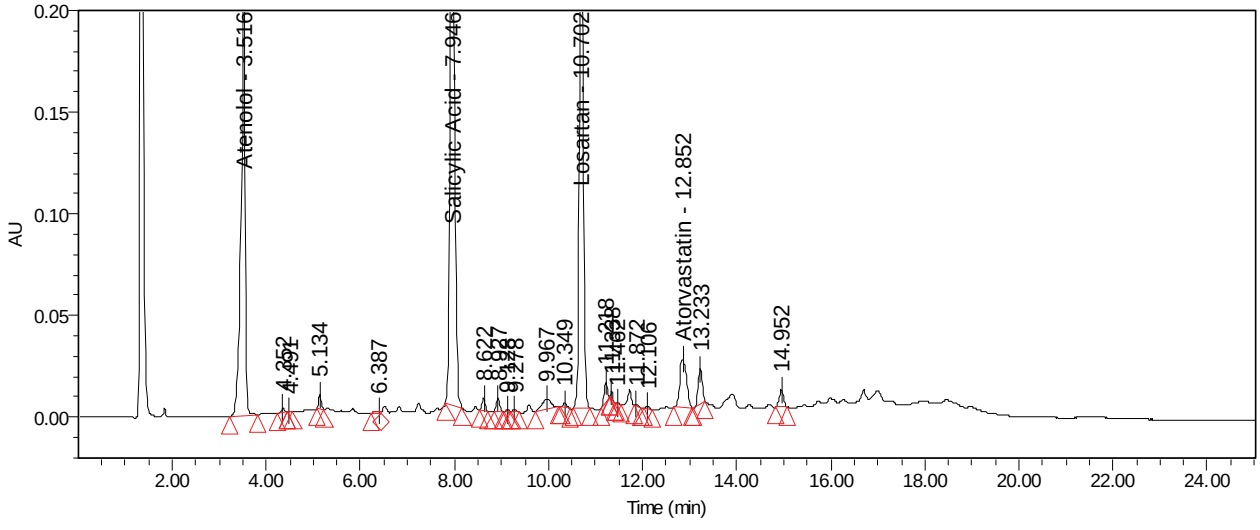

(c)

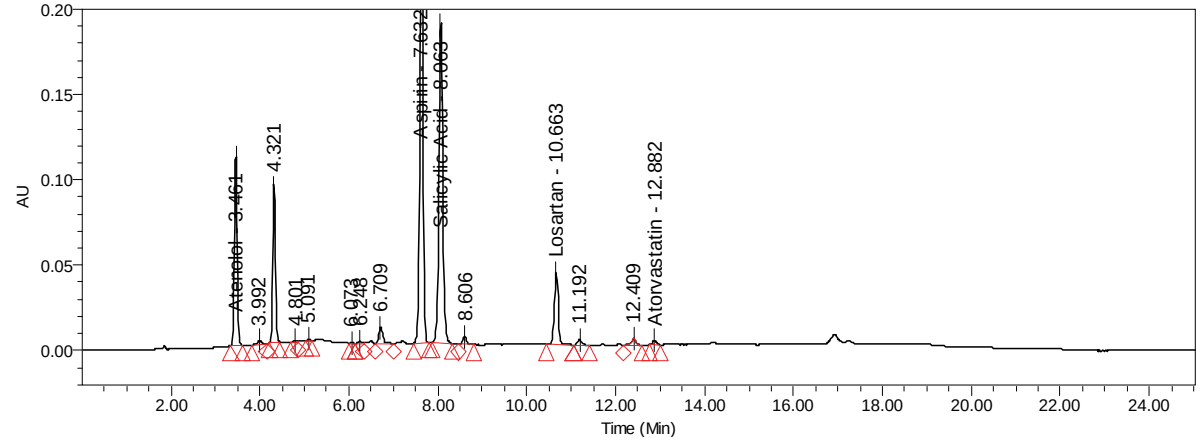

(d)

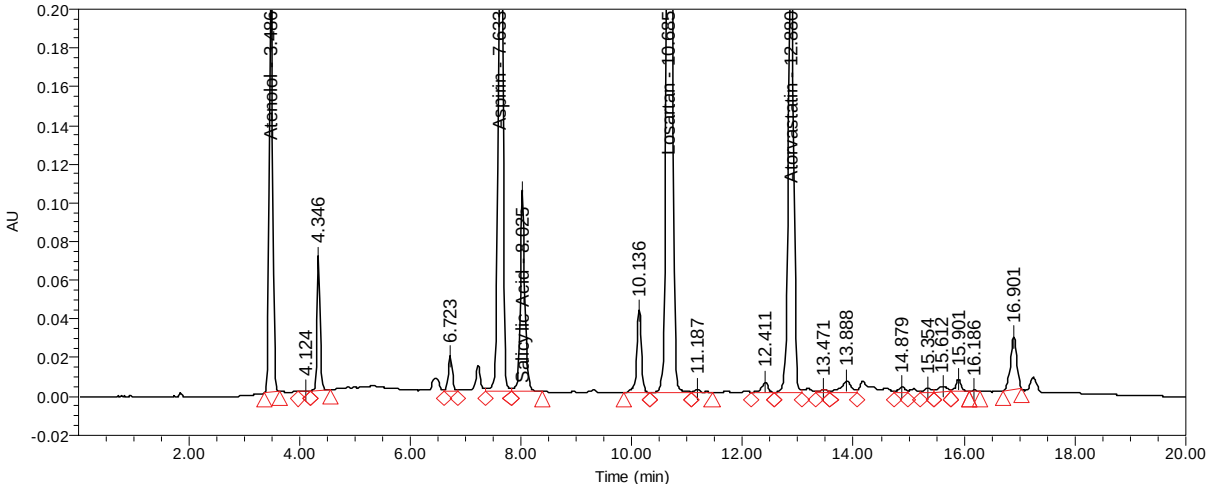

(e)

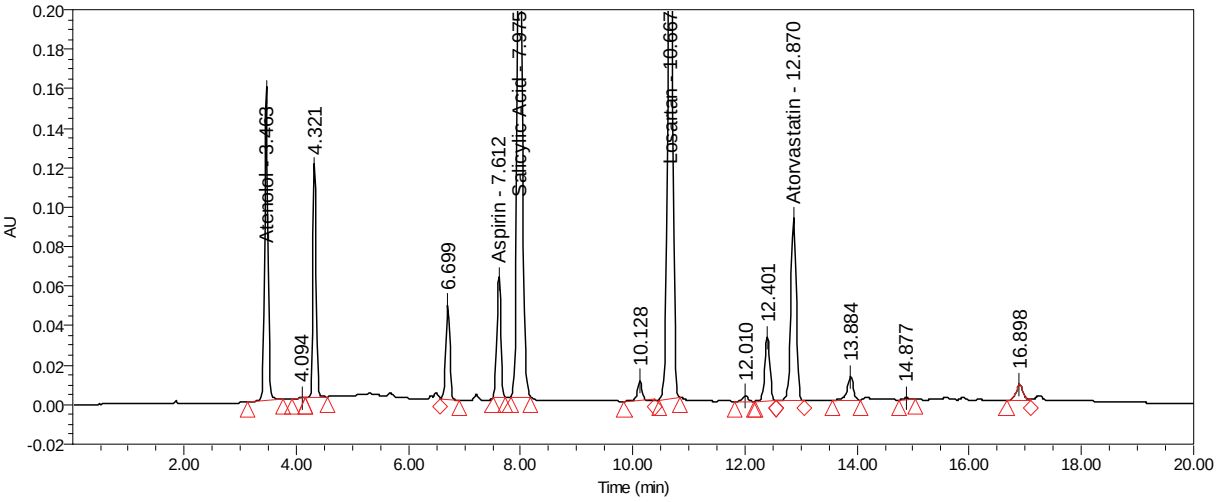

(f)

Figure 3. (a) Acid Degradation sample 0.1N HCl (1h, 100˚C); (b) Base Degradation sample: 0.1N NaOH (2h, Reflux); (c) Peroxide Dégradation sample: 5% Peroxide (48h, RT); (d) Photo stability degradation; (e) Thermal degradation: 60˚C for 8 h; (f) Accelerated 40˚C/75% RH degradation.

Table 6. Batch analysis for starpill drug product.

Batch No:	ATL (%assay)	ASP (%assay)	LST (%assay)	ATV (%assay)
STP/002	99.7	99.8	100.2	99.6
STP/005	99.6	100.3	99.4	99.8
STP/011	100.1	99.9	99.7	100.3

3.3. Application of the Method to Stability Study

Accelerated conditions stability studies are performed to establish the stability indicating nature of the method. Accelerated conditions (temperature 40 ± 2˚C, relative humidity 75 ± 5%) stored sample of the four drug combinations were analyzed by use of the developed LC method for period of 3 month both initially and after intervals of 1, 2, and 3, months .The results obtained clearly indicates that the method is able to separate all the drug-drug interaction impurities or any other degradation impurities formed during the storage conditions., indicating the method was stability-indicating and highly suitable for drug stability studies and for monitoring the quality of the Polypill.

3.4. Conclusions

The single gradient RP-LC method developed for simultaneous quantitative assay of ASP, ATV, ATL and LST in Polypill is precise, accurate and specific. The method was completely validated showing satisfactory data for all the method validation parameters tested. The developed method is stability indicating and can be used for the routine analysis of production samples and also to check the stability of Polypill tablets.

4. Acknowledgements

The authors wish to thank the management of United States Pharmacopeia laboratory-India for supporting this work.

5. References

[1] N. J. Wald and M. R. Law, "A Strategy to Reduce Cardiovascular Disease by More Than 80 Percent," *British Medical Journal*, Vol. 326, No. 7404, 2003, p. 1419.

[2] G. Sanz and V. Fuster, "Fixed-Dose Combination Therapy and Secondary Cardiovascular Prevention: Rationale, Selection of Drugs and Target Population," *Nature Clinical Practice Cardiovascular Medicine*, Vol. 6, No. 2, 2009, pp. 101-110.

[3] S. Yusuf, P. Pais, R. Afzal, *et al*., "Effects of a Polypill (Polycap) on Risk Factors in Middle-Aged Individuals without Cardiovascular Disease (TIPS): A Phase II, Double-Blind, Randomised Trial," *Lancet*, Vol. 373, No. 9672, 2009, pp. 341-351.

[4] M. R. Law and N. J. Wald, "Risk factor thresholds: their existence under scrutiny," *British Medical Journal*, Vol. 324, No. 7353, 2002, pp. 570-576.

[5] V. Kumar, R. P. Shah and S. Singh, **"**LC and LC-MS Methods for the Investigation of Polypills for the Treatment of Cardiovascular Diseases: Part.1Separation of Active Compo," *Journal of Pharmaceutical and Biomedical Analysis*, Vol. 47, 2008, pp. 508-515.

[6] V. Kumar, S. Malik and S. Singh, "Polypill for the treatment of cardiovascular diseases: Part 2. LC-MS/TOF characterization of interaction/degradation products of atenolol/lisinopril," *Journal of Pharmaceutical and Biomedical Analysis*, Vol. 48, No. 3, 2008, pp. 619-628.

[7] M. C. Koester, "An Overview of the Physiology and Pharmacology of Aspirin and Nonsteroidal Anti-Inflammatory Drugs," *Journal of Athletic Training*, Vol. 28, No. 3, 1993, pp. 252-254, 256-259.

[8] S. P. Clissold, "Aspirin and Related Derivatives of Salicylic Acid," *Drugs*, Vol. 32, Supplement 4, 1986, pp. 8-26.

[9] R. G. Bakker-Arkema, M. H. Davidson, R. J. Goldstein, "Efficacy and Safety of a New HMG-CoA Reductase Inhibitor, Atorvastatin, in Patients with Hypertriglyceridemia," *Journal of the American Medical Association*, Vol. 275, No. 2, 1996, pp. 128-133.

[10] A. N. Wadworth, D. Murdoch, R. N. Brogden, "Atenolol: A Reappraisal of its Pharmacological Properties and Therapeutic Use in Cardiovascular Disorders," *Drugs*, Vol. 42, No. 3, 1991, pp. 468-510.

[11] B. M. Psaty, T. D. Koepsell, J. P. LoGerfo, *et al*., "B-Blockers and Primary Prevention of Coronary Heart Disease in Patients with High Blood Pressure," *Journal of the American Medical Association*, Vol. 261, No. 14, 1989, pp. 2087-2094.

[12] K. L. Goa and A. J. Wag, "Losartan Potassium: A Review of its Pharmacology, Clinical Efficacy and Tolerability in the Management of Hypertension," *Drugs*, Vol. 51, No. 5, 1996, pp. 820-845.

[13] E. R. Montgomery, S. Taylor, J. Segretario, *et al*., "Development and Validation of a Reversed-Phase Liquid Chromatographic Method for Analysis of Aspirin and Warfarin in a Combination Tablet Formulation," *Journal of Pharmaceutical and Biomedical Analysis*, Vol. 15, No. 1, 1996, pp. 73-82.

[14] D. G. Sankar, M. S. M. Raju, K. Sumanth and P. V. M. Latha, "Asian HPLC Method for Estimation of Atorvastatin in Pure and Pharmaceutical Dosage Form," *Journal of Chemistry*, Vol. 17, 2005, pp. 2571-2574.

[15] S. Erturk, A. E. Sevinc, L. Ersoy and S. Ficicioglu, "HPLC Method for the Determination of Atorvastatin and its Impurities in Bulk Drug and Tablets," *Journal of Pharmaceutical and Biomedical Analysis*, Vol. 33, 2003, pp. 1017-1023.

[16] A. Puratchikody, R. Valarmathy, P. Shiju, "RP-HPLC Determination of Atorvastatin Calcium in Solid Dosage Forms," *Journal of Pharmaceutical Reviews*, 2003, pp. 79-80.

[17] B. Stanisz and L. Kania, "Validation of HPLC Method for Determination of Atorvastatin in Tablets and for Monitoring in Solid Phase," *Acta Poloniae Pharmaceutica*, Vol. 63, No. 6, 2006, pp. 471-476.

[18] G. Bahrami, B. Mohammadi, S. Mirzaeei and A. Kiani, "Determination of Atorvastatin in Human Serum by Reverse Phase High Performance Liquid Chromatography with UV Detection," *Journal of Chromatography B*: *Analytical Technologies in the Biomedical and Life Sciences*, Vol. 826, 2005, pp. 41-45.

[19] M. Jemal, Z. Ouyang, B. C. Chen and D. Teitz, "Quantitation of Atorvastatin and its Bio-Transformation Products in Human Serum by HPLC with Electro Spray Tandem Mass Spectrometry," *Rapid Communications in Mass Spectrometry*, Vol. 13, 1999, pp. 1003-1015.

[20] M. Hermann, H. Christensen and J. L. Reubsaet, "Determination of Atorvastatin and Metabolites in Human Plasma with Solid Phase Extraction Followed by LC-Tandem MS," *Analytical and Bioanalytical Chemistry*, Vol. 382, No. 5, 2005, pp. 1242-1249.

[21] S. R. Dhaneshwar, S. Yadav, A. Mhaske and S. Kadam, "HPTLC Method for Determination of Content Uniformity of Atorvastatin Calcium Tablets," *Indian Journal of Pharmaceutical Sciences*, Vol. 67, 2005, pp. 182-186.

[22] C. V. N. Prasad, C. Parihar, K. Sunil and P. Parimoo, "Simultaneous Determination of Amiloride, Hydrochlorothiazide and Atenolol in Combined Formulation by Derivative Spectroscopy," *Journal of Pharmaceutical and Biomedical Analysis*, Vol. 17, 1998, pp. 877-884.

[23] S. M. Al-Ghannam, "A Simple Spectrophotometric Method for the Determination of B-Blockers in Dosage Forms," *Journal of Pharmaceutical and Biomedical Analysis*, Vol. 40, No. 1, 2006, pp. 151-156.

[24] A. P. Agrekar and S. G. Powar, "Reverse Phase High Performance Liquid Chromatographic Determination of Ramipril and Amlodipine in Tablets," *Journal of Pharmaceutical and Biomedical Analysis*, Vol. 21, 2000, pp. 1137-1142.

[25] M. B. Shankar, F. A. Metha, K. K. Bhatt, R. S. Metha and M. Geetha, "Simultaneous Spectrophotometric Determination of Losartan Potassium and Hydrochlorothiazide in Tablets," *Indian Journal of Pharmaceutical Sciences*, Vol. 65, No. 2, 2003, pp. 167-170.

[26] C. F. Pedroso, J. G. de Oliveira, F. R. Campos, *et al*., "A Validated RP-LC Method for Simultaneous Determination of Losartan Potassium and Amlodipine Besilate in Pharmaceutical Preparations," *Chromatography*, Vol. 69, Supplement 2, pp. 201-206.

[27] D. D. Rao, N. V. Satyanarayana, S. S. Sait, Y. R. Reddy and K. Mukkanti, "Simultaneous Determination of Losartan Potassium, Atenolol and Hydrochlorothiazide in Pharmaceutical Preparations by Stability-Indicating UPLC," *Chromatography*, Vol. 70, No. 4, 2009, pp. 647-651.

[28] "ICH Stability Testing of New Drug Substances and Products Q1A (R2)," *International Conference on Harmonization*, IFPMA, Geneva, 2003.

[29] "ICH guidelines on Validation of Analytical procedures, Text and Methodology Q2 (R_1)," FDA, Published in the Federal Register 60, 1995.

[30] "United States Pharmacopoeia," 32nd Edition, United States Pharmacopeial Convention, Rockville, 2009.

[31] M. Bakshi and S. Singh, "Development of Validated Stability-Indicating Assay Methods-Critical Review," *Journal of Pharmaceutical and Biomedical Analysis*, Vol. 28, No. 6, 2002, pp. 1011-1040.

American Journal of Analytical Chemistry, **2010, 2, 70-72**
doi:10.4236/ajac.2010.12009 Published Online August 2010 (http://www.SciRP.org/journal/ajac)

A New Sesquiterpene from *Trichilia casarettii* (Meliaceae)

Ivo José Curcino Vieira[1,2]*, Elaine Rodrigues Figueiredo[2], Virginia Rodrigues Freitas[2], Leda Mathias[1], Raimundo Braz-Filho[3], Renata Mendonça Araújo[4]

[1]*Laboratório de Ciências Químicas-CCT, Universidade Estadual do Norte Fluminense Darcy Ribeiro, Campos dos Goytacazes, Brazil*

[2]*Laboratório de Tecnologia de Alimentos-CCTA, Universidade Estadual do Norte Fluminense Darcy Ribeiro, Campos dos Goytacazes, Brazil*

[3]*Universidade Estadual do Norte Fluminense Darcy Ribeiro, Campos dos Goytacazes, Brazil*

[4]*Departamento de Química-CCET, Universidade Federal do Rio Grande do Norte, Natal, Brazil*

E-mail: *curcino@uenf.br*

Received July 1, 2010; *revised July* 27, 2010; *accepted August* 2, 2010

Abstract

The dichloromethane extract of the air-dried stems of *Trichilia casarettii* afforded a new sesquiterpene (1), lupeol, stigmasterol, campesterol and sitosterol. The structure of 1 was elucidated by extensive one-and two-dimensional nuclear magnetic resonance and mass spectrometry.

Keywords: Trichilia Casarettii, *Meliaceae*, *Sesquiterpene*

1. Introduction

The Meliaceae family has attracted much interest among bioproduction phytochemists because of its very complex and diverse chemical structures and its biological activity, mainly against insects [1-3]. The *Trichilia* genus (Meliaceae) includes about 230 species distributed throughout tropical America which are recognized for their significant economic importance and high commercial value. The genus is rich in terpenoids, including triterpenes, limonoids, steroids and other terpenes derivatives [3-5].

In previous the activity of aqueous extract of leaves and twigs from *T. casarettii* was evaluated on *Spodoptera frugiperda* (J. E. Smith) development in laboratory conditions [6]. To the best of our knowledge, the literature reports no chemical investigation evaluation of *T. casarettii* native of Americas [7]. This stimulated our interest in the present work, involving isolation and structural elucidation of the constituents of the stems of this species. Then, we report the isolation of new sesquiterpene **1** (**Figure 1**) of *T. casarettii* DC. The stems also afforded lupeol, stigmasterol, campesterol, sitosterol and fatty acid esters.

The stems from *T. casarettii* DC., was collected on November 2006, at Vale do Rio Doce Cia., Linhares City, Espírito Santo State, Brazil. A voucher specimen (N° 449) was deposited at Vale do Rio Doce Cia. Herbarium.

2. Results and Discussion

Comound **1** (**Figure 1**) was obtained as white powder (MeOH), mp 121-122°C, and which is optically active with an $[\alpha]_D^{23}$ = -18.1° ($CHCl_3$, *c* 0.002). Its IR spectrum (KBr disk) obtained in spectrometer Shimadzu, model FTIR-8300, showed bands at ν_{max} 3433 (O-H stretching), 3394 (O-H stretching) cm^{-1}. Comparative analysis using spectrometer Brüker, DRX model [(operating at 400 (^{1}H) and 100 (^{13}C) MHz, respectively, in pyridine-d_5)] of the {^{1}H}- and DEPT 135°-^{13}C NMR spectra (**Table 1**) revealed signals corresponding to 15 carbon atoms. These data allowed us to recognize the presence of signals corresponding to three nonhydrogenated carbons [$(C)_3$: all sp^3 (including two bound to an oxygen atoms at δ_C 71.51 and 71.58)], two methine [$(CH)_2$: all sp^3, two α to a carbinolic carbon atom at δ_C 55.64/δ_H 1.58 and δ_C 51.14/δ_H 1.60, correlated in the HMQC spectrum with ^{1}H chemical

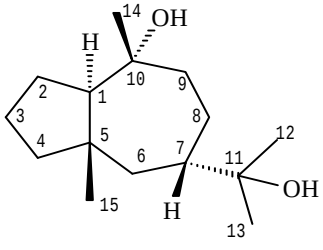

Figure 1. Chemical structure of ambrosanoli-10, 11-diol (1).

Table 1. ^{13}C (100 MHz) and ^{1}H NMR (400 MHz) data of compound 1 in pyridine-d_5, δ in ppm, J in Hz and multiplicities, in parenthesis.*

	HMQC		HMBC	
C	δ_C	δ_H	$^2J_{CH}$	$^3J_{CH}$
5	35.08	-	2H-4; 3H-15	H-7
10	71.51	-	2H-9; 3H-14	
11	71.58	-	H-7; 3H-12; 3H-13	
CH				
1	55.64	1.60-1.52 (m)		2H-9; 3H-14; 3H-15
7	51.14	1.62-1.54 (m)		3H-12; 3H-13
CH_2				
2	21.01	1.60-1.56 (m) 1.54-1.50 (m)		
3	23.47	1.85 (br s, 11.0) 1.60-1.57 (m)	2H-2; 2H-4	
4	45.77	1.44-1.40 (m) 1.14-1.12 (m)	2H-3	3H-15
6	42.08	1.38-1.36 (m) 1.10-1.02 (m)		2H-4; 3H-15
8	22.58	2.64 (br s, 12.0) 1.39-1.37 (m)		
9	44.55	1.98 (br s, 12.0) 1.75-1.78 (m)		3H-14
CH_3				
12	28.24	1.38 (s)		H-7; 3H-13
13	28.20	1.38 (s)		H-7; 3H-12
14	23.51	1.31 (s)		2H-9
15	19.56	0.93 (s)		2H-4; 2H-6

shifts, respectively], six methylene [$(CH_2)_6$, including one α to a carbinolic carbon atom at δ_C 44.55/δ_H 1.98 and 1.72] and four methyl [$(CH_3)_4$: including three linked to a carbinolic carbon atom at δ_C 28.24/δ_H 1.38, δ_C 28.20/δ_H 1.38 and δ_C 23.51/δ_H 1.31] carbon atoms, allowing us to deduce the expanded molecular formulae $(C)(C\text{-}OH)_2$ $(CH)_2$ $(CH_2)_6$ $(CH_3)_4$ = $C_{15}H_{28}O_2$ for **1**. The high-resolution electrospray ionization mass spectra (HR-ESIMS) of **1** obtained in mass spectrometer, model LCMS-IT-TOF (225- 07100-34, Shimadzu) showed a pseudomolecular ion at *m/z* 263.1988 $[M+Na]^+$, with the calculated value for $C_{15}H_{28}O_2Na$ being 263.1987. The molecular formula indicated an index of hydrogen deficiency of two. Thus, with ^{1}H and ^{13}C NMR spectral data and the compound bicyclic is compatible with the carbon skeleton sesquiterpenic of the ambrosanolide type [8].

In the ^{1}H NMR spectrum, three singlet signals were observed at δ_H 1.38 and δ_H 1.31, characteristic of a methyl groups linked to two carbinolic carbons, and one singlet signal at δ_H 0.93, corresponding to the signals at δ_C 28.24 (CH_3-12), 28.20 (CH_3-13), 23.51 (CH_3-14) and 19.56 (CH_3-15) in the ^{13}C NMR spectrum, suggesting the presence of two hydroxyl groups. The HMBC spectrum allowed us to confirm these long-range correlations (**Table 1**) through the signals corresponding to C-10 (δ_C 71.51) with the singlet observed at δ_H 1.31 (3H-14, $^2J_{CH}$) and C-11 (δ_C 71.58) with the two singlets observed at δ_H 1.38 (3H-12 and 3H-13, $^2J_{CH}$). This deduction was corroborated by the long-range correlations of methyne carbons CH-1 (δ_C 55.64) with both 3H-14 and 3H-15 (δ_H 1.31 and 0.93, $^3J_{CH}$) and CH-7 (δ_C 51.14) with both 3H-12 and 3H-13 (δ_H 1.38, $^3J_{CH}$) observed in the HMBC spectrum (**Table 1**). Thus, these data allowed us to recognize the presence of hydroxyl groups at C-10 (δ_C 71.51) and C-11 (δ_C 71.58).

The relative stereochemistry of **1** was determined from the spatial dipolar interaction revealed by the ^{1}H-^{1}H-NOESY spectrum, summarized in **Figure 2**. The ^{1}H-^{1}H-NOESY spectrum of **1** allowed characterization of the ring-junction (CH-1 with C-5) of the bicyclic system involving the seven and five-rings as *trans*. The relative stereochemistry indicated in **1** was deduced by the spatial dipolar interaction observed in the ^{1}H-^{1}H-NOESY spectrum between hydrogen atom H-7 with H_3-14 and H_3-15 indicating that both are β-oriented. The spatial dipolar interaction observed between H-1 and H-6b and absence of spatial interaction between H-1 with both, H_3-14 and H_3-15, respectively, indicating that H-1 was α-oriented in agreement with a *trans* ring-junction.

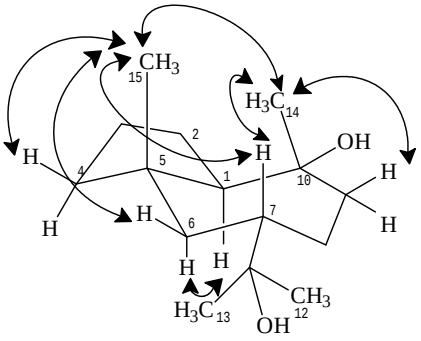

Figure 2. Selected NOESY correlations and relative stereochemistry for compound 1. Arrows denote the main NOESY correlations.

Additional spatial interaction is shown in **Figure 2**. Therefore, the structure of the new sesquiterpene (**Figure 1**) isolated from *T. casarettii* was defined as ambrosanoli-10,11-diol (**1**) (30 mg, 0.0433%).

The structures of lupeol [9], β-sitosterol [10] and stigmasterol [10] were deduced by comparison of their ^{1}H and ^{13}C NMR spectral data with those reported in the literature.

3. Acknowledgements

The authors are grateful to Fundação de Amparo à Pesquisa do Estado do Rio de Janeiro (FAPERJ) for grants and to Conselho Nacional de Desenvolvimento Científico (CNPq-Brazil) for a research fellowship and grants.

4. References

[1] Y. S. Xie, M. B. Isman, P. Gunning, S. Mackinnon, J. T. Arnason, D. R. Taylor, P. Sánchez, C. Hasbun and G. H. N. Towers, "Biological Activity of Extracts of *Trichilia* Species and the Limonoid Hirtin against Lepidopteran Larvae," *Biochemical Systematics and Ecology*, Vol. 22, No. 2, March 1994, pp. 129-136.

[2] T. D. Pennington and B. D. Styles, "A Generic Monograph of Meliaceae," *Blumea*, Vol. 22, No. 3, August-December 1975, pp. 419-540.

[3] M. T. Pupo, P. C. Vieira, J. B. Fernandes, M. F. G. F. Silva and J. R. Pirani, "Terpenoids and Steroids from *Trichilia* Species," *Journal of the Brazilian Chemical Society*, Vol. 13, No. 3, June 2002, pp. 382-388.

[4] M. C. Ramírez, R. A. Toscano, J. Arnason, S. Omar, C. M. Cerda-Garcia-Rojas and R. Mata, "Structure, Conformation and Absolute Configuration of New Antifeedant Dolabellanes from *Trichilia trifolia*," *Tetrahedron*, Vol. 56, No. 29, July 2000, pp. 5085-5091.

[5] D. A. G. Cortez, J. B. Fernandes, P. C. Vieira, M. F. G. F. Silva, A. G. Ferreira, Q. B. Cass and J. R. Pirani, "Meliacin Butenolides from *Trichilia estipulata*," *Phytochemistry*, Vol. 49, No. 8, December 1998, pp. 2493-2496.

[6] P. C. Bogorni and J. D. Vendramim, "Sublethal Effect of Aqueous Extracts of *Trichilia* spp. on *Spodoptera frugiperda* (J. E. Smith) (Lepidoptera: Noctuidae) Development on Maize," *Neotropical Entomolology*, Vol. 34, No. 2, March/April 2005, pp. 311-317.

[7] P. C. Patrício and A. C. Cervi, "O Gênero *Trichilia* P. Browne (Meliaceae) no estado do Paraná, Brasil," *Acta Biologica Paranaense*, Vol. 34, No. 1-4, January/April 2005, pp. 27-71.

[8] A. U. Rahman and V. U. Ahmad, "^{13}C-NMR of Natural Products: Monoterpenes and Sesquiterpenes," Hussain Ebrahim Jamal Research Institute of Chemistry, University of Karachi, Pakistan, Vol. 1, 1992.

[9] V. U. Ahmad and A. U. Rahman, "Handbook of Natural Products Data, Pentacyclic Triterpenoids," Elsevier Press, Karachi, Vol. 2, 1994.

[10] N. P. Rai, B. B. Adhikari, A. Paudel, K. Masuda, R. D. Mckelvey and M. D. Madandhar, "Phytochemical Constituents of the Flowers of *Sarcococca coriacea* of Nepalese Origin," *Journal of Nepal Chemical Society*, Vol. 21, 2006, pp. 1-7.

American Journal of Analytical Chemistry, **2010, 2, 73-82**
doi:10.4236/ajac.2010.12010 Published Online August 2010 (http://www.SciRP.org/journal/ajac)

Scientific Research

Application of H-Point Standard Addition Method and Multivariate Calibration Methods to the Simultaneous Kinetic-Potentiometric Determination of Cerium(IV) and Dichoromate

Mohammad Ali Karimi[1,2]*, Mohammad Hossein Mashhadizadeh[3], Mohammad Mazloum-Ardakani[4], Fatemeh Rahavian[2]
[1]*Department of Chemistry & Nanoscience and Nanotechnology Research Laboratory* (*NNRL*), *Faculty of Sciences, Payame Noor University* (*PNU*), *Sirjan, Iran*
[2]*Department of Chemistry, Faculty of Sciences, Payame Noor University* (*PNU*), *Ardakan, Iran*
[3]*Department of Chemistry, Tarbiat Moallem University of Tehran, Tehran, Iran*
[4]*Department of Chemistry, Faculty of Sciences, Yazd University, Yazd, Iran*
E-mail: *ma_karimi43@yahoo.com & m_karimi@pnu.ac.ir*
Received June 27, 2010; *revised July* 20, 2010; *accepted July* 26, 2010

Abstract

A kinetic-potentiometric method for simultaneous determination of Cerium(IV) and dichoromate ($Cr_2O_7^{2-}$) by H-point standard addition method (HPSAM), partial least squares (PLS) and principal component regression (PCR) using fluoride ion-selective electrode (FISE) is described. In this work, the difference between the rate of the oxidation reaction of Fe(II) to Fe(III) in the presence of Ce^{4+} and $Cr_2O_7^{2-}$ is based of the method. The rate of consume fluoride ion for making complex is detected with a FISE. The results show that simultaneous determination of Ce^{4+} and $Cr_2O_7^{2-}$ can be done in their concentration ranges of 1.0-30.0 and 0.1-20.0 μg/mL, respectively. The total relative standard error for applying the PLS and PCR methods on 8 synthetic samples was 2.97 and 3.19, respectively in the concentration ranges of 1.0-30.0 μg/mL of Ce^{4+} and 0.1-20.0 μg/mL of $Cr_2O_7^{2-}$. In order for the selectivity of the method to be assessed, we evaluated the effects of certain foreign ions upon the reaction rate and assessed the selectivity of the method. The proposed methods (HPSAM, PLS and PCR) were evaluated using a set of synthetic sample mixtures and then applied for simultaneous determination of Ce^{4+} and $Cr_2O_7^{2-}$ in different water samples.

Keywords: Multivariate Calibration, HPSAM, Simultaneous Kintic-Potentiometry, Dichromate, Cerium(IV)

1. Introduction

Dichromate ($Cr_2O_7^{2-}$) and cerium(IV) are strong oxidants in chemistry that are used widely as oxidizing agent in diverse chemical reactions in the laboratory and industry for the synthesis of many different kinds of chemical compounds. Dichromate is used as a common inorganic chemical reagent, most commonly used as an oxidising agent in various laboratory and industrial applications [1,2]. It also used to oxidize alcohols, determination ethanol, cleaning laboratory glassware of organic contaminants [3]. Cerium(IV) is also a common inorganic chemical reagent and industrially important and is used in nuclear reactors, alloys with nickel and chromium, microwave devices, lasers, agriculture and miscellaneous [4-6]. In analytical chemistry, standardized aqueous solutions of $Cr_2O_7^{2-}$ and Ce^{4+} are sometimes used as oxidizing titrants for redox titrations. Therefore, determination of these oxidants is very important. Several methods have been reported for the determination of them such as spectrophotometry [7,8], spectrofluorometry [9] and electroanalytical techniques [10,11]. In relation to the simultaneous analysis of $Cr_2O_7^{2-}$ and Ce^{4+}, Masin et al. have been reported a titrimetric method for the simultaneous determination of Ce^{4+}, MnO_4^- and $Cr_2O_7^{2-}$ using phosphate ion as precipitant of Ce^{4+} and Fe^{2+} as titrant [12]. To the best our knowledge, there is not any report for simultaneous determination of $Cr_2O_7^{2-}$ and Ce^{4+} using HPSAM and chemometrics methods.

In recent years the usage of chemometrics methods in electroanalytical chemistry, as in other areas of analytical chemistry, has received considerable attention as these methods can help us with extraction of more information from experimental data. Applications of HPSAM and chemometrics methods have been frequently reported for the calibration of overlapped voltammetric signals [13-16]. In the field of potentiometry, several methods have been reported based on flow injection system and titration using PLS, ANN and Kalman filter as modeling methods [17-21]. We are reported the first application of PLS and PCR multivariate calibration methods and HPSAM to the simultaneous kinetic-potentiometric determination of binary mixtures of hydrazine and its derivatives [22,23] and binary mixture of levodopa and carbidopa drugs [24]. The methods were based on the differences observed in the production rate of chloride ions in reaction of these species with *N*-chlorosuccinimide. The reaction rate of production of chloride ion was monitored by a chloride ion-selective electrode. Recently, we also reported the application of HPSAM, PLS and PCR methods for the simultaneous determination of binary mixtures of Fe(III) and Al(III) and ternary mixtures of Fe(III), Al(III) and Zr(IV) [25,26]. This method was based on the complex forming reaction of these metallic ions with fluoride ion that has a differential rate at certain reaction conditions. Therefore, the rate of fluoride-ion reaction with Fe(III), Al(III) and Zr(IV) was monitored by an fluoride ion-selective electrode (FISE).

This paper reports the first application of HPSAM, PCR and PLS to the simultaneous determination of oxidants binary mixtures such as $Cr_2O_7^{2-}$ and Ce^{4+} using potentiometric technique. The methods are based on the difference observed in the oxidation reaction rate of Fe(II) to Fe(III) in the presence of Ce^{4+} and $Cr_2O_7^{2-}$ as oxidants and complexing reaction between Fe(III) with fluoride ion at certain reaction conditions. The very fast response of the fluoride ion selective electrode (FISE) and its Nernstian behavior with respect to fluoride ions in acidic solutions indicated that this electrode might be employed effectively in kinetic studies of reactions involving changes in the fluoride ion concentration [25,26]. Therefore, rate of the complexing reaction of fluoride ion with Fe(III) was monitored by a FISE.

2. Experimental

2.1. Apparatus and Software

A solid-state Fluoride-selective electrode (Metrohm Model 6.0502.150) was used in conjunction with a double junction Ag/AgCl reference electrode (Metrohm Model 6.0726.100), whose outer compartment was filled with a saturated KCl solution. The Metrohm Model 780 potentiometer, attached to a Pentium (IV) computer, was used for recording the kinetic potentiometric data. All measurements were carried out in a thermostated (25.0 ± 0.2˚C), double-walled reaction cell with continuous magnetic stirring. The electrode was stored in 1×10^{-3} mol/L potassium fluoride solution when not in use. For pH measurements, a Metrohm Model 780 pH meter with a combination glass electrode was used. PLS and PCR analyses was performed using a MATLAB 7.0 software.

2.2. Materials and Reagents

All chemicals were of analytical reagent grade and doubly distilled water was used throughout. A stock solution of iron (1000 μg mL^{-1}) was prepared by dissolving 0.524 g of iron (II) sulfate ($FeSO_4 \cdot 7H_2O$) in water and diluted to 100 mL. Stock solutions $Ce^{4+}$and $Cr_2O_7^{2-}$ were prepared in 100-mL flasks by dissolving 0.2885 g of cerium sulfate tetrahydrate and 0.1369 g of potassium dichromate in water and diluting with water to the mark. Cerium(IV) sulfate and potassium dichromate and salts of Fe(II) and fluoride were purchased from Merck (Germany). Acetate buffer solution (0.05 mol/L, pH 3.0) was prepared using acetic acid and NaOH solutions and adjusting its pH with a pH meter.

2.3. Procedure

Twenty five milliliters of double distilled water, 2.0 mL of buffer solution, 1.0 mL of standard fluoride solution (0.1 mol/L) and 1.0 mL of 5×10^{-3} mol/L of iron (II) solution were added to the thermostated (25.0 ± 0.2˚C) reaction cell. Five milliliter of the standard or sample solution of $Cr_2O_7^{2-}$, Ce^{4+} or a mixture of them were injected into the cell quickly, and after the stabilization of the potential (about 30 s), all data were recorded. The potential changes versus time were recorded at the time intervals of 1.0 s. Synthetic samples containing different concentration ratios of $Cr_2O_7^{2-}$ and Ce^{4+} were prepared and standard additions of $Cr_2O_7^{2-}$ were made. Simultaneous determination of $Cr_2O_7^{2-}$ and Ce^{4+} was conducted by recording the potential changes for each solution from 10 to 500 s. After each run the cell was emptied and washed twice with doubly distilled water.

Using the standard analyte solutions, we can construct a calibration graph of ($10^{\Delta E/S}$-1) *versus* concentration (fixed-time method) [22-27], where ΔE is the potential variation in a selected time interval Δt and S is the slope of the fluoride electrode response, which is determined periodically by successive additions of micro-amounts of 100 μL of 1.0×10^{-5} -1.0 mol/L of NaF standard solutions in 25 mL of water mixed with 2 mL of buffer solution.

The simultaneous determination of $Cr_2O_7^{2-}$ and Ce^{4+} standard solutions with HPSAM was performed by measuring the potential changes (ΔE) at 60 and 80 s after

initiation of the reaction for each sample solution. Then plots of HPSAM of ($10^{\Delta E/S}$-1) *versus* added concentration of Ce^{4+} were constructed for mixtures of $Cr_2O_7^{2-}$ and Ce^{4+}. Simultaneous determination of $Cr_2O_7^{2-}$ and Ce^{4+} with PLS and PCR methods was performed by recording the potential for each solution from 10 to 500 s.

3. Results and Discussion

It is require finding the system that shows different kinetic behavior for the reaction with $Cr_2O_7^{2-}$ and Ce^{4+}. It is well-known that the rate of oxidation of Fe^{2+} with $Cr_2O_7^{2-}$ is much higher than that with Ce^{4+} [12]. Therefore, we could use from this different kinetic behavior for simultaneous determination of $Cr_2O_7^{2-}$ and Ce^{4+}. The concept for the simultaneous analysis of $Cr_2O_7^{2-}$ and Ce^{4+} in this work is based on the difference in their oxidizing power. Preliminary studies showed that iron(II) ion as reagent at presence of fluoride ion using FISE is suitable for our purpose. Upon the addition of the oxidant (Ce^{4+} and $Cr_2O_7^{2-}$) into solution of Fe^{2+} in the presence of F^-, the oxidation reaction of Fe^{2+} by Ce^{4+} and $Cr_2O_7^{2-}$ take place as follows:

$$Ce^{4+} + Fe^{2+} + 2\ F^- \rightarrow [FeF_2]^+ + Ce^{4+} \quad (1)$$

$$Cr_2O_7^{2-} + 2\ Fe^{2+} + 4\ F^- + 14\ H^+ \rightarrow 2\ [FeF_2]^{3+} + 2\ Cr^{3+} + 7\ H_2O \quad (2)$$

When using this ions and FISE for monitoring difference in the reaction rate, the linear range and differences of reaction rate for both two species ($Cr_2O_7^{2-}$ and Ce^{4+}) were suitable. In order to simultaneous kinetic potentiometric determination of $Cr_2O_7^{2-}$ and Ce^{4+} by HPSAM, PCR and PLS a series of experiments were conducted to establish the optimum system to achieve maximum sensitivity. Therefore, all experimental parameters affecting the reaction rate of Fe^{2+} with Ce^{4+} and $Cr_2O_7^{2-}$ (response time, concentration of F^- and Fe^{2+}, pH, etc) were carefully optimized.

3.1. Study of the Electrode Characteristics

The very fast response of FISE and its Nernstian behavior toward fluoride ions in acidic solutions indicates that this electrode might be employed effectively in the kinetic studies of reactions involving changes in the fluoride ion concentration [25,26]. The characteristics of the fluoride-selective electrode in the HNO_3-H_3BO_3-NaOH buffer were studied. In order to evaluate the operating characteristics of the FISE at pH < 5, calibration graphs were constructed for sodium fluoride in the concentration range of 1.0×10^{-5}-1.0×10^{-1} mol/L at pHs 4.0, 3.0, 2.5 and 2.0. The slope was found to be 56.9 mV/decade and remained almost constant to 0.2 mV over 6 months of usage in this system at pH 3.0.

3.2. Effect of Fluoride Concentration

The effect of F^- concentration over the ranges of 1.0×10^{-5}-1.0×10^{-1} mol/L fluoride ion on the linear range of calibration graph and reaction rate with Fe(II) was investigated (**Figure 1**). The results also indicate that the concentration of F^- has a great effect on the linear range and the change potential value. When the concentration of F^- is low, a gradual slope in the calibration graph is realized while a high concentration of F^- produces is high a steep slope in the calibration graph. So the fluoride concentration must be in excess, but by increasing the fluoride concentration, the potential change is decreased and the sensitivity is lower. Since, maximum differences in kinetic behaviour of Fe(III) (resulted from oxidation reaction of Fe^{2+} to Fe^{3+} by Ce^{4+} and $Cr_2O_7^{2-}$) and was observed in concentration of 1.0×10^{-3} mol L^{-1} fluoride and both species also had larger values of potential change (ΔE) in this concentration. Therefore, a concentration of 1.0×10^{-3} mol/L fluoride was selected as the optimum concentration for further studies.

3.3. Effect of Fe^{2+} Concentration

The effect of Fe^{2+} concentration over the ranges of 1.0×10^{-5}-1.0×10^{-1} mol/L Fe^{2+} ion on the reaction rate of Fe^{2+} with Ce^{4+} and $Cr_2O_7^{2-}$ and linear range of calibration graph was investigated (**Figure 2**). The results have shown that the increase of Fe^{2+} concentration, up to 5.0×10^{-3} mol/L, causes an increase in the reaction rate of Fe^{2+} with both Ce^{4+} and $Cr_2O_7^{2-}$ and the potential change, but decreased at higher concentrations. There- fore, a concentration of 5.0×10^{-3} mol/L Fe^{2+} ion was selected as the optimum concentration for further studies.

3.4. Effect of pH

Acidity of the solution influences potential response of

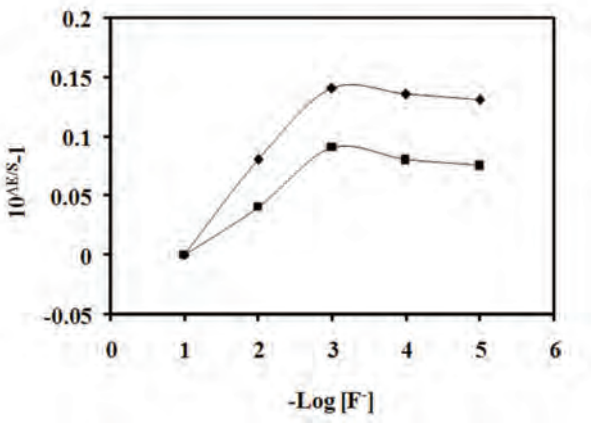

Figure 1. Effect of F^- concentration on the reaction of F^- and Fe^{2+} with 5.0 µg/mL of Ce^{4+} (■) and 10.0 µg/mL of $Cr_2O_7^{2-}$ (♦). Conditions: 5×10^{-3} M Fe^{2+}, pH 3.0, 25 °C.

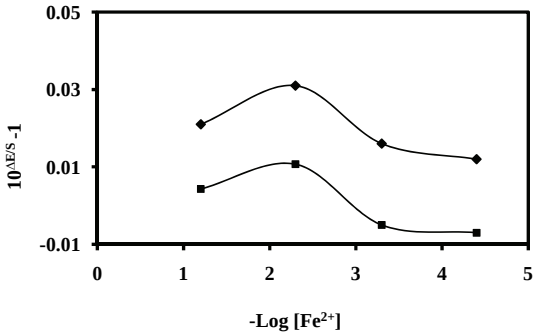

Figure 2. Effect of Fe^{2+} concentration on the reaction of F^- and Fe^{2+} with 5.0 µg/mL of Ce^{4+} (■) and 10.0 µg/mL of $Cr_2O_7^{2-}$ (♦). Conditions: 1×10^{-3} M F^-, pH 3.0, 25 °C.

FISE, the oxidation reaction rate of Fe^{2+} with Ce^{4+} and $Cr_2O_7^{2-}$ and complextion reaction rate of F^- with Fe^{3+}. The results show that maximum difference in kinetic behavior of Fe^{3+} was observed at pH 3.0 (**Figure 3**). In addition, Fe^{3+} had larger values of potential change (ΔE) in this pH. Above pH 3.0, the potential change decreased evidently due to the occurrence of the hydrolysis reaction competing with the complexation between fluoride and Fe^{3+}, and under pH 3.0, the potential change decreased too, probably owing to the formation of hydrogen fluoride, to which the fluoride electrode is insensitive. Thus, pH of 3.0 was selected as the optimum pH for further studies.

3.5. Composition Effect of Ground Buffer Solution

The change of potential value ($\triangle E$) for reaction of Fe^{2+} with Ce^{4+} and $Cr_2O_7^{2-}$ in the presence of certain amount fluoride ion in different acidic solutions was investigated (**Table 1**). The results have shown that in the solution of HNO_3–H_3BO_3 (pH 3.0), $\triangle E_{Fe^{3+}}$ has larger values. According to obtained results, the 0.1 mol L^{-1} boric acid-0.1 mol/L nitric acid- mixed solution (pH 3.0) containing 1.0×10^{-3} mol/L fluoride was chosen as the ground buffer solutions.

3.6. Temperature Effect of Reaction Rate

The temperature of solution evidently affects the reaction rate of the kinetic reaction. But higher temperatures do not have a positive effect on the reaction of Fe^{2+} with Ce^{4+} and $Cr_2O_7^{2-}$ and complexing reaction of Fe^{3+} with fluoride. Therefore, the temperature of solution was kept at 25 ± 0.2˚C by thermostatic water bath in all of the measurements.

3.7. Potential-Time Behavior

The potential-time behavior of reactions of Fe^{2+} with Ce^{4+} and $Cr_2O_7^{2-}$ in the presence of F^- under the optimized conditions is shown in **Figure 1**. **Figure 2** shows typical reaction curves for the reaction of Fe^{2+} with Ce^{4+} and $Cr_2O_7^{2-}$ at different concentrations. As can be seen in **Figures 4** and **5**, the reaction of $Cr_2O_7^{2-}$ is faster Ce^{4+} and was almost completed in 60 s after initial reaction but the reaction of Ce^{4+} was completed almost in 500 s. This difference in the reaction rates allowed us to design the HPSAM, PCR and PLS methods for simultaneous determination of Ce^{4+} and $Cr_2O_7^{2-}$. Characteristics of calibration graphs for the determination of Ce^{4+} and $Cr_2O_7^{2-}$, under the optimum conditions, are also given in **Table 2**. Therefore, above difference mentioned in the reaction rates allowed us to design the HPSAM, PCR and PLS a method for simultaneous determination of Ce^{4+} and $Cr_2O_7^{2-}$, in the concentration ranges of 1.0-30.0 and 0.1-20.0 µg/mL, respectively.

3.8. Requirements for Applying HPSAM

The basis of using HPSAM for treating kinetic data under the conditions that the reaction of one component is

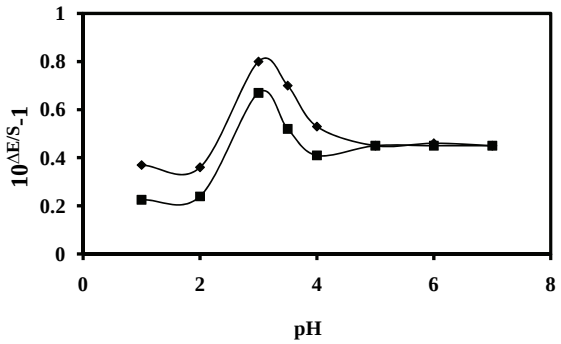

Figure 3. Effect of pH on the reaction of F^- and Fe^{2+} with 5.0 µg/mL of Ce^{4+} (■) and 10.0 µg/mL of $Cr_2O_7^{2-}$ (♦). Conditions: 1×10^{-3} M F^-, 5×10^{-3} M Fe^{2+}, 25 °C.

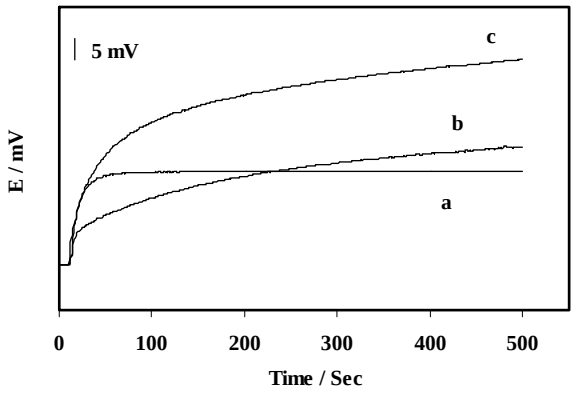

Figure 4. Potential-time curves for the reaction of F^- and Fe^{2+} with 10.0 µg/mL of $Cr_2O_7^{2-}$(a), 5.0 µg/mL of Ce^{4+} (b) and mixture of them (c).

Table 1. The values of ΔE for reaction of 10 µg/mL of Fe^{2+} with Ce(IV) and $Cr_2O_7^{2-}$ in the presence of 1.0×10^{-3} M F^- ion in different acid solutions (pH = 3.0).

Acid solution	H_3PO_4-H_3BO_3	KCl-HCl	HNO_3-CH_3COOH	HNO_3-H_3BO_3
ΔE_{Fe}^{3+} (for $Cr_2O_7^{2-}$)/mv	2.3	7.5	8.5	13.0
ΔE_{Fe}^{3+} (for Ce^{4+}/mv	1.8	5.5	6.7	10.4

Table 2. Characteristics of calibration graphs for the determination of Ce^{4+} and $Cr_2O_7^{2-}$.

Species	Linear range	Slope	Intercept	Correlation coefficient	Detection limit[(a)]
	(µg/mL)	(mL/µg)			(µg/mL)
Ce^{4+}	1.0-30.0	0.0681	0.0177	0.9995 (n = 10)	0.450
$Cr_2O_7^{2-}$	0.1-20.0	0.1119	0.2975	0.9994 (n = 10)	0.086

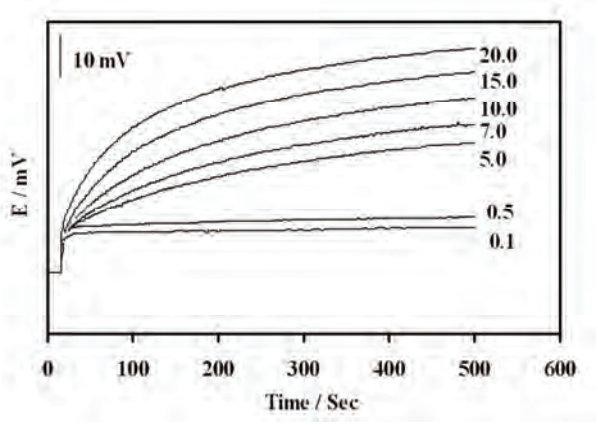

(a)

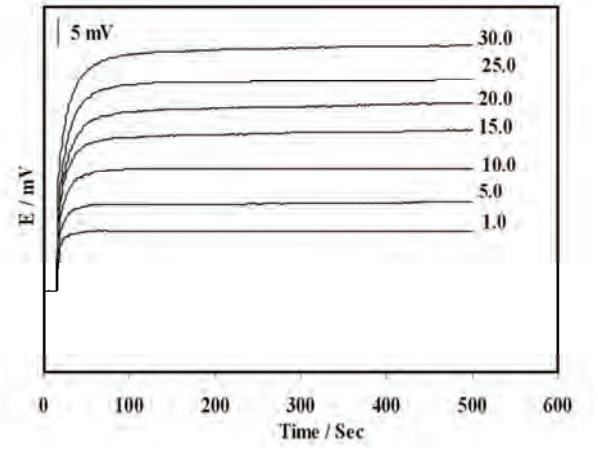

(b)

Figure 5. Typical potential-time curves for the reaction of F^- and Fe^{+2} with Ce^{4+}(a) and $Cr_2O_7^{2-}$ (b) at different concentrations (µg/mL).

completed, while that of other component is not completed yet, is described below. In this case, the vari- ables to be fixed were the time variables t_1 and t_2, at which the product of the reaction of Ce^{4+} had the same amount of ($10^{\Delta E/S}$-1) over the range between these two times, and also there is an appropriate difference between the slopes of the calibration lines.

Considering a binary mixture of Ce^{4+} and $Cr_2O_7^{2-}$, for example, assume that the amount of R ($10^{\Delta E/S}$-1) of the oxidation in the reaction of Fe^{2+} with Ce^{4+} and then complexation in the reaction of Fe^{3+} with F^- at time variables t_1 and t_2 are P_i and Q_i, respectively, while those for the $Cr_2O_7^{2-}$-Fe^{2+}-F^- reaction under the same conditions are P and Q, respectively (**Figure 6**). They are equal in this case.

The following equations show the relation between them:

For Ce^{4+}: $Q_i = P_i + m_i t_j$ ($t_1 \le t_j \le t_2$; $i = 0,1,\ldots, n$) (1)

For $Cr_2O_7^{2-}$: $Q = P + mt_j$ ($m = 0$) (2)

where subscripts i and j denote different solutions for n additions of Ce^{4+} concentration prepared to apply to HPSAM and the time comprising the t_1-t_2 range, respectively.

Thus, the overall amounts of ($10^{\Delta E/S}$-1) (or R) of the Ce^{4+}-$Cr_2O_7^{2-}$ mixture are:

At t_1 $Rt_1 = P + P_i$ (3)

At t_2 $Rt_2 = Q + Q_i$ (4)

Simultaneous kinetic determination of concentration of Ce^{4+} and $Cr_2O_7^{2-}$ by HPSAM requires the selection of two times t_1 and t_2. To select the appropriate times, the following principles were observed. At the two selected times t_1 and t_2, the amount of R of the Ce^{4+} must be linear with the concentrations, and the amount of R for Fe^{3+} must remain constant even if the $Cr_2O_7^{2-}$ concentrations are changed. The amount of R for the mixture of Ce^{4+} and $Cr_2O_7^{2-}$ should be equal to the sum of individual Rs of the two compounds. In addition, the slope difference of the two straight lines obtained at both t_1 and t_2 must be

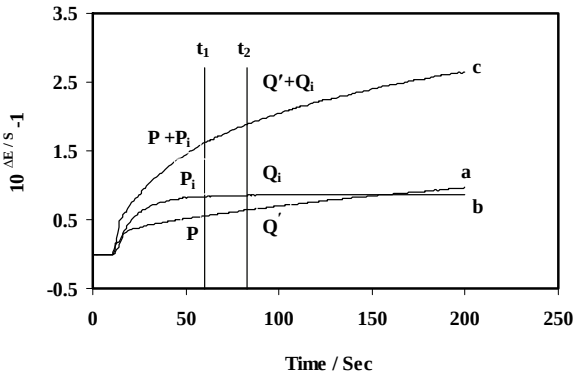

Figure 6. Plot of potential changes ($10^{\Delta E/S}$-1) for the reaction of F^- and Fe^{2+} with 10.0 µg/mL of Ce^{4+} (a), 5.0 µg/mL of $Cr_2O_7^{2-}$ (b) and mixture of them (c).

as large as possible to achieve good accuracy. Then known amounts of Ce^{4+} are successively added to the mixture and resulting potential changes are measured at the two times and expressed:

$$R_{t1} = (10^{\Delta E(t1)/S}\text{-}1)_{t1} = P_0 + P + M_{t1}C_i \quad (5)$$

$$R_{t2} = (10^{\Delta E(t2)/S}\text{-}1)_{t2} = Q_0 + Q + M_{t2}C_i \quad (6)$$

where $\Delta E(t_1)$ and $\Delta E(t_2)$ are the potential changes measured at t_1 and t_2, respectively. P_0 and Q_0 are the amounts of R for Ce^{4+} at a sample at t_1 and t_2, respectively. P and Q are the amounts of R for $Cr_2O_7^{2-}$ at t_1 and t_2, respectively (**Figure 7**).

M_{t1} and M_{t2} are the slopes of the standard addition calibration lines at t_1 and t_2, respectively. C_i is the added Ce^{4+} concentration. The two obtained straight lines intersect at the so-called H-point ($-C_H$, R_H), which at point H (**Figure 7**), since $R_{t1} = R_{t2}$, $H(-C_H, R_H) \approx (-C_{\text{Ceric}}, R_{Dichromate})$ from Equations (1) and (2) we have:

$$P_0 + P + M_{t1}(-C_H) = Q_0 + Q + M_{t2}(-C_H) \quad (7)$$

$$-C_H = [(Q - P) + (Q_0 - P_0)]/(M_{t1} - M_{t2}) \quad (8)$$

as species $Cr_2O_7^{2-}$ is assumed not to evolve over the considered range of time,

$$Q = P$$

and

$$C_H = (Q_0 - P_0)/(M_{t1} - M_{t2}) \quad (9)$$

which is equivalent to the existing C_{Ceric} ($=P_0/M_{t1} = Q_0/M_{t2}$). Combining this with Equation (5) yields $R_H = P$. The overall equation for the potential at the H-point is simply represented as:

$$Q = P = R_H = R_{Fe} \quad (10)$$

The intersection of the straight lines (Equations (5) and (6) directly yields the unknown Ce^{4+} concentration (C_{Ceric}) and the R for $Cr_2O_7^{2-}$ species ($R_{Dichromate}$) corresponding to t_1 and t_2 in the original samples, as the two times were chosen in such a way that the later species had the same R at both times. This analytical signal enables us to calculate the concentration of $Cr_2O_7^{2-}$ from a calibration curve.

Since Ce^{4+} is selected as the analyte, it is possible to select several pairs of time ranges which present the same R for $Cr_2O_7^{2-}$. Some of the selected time pairs were 60-80, 80-110, 150-200, 250-300 and 350-420 s. Greater time increments caused higher sensitivity and steeper slopes of the two time axes, as shown previously by Campins-Falco *et al.* [29]. Also, the accuracy of determinations was affected by the slope increments of H-point plots. However, the time pair that gives the greatest slope increment, lower error, and shortest analysis time was selected. For this reason, the time pair of 60-80 s as the most suitable times was employed.

A summary of the results obtained for various analyte concentrations is given in **Tables 3** and **4**. The concentration was calculated directly by solving a system of equations of two straight lines. $Cr_2O_7^{2-}$ concentrations were calculated in each test solution by the calibration method with a single standard and ordinate value of R.

3.9. Multivariate Calibration

Multivariate calibration consists of establishment of a relationship between matrices of chemical data. These methods are based on a first calibration step in which a mathematical model is built using a chemical data set

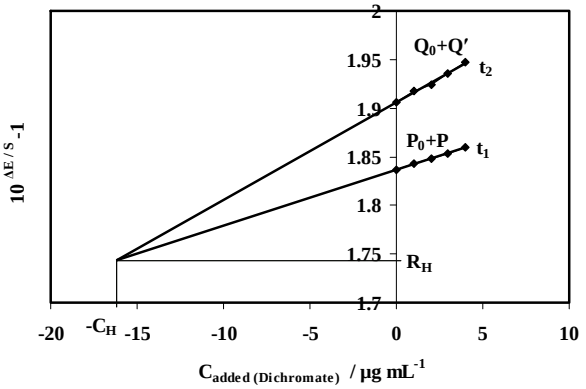

Figure 7. Plot of HPSAM for simultaneous determination of a mixture of $Cr_2O_7^{2-}$ (15 µg/mL) and Ce^{4+} (25 µg/mL).

Table 3. Results of several experiments for analysis of Ce^{4+} and $Cr_2O_7^{2-}$ mixtures in different concentration ratios using HPSAM (T = 25˚C).

R-C equation	r	Spiked (µg/mL)		Found (µg/mL)	
		Ce^{4+}	$Cr_2O_7^{2-}$	Ce^{4+}	$Cr_2O_7^{2-}$
$R_{80} = 0.0322C_i + 0.4665$	0.9994	5.0	2.0	4.90 ± 0.10	2.12 ± 0.08
$R_{60} = 0.0509C_i + 0.5069$	0.9990				
$R_{80} = 0.0209C_i + 0.3056$	0.9990	3.0	3.0	3.14 ± 0.11	3.10 ± 0.10
$R_{60} = 0.0286C_i + 0.3334$	0.9999				
$R_{80} = 0.0164Ci + 0.5153$	0.9991	5.0	10.0	5.16 ± 0.13	9.85 ± 0.18
$R_{60} = 0.0239Ci + 0.5880$	0.9990				
$R_{80} = 0.0057Ci + 0.9900$	0.9930	13.0	15.0	13.20 ± 0.2	15.32 ± 0.21
$R_{60} = 0.0153Ci + 1.1312$	0.9970				
$R_{80} = 0.0052Ci + 1.5450$	0.9999	20.0	10.0	19.76 ± 0.28	10.12 ± 0.15
$R_{60} = 0.0155Ci + 1.6895$	0.9930				
$R_{80} = 0.0101Ci + 1.9061$	0.9950	25.0	15.0	24.70 ± 0.24	15.38 ± 0.28
$R_{60} = 0.0058Ci + 1.8365$	0.9995				
$R_{80} = 0.0014Ci + 0.9954$	0.9920	15.0	5.0	15.27 ± 0.23	5.34 ± 0.15
$R_{60} = 0.0107Ci + 1.0391$	0.9992				

Table 4. Results of six replicate experiments for analysis of Ce^{4+} and $Cr_2O_7^{2-}$ mixture using HPSAM (T = 25ºC).

R-C equation	*r*	Spiked (μg/mL)		Found (μg/mL)	
		Ce^{4+}	$Cr_2O_7^{2-}$	Ce^{4+}	$Cr_2O_7^{2-}$
$R_{80} = 0.1090C_i + 1.0720$	0.9902	13	15	12.98(99.8)	15.51(103.4)
$R_{60} = 0.0046C_i + 0.9736$	0.9900				
$R_{80} = 0.0094C_i + 1.0276$	0.9980	13	15	12.79(98.3)	14.75(98.3)
$R_{60} = 0.0040C_i + 0.9479$	0.9999				
$R_{80} = 0.0153C_i + 1.1312$	0.9980	13	15	13.10(100.7)	14.80(98.6)
$R_{60} = 0.0057C_i + 0.9900$	0.9933				
$R_{80} = 0.0104C_i + 1.0300$	0.9990	13	15	12.70(97.7)	14.40(96.0)
$R_{60} = 0.0056C_i + 0.9611$	0.9930				
$R_{80} = 0.0154C_i + 1.1488$	0.9930	13	15	13.30(102.3)	14.80(98.6)
$R_{60} = 0.0056C_i + 1.0034$	0.9940				
$R_{80} = 0.0156C_i + 1.0520$	0.9990	13	15	12.60(96.9)	15.0(100.0)
$R_{60} = 0.0055C_i + 0.9567$	0.9940				
Mean				13.01	14.87
SD				0.28	0.39
RSD (%)				2.16	2.60

(e.g., potential values) and a concentration matrix data set [30-34]. The calibration is followed by a prediction set in which this model is used to estimate unknown concentrations of a mixture from kinetic profile. Multivariate calibration methods are being successfully applied to the multi-component kinetic determination to overcome some of the drawbacks of classical methods. The theories and applications of chemometrics methods such as PCR and PLS, to the analysis of multi-component mixtures, have been discussed by several workers [31-35]. PCR and PLS modeling are powerful multivariate statistical tools, which are successfully applied to the quantitative analysis of spectrochemical and electrochemical data [33-36]. The first step in the simultaneous determination of the species by PCR and PLS methodologies involves the construction of calibration matrix for the binary mixture of Ce^{4+} and $Cr_2O_7^{2-}$. For constructing the calibration set, factorial design was applied to five levels in order to extract a great deal of quantitative information, using only a few experimental trials. In this research, a synthetic set of 34 solutions, including different concentrations of Ce^{4+} and $Cr_2O_7^{2-}$, was prepared. A collection of 26 solutions was selected as the calibration set (**Table 5**) and the other 8 solutions were used as the prediction set (**Table 6**). Their composition was randomly designed to obtain more information from the calibration procedure. Changes in the solution potential were recorded during a time period of 500 seconds.

To select the number of factors in the PCR and PLS algorithm, as a cross-validation method, leaving out one sample method was employed [37]. The prediction error was calculated for each species of the prediction set. This error was expressed as the prediction residual error sum of squares (PRESS):

$$PRESS = \sum_{i=1}^{m} \left(\hat{C}_i - C_i \right)^2 \quad (11)$$

Where m is the total number of calibration sample, $\hat{C}_i$ represents the estimated concentration while C_i is the reference concentration for the *i*th sample left out of the

Table 5. Calibration set for constructing PCR and PLS methods in determination of Ce^{4+} and $Cr_2O_7^{2-}$ (μg/mL).

Sample	Ce^{4+}	$Cr_2O_7^{2-}$	Sample	Ce^{4+}	$Cr_2O_7^{2-}$
1	5.0	2.0	14	22.0	15.0
2	5.0	6.0	15	22.0	18.0
3	5.0	12.0	16	1.0	0.5
4	5.0	20.0	17	1.0	6.0
5	10.0	10.0	18	1.0	4.0
6	10.0	15.0	19	25.0	17.0
7	10.0	19.0	20	25.0	19.0
8	13.0	17.0	21	25.0	20.0
9	13.0	20.0	22	18.0	7.0
10	3.0	3.0	23	18.0	15.0
11	3.0	9.0	24	15.0	5.0
12	3.0	17.0	25	15.0	9.0
13	22.0	14.0			

Table 6. Prediction set for constructing PLS and PCR methods in determination of Ce^{4+} and $Cr_2O_7^{2-}$.

Solution	Synthetic (μg/mL)		Predicted (μg/mL)			
			PLS[a]		PCR[a]	
	Ce^{4+}	$Cr_2O_7^{2-}$	Ce^{4+}	$Cr_2O_7^{2-}$	Ce^{4+}	$Cr_2O_7^{2-}$
1	13.0	15.0	13.40(103.0)	15.80(105.3)	13.70(105.3)	15.60(104.0)
2	3.0	13.0	2.80(93.3)	13.40(103.0)	2.78(92.6)	13.00(100.0)
3	5.0	10.0	5.10(102.0)	10.20(102.0)	4.80(96.0)	9.90(99.0)
4	13.0	18.0	13.50(103.8)	18.50(102.7)	13.50(103.8)	17.80(98.8)
5	13.0	16.0	12.50(96.1)	15.40(96.2)	12.60(96.9)	15.30(95.6)
6	22.0	16.0	22.30(101.3)	15.70(98.1)	22.60(102.7)	15.40(96.3)
7	10.0	13.0	9.60(96.0)	12.70(97.7)	9.80(98.0)	13.10(100.7)
8	3.0	5.0	3.20(106.6)	5.30(106.0)	3.10(103.3)	4.90(98.0)
Mean recovery			100.2	101.3	99.8	99.1
RMSEP			2.97	3.40	3.03	2.90
RSEP(%)			3.19		2.97	

[a] Predicted mean (recovery percent)

calibration during the cross validation. **Figure 8** shows a plot of PRESS against the number of factors for a mixture of components. To find out minimum factors, we also used the F-statistics to carry out the significant determination [33]. The optimal number of factors, for the two components, was obtained as 2 for both PCR and PLS.

For evaluating the predictive ability of a multivariate calibration model, the root mean square error of prediction (RMSEP), relative standard error of prediction (RSEP) and squares of correlation coefficient (R^2), which is an indication of the quality fit of all the date to a straight line, can be used as follows [33,37]:

$$RMSEP = \left(\sum_{i=1}^{N} \left(\hat{C}_i - C_i \right)^2 / n \right)^{1/2} \quad (12)$$

$$RSEP(\%) = \left(\sum_{i=1}^{N} \left(\hat{C}_i - C_i \right)^2 / \sum_{i=1}^{N} \left(C_i \right)^2 \right)^{1/2} \times 100 \quad (13)$$

$$R^2 = \sum_{i=1}^{N} \left(\hat{C}_i - C' \right)^2 / \sum_{j=1}^{N} \left(C_i - C' \right)^2 \quad (14)$$

where $\hat{C}_i$ represents the estimated concentration, C_i and n are the actual analyte concentration and the number of samples, respectively.

Table 7 shows the values of RSEP, RMSEP and R^2 for each component using PLS and PCR. It is shown that the obtained values, for the statistical parameters, are almost the same for both PLS and PCR methods.

3.10. Interference Study

The study of interference ions was performed by a standard mixture solution containing 10.0 μg/mL of each Ce^{4+} and $Cr_2O_7^{2-}$ and a certain amount of foreign ions. The following excesses of ions do not interfere (*i.e.*, caused a relative error of less than 5%): more than a 1000-fold (largest amount tested) amount of K^+, Zn^{2+}, Cu^{2+}, Bi^{3+}, As^{3+}, Cd^{2+}, Mg^{2+}, Be^{2+}, Cl^-, NO_3^-, BO_3^{3-}, $C_2O_4^{2-}$ a 100-fold amount of Mn^{2+}, Ni^{2+}, Co^{2+}, pb^{2+}, Cr^{3+}, Ca^{2+}; a 10-fold amount of SO_4^{2-}, PO_4^{3-}, Hg^{2+} and a 1-fold amount of Al^{3+}, Fe^{3+}, Zr^{4+}, Ti^{4+}, I . As was to be expected, Al^{3+}, Fe^{3+}, Zr^{4+}, Ti^{4+} have a interference effect because complex forming reaction of these metallic ions with fluoride ion. The interference of iodide ion was also because oxidation reaction with Ce^{4+} and $Cr_2O_7^{2-}$ as oxidants.

3.11. Application

To evaluate the analytical applicability of the proposed methods (PCR, PLS and HPSAM), we spiked known amounts of both Ce^{4+} and $Cr_2O_7^{2-}$ into some water samples. The proposed methods were applied to determine analytes simultaneously and satisfactory results were obtained. The results are given in **Table 8**. The results show that the proposed methods could accurately determine the concentration of these oxidants mixture under investigation in real water samples, and there is no significant difference between the results of PCR, PLS and HPSAM for their simultaneous determination.

Table 7. Statistical parameters calculated for the prediction set using PLS and PCR models.

	RSEP (%)		RMSEP		R^2	
Component	PLS	PCR	PLS	PCR	PLS	PCR
Ce^{4+}	2.97	3.03	0.35	0.36	0.9980	0.9990
$Cr_2O_7^{2-}$	3.40	2.90	0.64	0.40	0.9993	0.9988

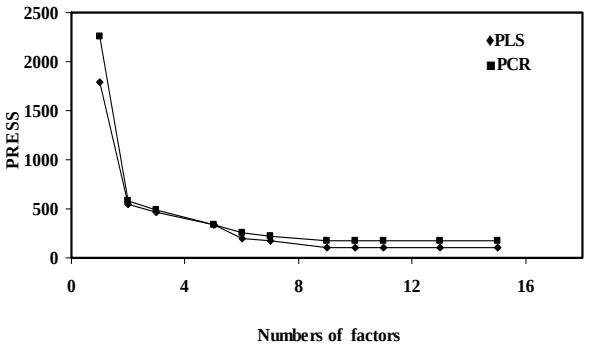

Figure 8. Plot of PRESS against the numbers of factors PLS(♦)and PCR(■).

Table 8. Simultaneous determination of Ce^{4+} and $Cr_2O_7^{2-}$ in different water samples using HPSAM, PCR and PLS methods.

Sample	Spiked (μg/mL)		Found (μg/mL)					
			HPSAM		PLS		PCR	
	Ce^{4+}	$Cr_2O_7^{2-}$	Ce^{4+}	$Cr_2O_7^{2-}$	Ce^{4+}	$Cr_2O_7^{2-}$	Ce^{4+}	$Cr_2O_7^{2-}$
1	4.0	0.5	4.20 ± 0.12	0.51 ± 0.10	4.10 ± 0.11	0.46 ± 0.05	3.97 ± 0.20	0.48 ± 0.02
	10.0	10.0	10.20 ± 0.24	10.40 ± 0.30	10.10 ± 0.22	9.88 ± 0.20	9.79 ± 0.14	9.90 ± 0.10
2	3.0	15.0	2.90 ± 0.06	15.40 ± 0.25	2.97 ± 0.05	14.80 ± 0.28	3.10 ± 0.10	15.20 ± 0.20
	7.0	15.0	7.20 ± 0.21	15.30 ± 0.33	7.14 ± 0.18	14.88 ± 0.15	6.85 ± 0.13	14.90 ± 0.11
3	25.0	4.0	24.60 ± 0.36	4.10 ± 0.10	24.8 ± 0.33	3.88 ±0.09	25.4 ± 0.28	4.16 ± 0.15
	18.0	20.0	17.80 ± 0.28	19.30 ± 0.20	17.65 ± 0.37	19.10 ± 0.12	18.20 ± 0.13	19.8 ± 0.21

4. Conclusions

This work as the first application of PCR, PLS and HPSAM in the simultaneous determination of the binary mixture of Ce^{4+} and $Cr_2O_7^{2-}$ shows the ability and excellent performance of ISEs as detectors not only for individually determination of produced or consumed ions, but also in the simultaneous kinetic-potentiometric analysis. In addition, this paper has also demonstrated that the ability and advantages of the HPSAM and chemometrics methods such as PCR and PLS, ISEs and kinetic methods produce a very attractive and excellent technique for the analysis of multi-component oxidant mixtures. Other chemometrics approaches like ANN, ISEs (flouride, bromide, iodide, etc) and other kinetic reactions in which the rate of production or consumption of the corresponding ion is different can also be used. Our team has obtained good results for the simultaneous determination of other species using HPSAM, chemometrics methods, different ISEs and various reaction systems and our complete results will be presented for publication in the future.

5. Acknowledgements

The authors would like to express their appreciations to Professor Afsaneh Safavi and Professor Hamid Abdollahi for their valuable discussion and useful suggestions. This research was supported by the Payame Noor Universities of Ardakan and Sirjan.

6. References

[1] K. Basavaiah and B. C. Somashekar, "Quantitation of Ranitidine in Pharmaceuticals by Titrimetry and Spectrophotometry Using Potassium Dichromate as the Oxidimetric Reagent," *Journal of the Iranian Chemical Society*, Vol. 4, No. 1, 2007, pp. 78-88.

[2] O. Z. Zhai, "Catalytic Kinetic Spectrophotometric Determination of Trace Amounts of Ethylenediaminetetraacetic Acid Based on its Catalytic Effect on the Reaction of Rhodamine B and Potassium Dichromate," *Instrumentation Science and Technology*, Vol. 29, No. 38, 2010, pp. 72-82.

[3] J. C. Dacons, H. G. Adolph and M. J. Kamlet, "Selective Solvent-Free Oxidation of Alcohols with Potassium Dichromate," *Tetrahedron Letters*, Vol. 43, No. 49, 2002, pp. 8843-8844.

[4] J. Sumaoka, W. Chen, Y. Kitamura, T. Tomita, J. Yoshida and M. Komiyama, "Application of Cerium(IV)/ EDTA Complex for Future Biotechnology," *Journal of Alloys and Compounds*, Vol. 408-412, 2006, pp. 391-395.

[5] I. D. Nickson, C. Boxall, A. Jackson and G. O. H. Whillock, "A Spectrophotometric Study of Cerium IV and Chromium VI Species in Nuclear Fuel Reprocessing Process Streams," *IOP Conference Series*: *Materials Science and Engineering*, Vol. 9, No. 1, 2010.

[6] H. J. Vieira and O. Fatibello-Filho, "Indirect Flow Injection Determination of N-acetyl-L-cysteine Using Cerium (IV) and Ferroin," *Química Nova*, Vol. 28, No. 5, 2005, pp. 797-800.

[7] Y. Liu and P. Wang, "Kinetic Spectrophotometric Method for the Determination of Cerium(IV) with Naphthol Green B," *Rare Metals*, Vol. 28, No. 1, 2009, pp. 5-8.

[8] A. M. Stoyanova, "Catalytic Spectrophotometric Determination of Chromium", *Turkish Journal of Chemistry*, Vol. 29, No. 4, 2005, pp. 367-375.

[9] M. M. Karim, S. H. Lee, Y. S. Kim, H. S. Bae and S. B. Hong, "Fluorimetric Determination of Cerium(IV) with Ascorbic Acid," *Journal of Fluorescence*, Vol. 16, No. 1, 2006, pp. 17-22.

[10] M. Mazloum-Ardakani, M. Salavati-Niasari, A. Dastanpour, "Determination of Chromate and Dichromate by Highly Selective Coated-Wire Electrode Based on Bis (Acetylacetonato)Copper(II)," *Bulletin of Electrochemistry*, Vol. 20, No. 5, 2004, pp. 193-197.

[11] H. Rajantie and D. E. Williams, "Electrochemical Titration of Thiosulfate, Sulfite, Dichromate and Permanganate Using Dual Microband Electrodes," *Analyst*, Vol. 126, No. 1, 2001, pp. 86-90.

[12] V. Mašín and J. Doležal, "Simultaneous Determination of Ce^{4+}, MnO_4^- and $Cr_2O_7^{2-}$ without Separation," *Fresenius' Journal of Analytical Chemistry*, Vol. 301, No. 1, 1980, p. 25.

[13] E. Shams, H. Abdollahi, M. Yekehtaz and R. Hajian, "H-Point Standard Addition Method in the Analysis by Differential Pulse Anodic Stripping Voltammetry. Simultaneous Determination of Lead and Tin," *Talanta*, Vol. 63, No. 2, 2004, pp. 359-364.

[14] E. Shams, H. Abdollahi and R. Hajian, "Simultaneous Determination of Copper and Bismuth by Anodic Stripping Voltammetry Using H-Point Standard Addition Method with Simultaneous Addition of Analytes," *Electroanalysis*, Vol. 17, No. 17, 2005, pp. 1589-1594.

[15] K. Zarei, M. Atabati and M. Karami, "H-Point Standard Addition Method Applied to Simultaneous Kinetic Determination of Antimony(III) and Antimony(V) by Adsorptive Linear Sweep Voltammetry," *Journal of Hazardous Materials*, Vol. 179, No. 1-3, 2010, pp. 840-844.

[16] F. Ahmadi and F. Bakhshandeh-Saraskanrood, "Simultaneous Determination of Ultra Trace of Uranium and Cadmium by Adsorptive Cathodic Stripping Voltammetry Using H-Point Standard Addition Method," *Electroanalysis*, Vol. 22, No. 11, 2010, pp. 1207-1216.

[17] J. Mortensen, A. Legin, A. Ipatov, A. Rudnitskaya, Y. Vlasov and K. Hjuler, **"**A Flow-Injection System Based on Chalcogenide Glass Sensors for Determination of Heavy Metals**,**" *Analytica Chimica Acta*, Vol. 403, No. 1-2, 2000, pp. 273-277.

[18] M. Slama, C. Zaborosch, D. Wienke and F. Spener, "Chemometrical Studies on Mixture Analysis with a Single Dynamic Microbial Sensor," *Sensors and Actuators B*: *Chemical*, Vol. 44, No. 1-3, 1997, pp. 286-290.

[19] N. Garcia-Villar, J. Saurina and S. Hernández-Cassou, "Flow Injection Differential Potentiometric Determination of Lysine by Using a Lysine Biosensor," *Analytica Chimica Acta*, Vol. 477, No. 2, 2003, pp. 315-324.

[20] M. Akhond, J. Tashkhourian and B. Hemmateenejad, "Simultaneous Determination of Ascorbic, Citric and Tartaric Acids by Potentiometric Titration with PLS Calibration," *Journal of Analytical Chemistry*, Vol. 61, No. 8, 2006, pp. 804-808.

[21] Y. Z. Ye and Y. Luo, "Kinetic Potentiometry Simultaneous Determination of Iron(III) and Zirconium(IV) by Using the Kalman Filter," *Laboratory Robotics and Automation*, Vol. 10, No. 5, 1998, pp. 283-287.

[22] M. A. Karimi, M. Mazloum-Ardakani, H. Abdollahi and F. Banifatemeh, "Application of H-Point Standard Addition Method and Partial Least Squares to the Simultaneous Kinetic-Potentiometric Determination of Hydrazine and Phenylhydrazine," *Analytical Science*, Vol. 24, No. 2, 2008, pp. 261-266.

[23] M. A. Karimi, H. Abdollahi, H. Karami and F. Banifatemeh, "Simultaneous Kinetic-Potentiometric Determination of Hydrazine and Thiosemicarbazide by Partial Least Squares and Principle Component Regression Methods," *Journal of the Chinese Chemical Society*, Vol. 55, No. 1, 2008, pp. 129-136.

[24] M. A. Karimi, M. H. Mashhadizadeh, M. Mazloum-Ardakani and N. Sahraei, "Simultaneous Kinetic-Potentiometric Determination of Levedopa and Carbidopa Using Multivariate Calibration Methods", *Journal of Food and Drug Analysis*, Vol. 16, No. 5, 2008, pp. 39-47.

[25] M. A. Karimi, M. Mazloum Ardakani, R. Behjatmanesh Ardakani and M. R. Zand Monfared, "Simultaneous Kinetic-Potentiometric Determination of Fe^{3+} and Al^{3+} Using H-point Standard Addition and Partial Least Squares Methods," *Chemical Analysis* (*Warsaw*), Vol. 54, No. 6, 2009, pp. 1321-1337.

[26] M. A. Karimi, M. Mazloum-Ardakani, R. Behjatmanes Ardakani, M. H. Mashhadizadeh, M. R. Zand Monfared and M. Tadayon, "Chemometrics-Assisted Kinetic-Potentiometric Methods for Simultaneous Determination of Fe(III), Al(III), and Zr(IV) Using a Fluoride Ion-Selective Electrode," *Journal of AOAC International*, Vol. 93, No. 1, 2010, p. 327.

[27] E. Athanasiou-Malaki, M. A. Koupparis and T.P. Hadjiioannou, "Kinetic-Potentiometric Study and Analytical Applications of Micellar-Catalysed Reactions of 1- Fluoro-2,4-Dinitrobenzene with Amino Compounds," *Analytica Chimica Acta*, Vol. 219, No. 2, 1989, pp. 295-307.

[28] K. Srinivasan and G. A. Rechnitz, "Activity Measurements with a Fluoride-Selective Membrane Electrode," *Analytical Chemistry*, Vol. 40, No. 3, 1968, pp. 509-512.

[29] F. Bosch-Reig, P. Campins-Falco, A. Sevillano-Cabeza, R. Herraez-Hernandez and C. Molins-Legua, "Development of the H-Point Standard Additions Method for Ultraviolet-Visible Spectroscopic Kinetic Analysis of Two-Component Systems," *Analytical Chemistry*, Vol. 63, No. 21, 1991, pp. 2424-2429.

[30] M. Bahram, K. Farhadi, A. Afkhami, D. Shokatynia and F. Arjmand, "Simultaneous Kinetic Spectrophotometric Determination of Cu(II), Co(II) and Ni(II) Using Partial Least Squares (PLS) Regression," *Central European Journal of Chemistry*, Vol. 7, No. 3, 2009, pp. 375-381.

[31] M.A. Karimi, M. Mazloum-Ardakani, R. Behjatmanesh-Ardakani, M. H. Mashhadizadeh and N. Zarea Zadeh, "Application of H-Point Standard Addition Method and Multivariate Calibration Methods to the Simultaneous Kinetic-Potentiometric Determination of Hydrogen Peroxide and Peracetic Acid," *Analytical & Bioanalytical Electrochemistry*, Vol. 1, No. 3, 2009, pp. 142-158.

[32] M. Chamsaz, A. Safavi and J. Fadaee, "Simultaneous Kinetic-Spectrophotometric Determination of Carbidopa, Levodopa and Methyldopa in the Presence of Citrate with the Aid of Multivariate Calibration and Artificial Neural Networks," *Analytica Chimica Acta*, Vol. 603, No. 2, 2007, pp. 140-146.

[33] M. Otto and W. Wegscheider, "Spectrophotometric Multicomponent Analysis Applied to Trace Metal," *Analytical Chemistry*, Vol. 57, No. 1, 1985, pp. 63-69.

[34] M. A. Karimi, M. Mazloum-Ardakani, R. Behjatmaneh-Ardakani, M. R. Hormozi Nezhad and H. Amiryan, "Individual and Simultaneous Determinations of Phenothiazine Drugs Using PCR, PLS and (OSC)–PLS Multivariate Calibration Methods," *Journal of the Serbian Chemical Society*, Vol. 72, No. 2, 2008, pp. 233-247.

[35] M. A. Karimi, M. Mazloum-Ardakani, O. Moradlou, R. Behjatmanesh-Ardakani and F. Banifatemeh, "Simultaneous Kinetic-Spectrophotometric Determination of Hydrazine and its Derivatives by Partial Least Squares and Principle Component Regression Methods," *Journal of the Chinese Chemical Society*, Vol. 54, No. 1, 2007, pp. 15-21.

[36] D. M. Haaland and E. V. Thomas, "Partial Least-Squares Methods for Spectral Analyses. 1. Relation to other Quantitative Calibration Methods and the Extraction of Qualitative Information," *Analytical Chemistry*, Vol. 60, No. 11, 1988, pp. 1193-1202.

[37] M. A. Karimi, M. Mazloum-Ardakani, M. H. Mashhadizadeh and F. Banifatemeh, "Simultaneous Kinetic Spectrophotometric Determination of Hydrazine and Isoniazid Using H-Point Standard Addition Method and Partial Least Squares Regression in Micellar Media," *Croatica Chemica Acta*, Vol. 84, No. 4, 2009, pp. 729-738.

American Journal of Analytical Chemistry, 2010, 2, 83-90
doi:10.4236/ajac.2010.12011 Published Online August 2010 (http://www.SciRP.org/journal/ajac)

Degradation Pathway for Pitavastatin Calcium by Validated Stability Indicating UPLC Method

Antony Raj Gomas[1,2], Pannala Raghu Ram[1,2], Nimmakayala Srinivas[1], Jadi Sriramulu[2]
[1]*Shasun Pharmaceuticals Limited, Chennai, India*
[2]*Department of Chemistry, Sri Krishna Devaraya University, Anantapur, India*
E-mail: *ramp.raghu@gmail.com*
Received July 7, 2010; *revised July* 30, 2010; *accepted August* 3, 2010

Abstract

Degradation pathway for pitavastatin calcium is established as per ICH recommendations by validated and stability indicating reverse phase liquid chromatographic method. Pitavastatin is subjected to stress conditions of acid, base, oxidation, thermal and photolysis. Significant degradation is observed in acid and base stress conditions. Four impurities are studied among which impurity-4 is found prominent degradant. The stress samples are assayed against a qualified reference standard and the mass balance is found close to 99.5%. Efficient chromatographic separation is achieved on a BEH C18 stationary phase with simple mobile phase combination delivered in gradient mode and quantification is carried at 245 nm at a flow rate of 0.3 mL min^{-1}. In the developed UPLC method the resolution between pitavastatin calcium and four potential impurities is found to be greater than 4.0. Regression analysis shows an r value (correlation coefficient) of greater than 0.998 for pitavastatin calcium and four potential impurities. This method is capable to detect the impurities of pitavastatin calcium at a level of 0.006% with respect to test concentration of 0.10 mg/mL for a 2-µL injection volume. The developed UPLC method is validated with respect to specificity, linearity & range, accuracy, precision and robustness for impurities determination and assay determination.

Keywords: Column Liquid Chromatography; Pitavastatin Calcium; Forced Degradation; Validation; Stability Indicating.

1. Introduction

Pitavastatin: (E)-7-[2-cyclopropyl-4-(4-fluorophenyl)quinolin-3-yl]-3,5-dihydroxy-hept-6-enoic acid. Pitavastatin (usually as a calcium salt) is a novel member of the medication class of statins. Like the other statins, it is an inhibitor of HMG-CoA reductase, the enzyme that catalyses the first step of cholesterol synthesis. It has been available in Japan since 2003, and is being marketed under license in South Korea and in India. It is likely that pitavastatin will be approved for use in hypercholesterolaemia [1-2]. There are some mass detection methods reported for determination of pitavastatin in plasma and biological fluids and two methods for pitavastatin quantification in tablets by HPLTC were reported [3-6]. As far as we are aware there is no stability-indicating LC method for determination of related substances and assay determination of pitavastatin calcium. In this paper we describe validation of related substances and assay methods for accurate quantification of four potential process impurities in pitavastatin calcium samples as per ICH recommendations. Intensive stress studies are carried out on pitavastatin calcium; accordingly a stability-indicating method is developed, which could separate various degradation products.

The present active pharmaceutical Ingredient (API) stability test guideline Q1A (R2) issued by international conference on harmonization (ICH) [7] suggests that stress studies should be carried out on active pharmaceutical ingredient (API) to establish its inherent stability characteristics, leading to separation of degradation products and hence supporting the suitability of the proposed analytical procedures. It also requires that analytical test procedures for stability samples should be stability indicating and they should be fully validated. Accordingly, the aim of present study is to establish degradation pathway of pitavastatin calcium through stress studies under a variety of ICH recommended test conditions [7-9].

2. Experimental Design

2.1. Chemicals

Samples of pitavastatin calcium with purity more than 99.8% and its related impurities having purity more than 99.0% are received from Shasun research centre, Chennai, India (**Figure 1**). HPLC grade acetonitrile is purchased from Merck, Darmstadt, Germany. Analytical reagent grade orthophosphoric acid and is purchased from Merck, Darmstadt, Germany. High purity water is prepared by using Millipore Milli-Q plus water purification system.

2.2. Procedure

2.2.1. Equipments

The LC system, used for method development and method validation is Waters-Acquity UPLC. The output signal is monitored and processed using Empower 2 software on Pentium computer (Digital equipment Co). UPLC is equipped with Binary gradient pump, Auto Sampler, thermostatted column compartment, Tunable UV Detector, Auto sampler thermostatted, Computer with windows based Empower 2 Method validation manager software.

2.2.2. Chromatographic Conditions

The chromatographic column used is Waters BEH C18 (100 × 2.1 mm) with 1.7µm particles. The mobile phase- A contains a 0.03% of orthophosphoric acid buffer (0.3mL/L). Acetonitrile is used as mobile phase-B. The flow rate of the mobile phase is 0.3 mL/min with a gradient program of 0/45, 2/45, 2.5/100, 4/100, 4.5/45 and 5/45 (time (min)/%B).

The column temperature is maintained at 40°C and the detection is monitored at wavelength of 245 nm. The injection volume is 2 µL. Diluent consists water and acetonitrile in the ratio 90:10.

2.2.3. Preparation of Solutions

All the impurities are dissolved initially by adding 5 mL of acetonitrile then make up to the volume with diluent. A Stock solution of pitavastatin calcium (0.10 mg/mL) is prepared by dissolving appropriate amount in the diluent. Working solution 10 µg/mL is prepared from above stock solution for assay determination.

2.3. Method development and optimization

Impurities and pitavastatin calcium solutions are prepared in diluent at a concentration of 100 ppm and scanned in UV-visible spectrometer; all the 4 impurities and pitavastatin calcium are having UV maxima at around 245 nm which is selected for method development purpose. Mobile phase of ammonium acetate (0.05 M) and acetonitrile (60:40, *v/v*) is selected for initial trial on a C18 stationary phase column [150 × 4.6 mm, 5 µm] and flow rate at

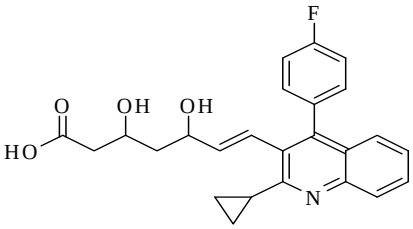

(a)

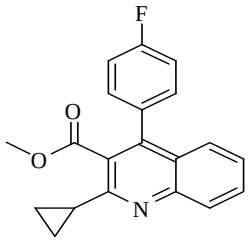

(b)

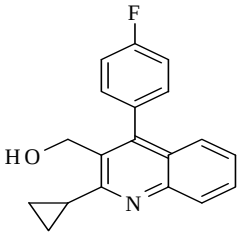

(c)

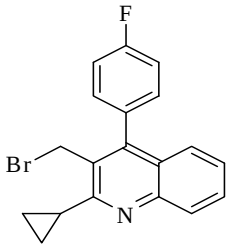

(d)

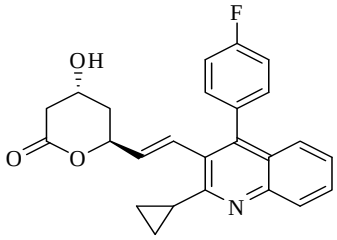

(e)

Figure 1. Chemical Structures and labels of pitavastatin calcium and its impurities. Pitavastatin calcium: (E)-7-[2-cyclopropyl-4-(4-fluorophenyl)quinolin-3-yl]-3,5-dihydroxy-hept-6-enoic acid; Impurity-1: Methyl 4-(4'-fluorophenyl)-2-cyclopropyl-quinolin-3-yl-carboxylate; Impurity-2: 3-hydroxymethyl-2-cyclopropyl-4-(4-fluorophenyl)-quinoline; Impurity-3: 3-Bromomethyl-2-cyclopropyl-4-(4-fluorophenyl)quinoline; Impurity-4: (4R,6S)-6-{(E)-2-[2-cyclopropyl-4-(4-fluorophenyl)-3-quinolyl]etheynyl}-4-hydroxy-3,4,5,6-tetrahydro-2H-pyran-2-one.

1 mL/min. Spike sample analysis revealed that principal peak RT is late and impurities 1 and 3 are not resolved properly. Similar results are obtained with other C18 columns length with the 250 mm. To further resolve the impurity-1 and impurity-3 triethyl- amine is added to buffer then impurity-1 and impurity-3 are separated but the retention time of pitavastatin calcium is late.

Gradient program is introduced for better resolution between Impurity-1 and impurity-3, 0.03% H_3PO_4 buffer used as mobile phase-A and 100% acetonitrile is used as mobile phase-B. Initial ratio of buffer: acetonitrile tried as 80:20 in this case impurity-1 and impurity-3 are well resolved but peak shapes are not good for all components and retention time of pitavastatin calcium is not decreased. Shorter length columns are selected like 50mm and 100 mm with the 4.6 mm diameter of symmetry C18 and C8 for decreasing of retention time for pitavastatin calcium peak in this case pitavastatin calcium retention is decreased but impurities all are not resolved well. Keeping these disadvantages the shorter length and less internal diameter column like waters BEH C18 column is selected with the dimensions 50 × 2.1 mm 1.7µm in this column all components are separated with the minimum resolution 1.5.

To increase the resolution between each component 100 × 2.1 mm column is selected. After several other trails satisfactory results (Retention time of pitavastatin calcium is ~1.16 min and the resolution between all the impurities is > 4.0) are obtained with optimized conditions. In the optimized conditions pitavastatin calcium, Impurity-1, Impurity-2, Impurity-3 and Impurity-4 are well separated with a resolution greater than 4.0 and the typical retention times of pitavastatin calcium, Impurity-1, Impurity-2, Impurity-3 and Impurity-4 are about 1.169, 3.763, 1.763, 3.984 and 2.361 min respectively meeting the chromatographic system suitability requirements (**Table 1)**.

2.4. Analytical Method Validation

The developed chromatographic method is validated for specificity and stress studies, sensitivity, linearity & range, precision, accuracy, and robustness and system suitability [10-15].

2.4.1. Specificity and Stress Studies

Specificity is the ability of the method to measure the analyte response in the presence of its potential impurities. The specificity [10-11] of the developed LC method for pitavastatin calcium is determined in the presence of its impurities namely Impurity-1, Impurity-2, Impurity-3 and Impurity-4 at a concentration of 0.15 µg/mL and

Table 1. System suitability report.

Component	USP Resolution (R_S)	USP Tailing factor	Theoretical plates	%RSD at Precision study
Pitavastatin calcium	--	1.2	3752	1.04
Impurity -2	7.1	1.2	6554	1.50
Impurity -4	6.1	1.1	8024	1.43
Impurity -1	17.6	1.1	86618	1.91
Impurity -3	4.2	1.1	90439	2.19

degradation products. The stress conditions employed for degradation study includes photolytic (carried out as per ICH Q1B), thermal (100°C), acid hydrolysis (1N HCl), base hydrolysis (1N NaOH), hydrolysis and oxidation (10% H_2O_2). All stressed samples of pitavastatin calcium are analysed for an extended run time of 10 min to check the late eluting degradants. Assays are carried out for stress samples against qualified reference standard and the mass balance (%assay + %of impurities + %of degradation products) is calculated for all the samples.

2.4.2. Precision

The precision of the related substance method is checked by injecting six individual preparations of (100 µg mL^{-1}) pitavastatin calcium spiked with 0.02% each impurity.

The %RSD for percentage of each impurity is calculated.

The intermediate precision (ruggedness) of the method is evaluated by different analyst using different column, different day and different analyst in the same laboratory.

The precision of the assay method is evaluated by carrying out six independent assay of test sample of pitavastatin calcium against a qualified reference standard. The %RSD of six obtained values is calculated.

2.4.3. Sensitivity

Sensitivity was determined by establishing the Limit of detection (LOD) and Limit of quantification (LOQ) for each component estimated by based on the Signal to noise ratio method. The precision study was also carried out at the LOQ level by injecting six replicates and calculated the % RSD for the area of each component.

2.4.4. Linearity and Range

Linearity test solutions from LOQ to 150% with respect to test concentration are prepared by diluting the impurity stock solution to the required concentrations. For assay method test solutions from 50% to 150% with respect to test concentration are prepared by diluting the stock solution to the required concentrations. The correlation coefficient, slope and Y-intercept of the calibration curve are calculated for the both related substances and assay methods.

2.4.5. Accuracy

A known amount of the impurity stock solutions are

spiked to the previously analysed samples at LOQ, 100 and 150% of the analyte concentration (100 µg/mL). The percentage of recoveries for Impurity-1, Impurity-2, Impurity-3 and Impurity-4 are calculated. A known amount of pitavastatin calcium stock solution spiked to the sucrose at 50%, 100% and 150% of the analyte concentration (10 µg/mL). Each concentration level is prepared for three times. The percentage of recoveries is calculated.

2.4.6. Robustness
To determine the robustness of the developed method, experimental conditions are deliberately changed and the resolution between each component is evaluated. The flow rate of the mobile phase is 0.3 mL/min. To study the effect of flow rate on the resolution, 0.03 units changed *i.e.* 0.27 and 3.3 mL/min. The effect of column temperature on resolution is studied at 35˚C and 45˚C instead of 40˚C. In the all above varied conditions, the components of the mobile phase are held constant.

2.4.7. Solution Stability and Mobile Phase Stability
The solution stability of pitavastatin calcium and its related impurities are carried out by leaving spiked sample solution in tightly capped volumetric flask at room temperature for 48 h. Impurity content is determined for every 6 h interval up to the study period. Mobile phase stability is also carried out for 48 h by injecting the freshly prepared sample solutions for every 6 h interval. Impurity content is checked in the test solutions. Mobile phase prepared is kept constant during the study period.

3. Results and Discussion

3.1. Specificity and Stress studies
Stress studies on pitavastatin calcium under different stress conditions suggested the following degradation behavior (**Table 2**).

3.1.1. Degradation in Acid Stress Condition
Pitavastatin calcium gradually undergone degradation with time in 1 N HCl upon heating for 2 h and prominent degradation is observed as impurity-4.

3.1.2. Degradation in Base Stress Condition
Pitavastatin calcium is gradually undergone degradation with time in 1 N NaOH upon heating for 2 h and prominent degradation is observed as impurity-2 and impurity-4.

3.1.3. Degradation in Peroxide Stress Condition
Pitavastatin calcium is gradually undergone degradation with time in 10% H_2O_2 upon heating for 2 h and mild degradation is observed as impurity-4.

3.1.4. Degradation in Neutral (Water) Stress Condition
Pitavastatin calcium is exposed water heating for 2 h, no degradation is observed.

3.1.5. Photolytic Stress Condition
Pitavastatin calcium is exposed to light for an overall illumination of 1.2 million Klux hours and an integrated near ultraviolet energy of 200-watt hours/square meter (w/mhr) (in photo stability chamber), mild degradation is observed.

3.1.6. Thermal Stress Condition
Pitavastatin calcium exposed to dry heat at 100˚C for 48 hours, no degradation is observed.

The mass balance of stressed samples is close to 99.5%. The assay of pitavastatin calcium is unaffected in the presence of four impurities and its degradation products confirm the stability indicating power of the developed method.

3.2. Method Validation

3.2.1. Precision
The %RSD of area of pitavastatin calcium, Impurity-1, Impurity-2, Impurity-3 and Impurity-4 and %RSD of area% of each impurity in precision study are within 5.0% confirming the good precision of the developed analytical method. The %RSD obtained in intermediate precision study for pitavastatin calcium, Impurity-1, Impurity-2, Impurity-3 and Impurity-4 are well within 5.0%, confirming the intermediate precision of the method. The %RSD obtained in precision and intermediate precision studies for pitavastatin calcium are well within 1.0% of assay determination method.

3.2.2. Sensitivity
The limit of detection of pitavastatin calcium, impurity-1, impurity-2, impurity-3 and impurity-4 is 0.006% (of analyte concentration, *i.e.* 100 µg/mL) for 2 µL injection volume. The limit of quantification of pitavastatin calcium, Impurity-1, Impurity-2, Impurity-3 and Impurity-4 is 0.02% (of analyte concentration, *i.e.* 100 µg/mL) for 2 µL injection volume. The % RSD for area of pitavastatin calcium, Impurity-1, Impurity-2, Impurity-3 and Impurity-4 are below 5 for precision at LOQ level.

3.2.3. Linearity and Range
Calibration curve obtained by the least square regression analysis between average peak area and concentration showed linear relationship with a correlation coefficient of 0.998 over the calibration ranges tested. Linear calibration plot for related substance method is obtained over the calibration ranges tested, *i.e.* LOQ to 0.225% for Impurity-1, Impurity-2, Impurity-3 and Impurity-4 and LOQ to 0.15% for pitavastatin calcium. The correlation coefficient obtained is greater than 0.998 for all four impurities and pitavastatin calcium. The result shows an excellent correlation existed between the peak area and concentration of pitavastatin calcium and all impurities. Linear calibration plot for assay determination method is ob-

tained over the calibration ranges tested, *i.e.* 50 to 150% for pitavastatin calcium and found the correlation coefficient more than 0.999. The results shows an excel- lent correlation existed between the peak area and con- centration of pitavastatin calcium in assay determination method (**Figure 3**, **Table 3**).

3.2.5. Robustness

Close observation of analysis results for deliberately changed chromatographic conditions (flow rate and column temperature) revealed that the resolution between closely eluting impurities, namely impurity-1 and impurity-3 is greater than 4.0, illustrating the robustness of the method.

3.2.6. Solution Stability and Mobile phase Stability

The %RSD of assay of pitavastatin calcium during solution stability and mobile phase stability experiments is within 1.0. No significant changes are observed in the content of impurity-1, impurity-2, impurity-3 and impurity-4 during solution stability and mobile phase stability experiments. The solution stability and mobile phase sta-

Table 2. Summary on forced degradation results.

Stress condition	Time	% Assay of active substance	%impurities + % Degradation products	Mass balance (%Assay + %impurities + % Degradation products)	Remarks
Acid Stressed sample (1N HCl)	**2 hrs heating**	**93.0**	**6.60**	**99.6**	**Formed as Impurity-4**
Base Stressed sample (1N NaOH)	**2 hrs heating**	**95.1**	**4.40**	**99.5**	**Formed as Impurity-4**
Peroxide stressed sample (10% H_2O_2)	**2 hrs heating**	**98.8**	**1.32**	**100.1**	**Formed as Impurity-2 and Impurity-4**
Thermal stressed sample (Heated at 100˚C)	**48 hours**	**99.7**	**0.08**	**99.8**	**No degradation is observed**
Photo light stressed sample	**1200 Klux hours**	**99.5**	**0.34**	**99.8**	**No prominent degradation is observed**

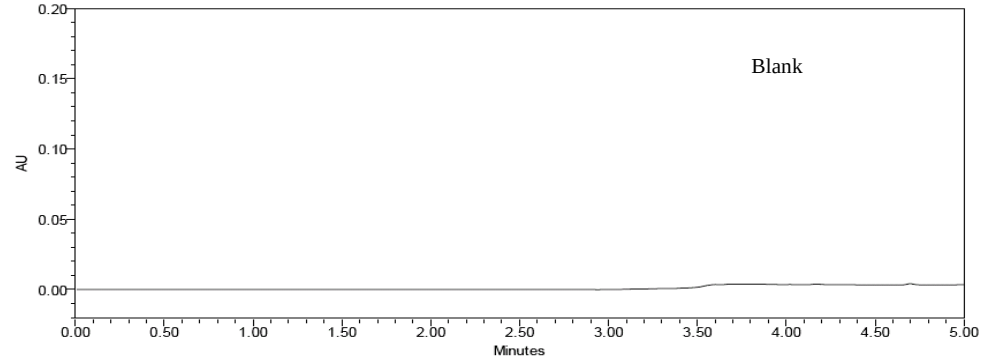

(a)

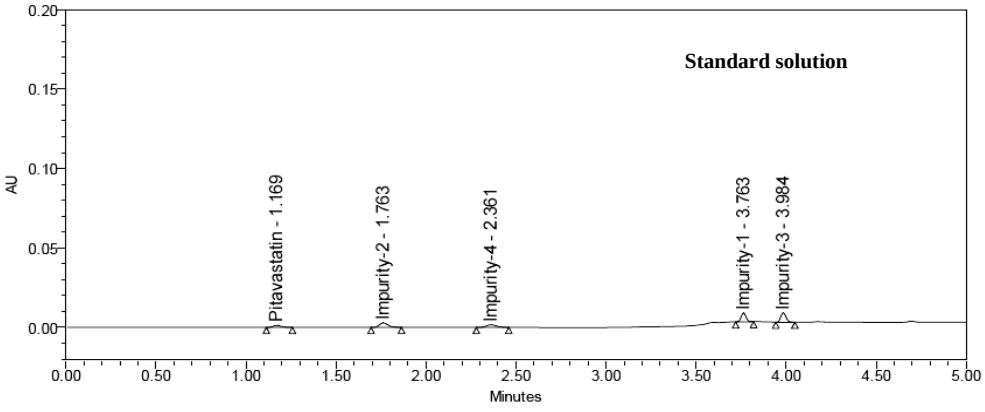

(b)

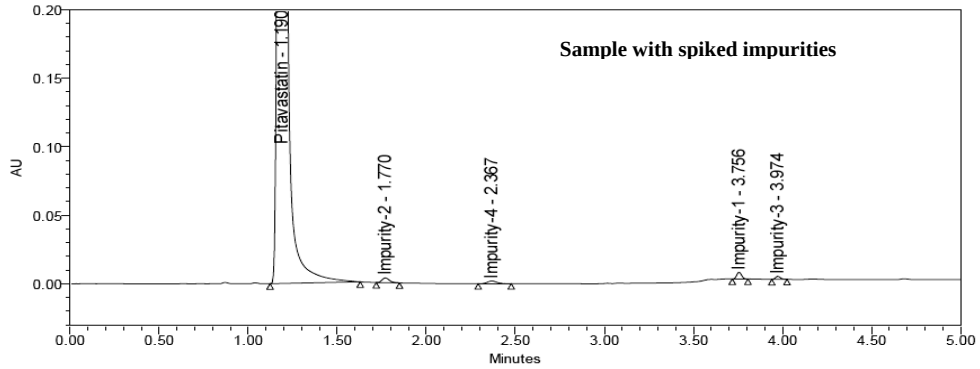

(c)

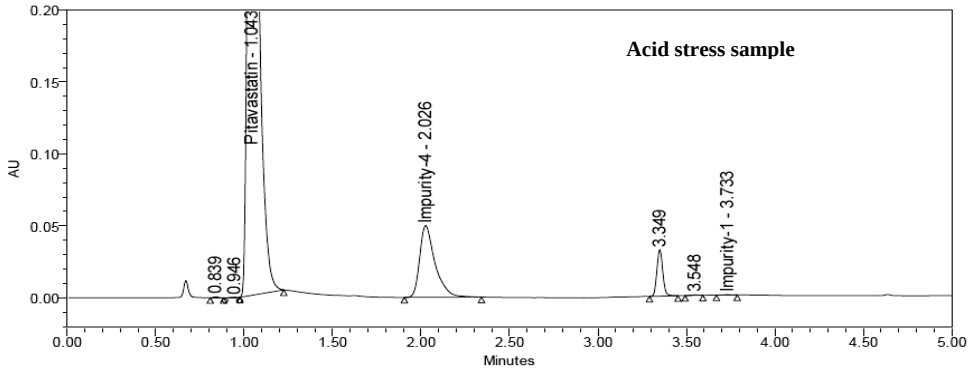

(d)

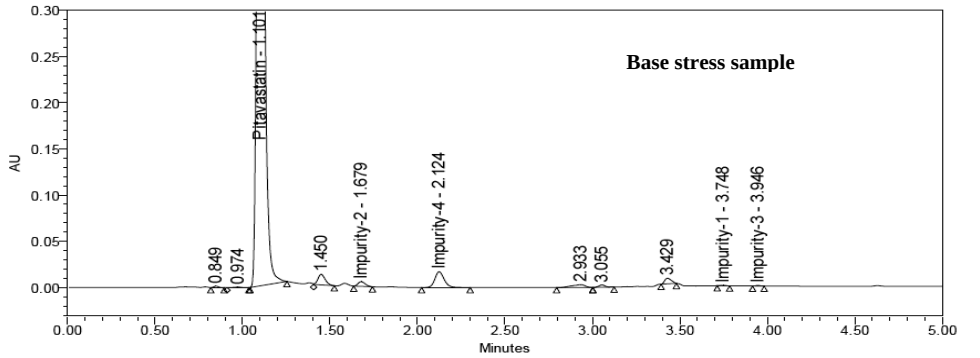

(e)

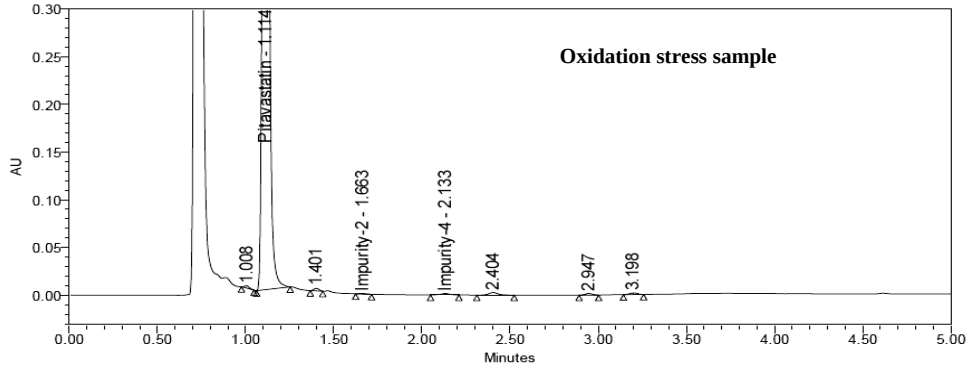

(f)

Figure 2. Typical chromatogram of blank, standard solution and pitavastatin calcium spiked with impurities & Stress sample Chromatograms.

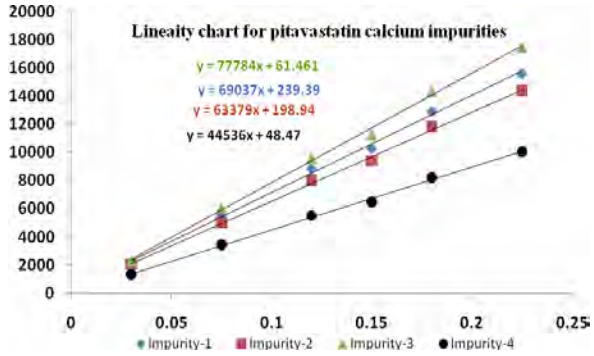

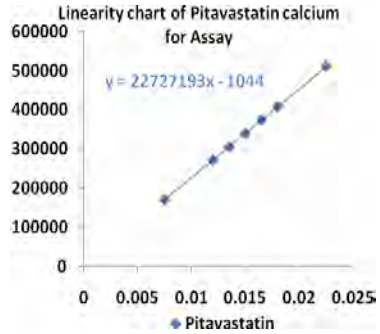

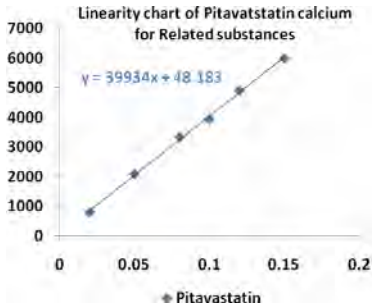

Figure 3. Typical charts and for pitavastatin calcium and its impurities.

bility experiments data confirms that sample solutions and mobile phase used related substance determination are stable up to the study period of 48 h.

Analysis is performed for different samples of pitavastatin calcium (n = 3). All the four impurities in these samples are less than 0.1% and Assay is more than 99.5%.

Table 3. Linearity table.

Component		Trendline equation	Range	Correlation coefficient	% Intercept	Residual sum of squares
Impurity-1		69037X+239.39	0.02-0.225	0.99843	2.32	75426
Impurity-2		63379X+198.94	0.02-0.225	0.99899	2.12	68828
Impurity-3		77784X+61.46	0.02-0.225	0.99880	0.54	82815
Impurity-4		44536X+48.47	0.02-0.225	0.99910	0.74	47613
Pitavastatin calcium	Related substances	39934X+48.18	0.02-0.15	0.99910	1.22	43281
	Assay determination	22727193X-1044	50%-150%	0.99998	–0.31	24868238

Table 4. Table for accuracy study.

Amount of impurity added (µg) to the 100% sample	% of Recovery					
					Assay determination	
	Imp-1	Imp-2	Imp-3	Imp-4	Amount of substance added	%Recovery (Pitavastatin calcium)
0.02	98.2	101.1	96.5	99.0	50%	99.48
0.10	97.5	102.5	98.0	97.1	100%	100.00
0.15	96.4	98.5	93.6	101.8	150%	100.11

4. Conclusions

The degradation pathway of pitavastatin calcium is established as per ICH recommendations. The gradient UPLC method developed and used for stress studies is also fit for quantitative, related substance and assay determination of pitavastatin calcium. The method is validated as per ICH requirements. The developed method is stability indicating which can be used for the impurity testing and assay determination in routine analysis of production samples and also to analyze stability samples.

5. Acknowledgements

The authors wish to thank the management of Shasun Chemicals & Drugs Limited for supporting this work.

6. References

[1] K. Kajinami, N. Takekoshi and Y Saito, "Pitavastatin: Efficacy and Safety Profiles of a Novel Synthetic HMG-CoA Reductase Inhibitor," *Cardiovascular Drug Reviews*, Vol. 21, 2003, pp. 199-215.

[2] R. Y. Mukhtar, J. Reid and J. P. Reckless, "Pitavastatin," *International Journal of Clinical Practice*, Vol. 59, 2005, pp. 239-252.

[3] N. Satheesh Kumar and J. Baghyalakshmi, "Determination and Quantification of Pitavastatin Calcium in Tablet Dosage Formulation by HPTLC Method," *Analytical Letters*, Vol. 40, No. 14, 2007, pp. 2625-2632.

[4] H. J. Panchal, B. N. Suhagia, N. J. Patel and B. H. Patel, "A Simple and Sensitive HPTLC Method for Quantitative Analysis of Pitavastatin Calcium in Tablets," *Journal of Planar Chromatography—Modern TLC*, Vol. 21, No. 4, 2008, pp. 267-270.

[5] R. Nirogi, K. Mudigonda and V. Kandikere, "Chromatography–Mass Spectrometry Methods for the Quantitation of Statins in Biological Samples," *Journal of Pharmaceutical and Biomedical Analysis*, Vol. 44, No. 2, 2007, pp. 379-387.

[6] J. Z. Shen-Tu, X. Xu, J. Liu, X. J. Hu, J. C. Chen, L. H. Wu, M. Z. Huang and H. L. Zhou, "Determination of Pitavastatin in Human Plasma by LC–MS–MS," *Chromatographia*, Vol. 69, No. 9-10, 2009, pp. 1041-1047.

[7] ICH, "Stability Testing of New Drug Substances and Products", Q1A(R2), 2005.

[8] ICH, "Photo stability Testing of New Drug Substances and Products," Q1B, 2005.

[9] S. W. Baertschi, K. Alsante and R. A. Reed, "Pharmaceutical Stress Testing: Predicting Drug Degradation," *Informa Healthcare*, 2005.

[10] US FDA Guidance, "Analytical Procedures and Methods Validation," 2000.

[11] Validation of Compendial Methods <1225>, "The United States Pharmacopeia," 2009.

[12] M. E. Swartz and I. S. Krull, "Developing and Validating Stability-Indicating Methods," Pharmaceutical Technology July 2006.

[13] ICH, "Validation of Analytical Procedures: Text and Methodology", Q2(R1), 2005.

[14] J. Ermer and J. H. McB. Miller, "Method Validation in Pharmaceutical Analysis: A Guide to Best Practice," Wiley, January 2005.

[15] D. M. Bliesner, "Validating Chromatographic Methods: A Practical Guide," Wiley, 2006.

American Journal of Analytical Chemistry, **2010, 2, 91-94**
doi:10.4236/ajac.2010.12012 Published Online August 2010 (http://www.SciRP.org/journal/ajac)

A Simple Colorimetric Method for the Evaluation of Chitosan

Mohamed Abou-Shoer
Department of Pharmacognosy, Faculty of Pharmacy, Alexandria University, Alexandria, Egypt
E-mail: *aboushoerm@yahoo.com*
Received June 19, 2010; *revised August* 7, 2010; *accepted August* 12, 2010

Abstract

A simple sensitive and rapid colorimetric method has been developed, and herein described, for the qualitative and quantitative chemical assessment of the commercially available chitosan products. The described method relies on the reactivity of the basic amino function of chitosan with the acid dye bromocresol purple. The applied technique allows assessment of variability and selectivity changes in the quality of the marketed chitosan products.

Keywords: Chitosan, Dye, Colorimetric, Bromocresol Purple

1. Introduction

Chitosan is a natural biocompatible polymer derived from the naturally-occurring polysaccharide-based biopolymer, chitin, by deacetylation with an alkali leaving behind a free amino group (-NH2) (**Figure 1**) [1]. Chitosan naturally exists only in a few species of fungi but it is mainly extracted from the cuticular and exoskeletons of invertebrates like crustaceans, mollusks, crabs and shrimp. Crabs obtained from seafood processing waste are an important commercial source. Chitin is the second, after cellulose, most abundant naturally occurring polysaccharide. Chitin is composed of 2-acetamido-2-deoxy-β-D-glucose units that are combined by 1-4 glycosidic linkages, forming long un-branched linear polymeric chains. Therefore, the biopolymer chitosan is composed of β-2-amino-2-deoxy-D-glucopyranose(glucosamine units) and β-2-acetamido-2-deoxy-D-glucopyranose [2]. Chitosan possesses unique properties like its ability to form films, and possesses a positive ionic charge which develops its ability to chemically bind with negatively charged fats, lipids and bile acids. Chitosan has a wide range of applications in diverse fields like in health (ranging from medical sutures to beauty aids), water purification (coagulants for waste treatment), biomedical applications, agriculture (seed coatings), biotechnology, nutrition (dietary supplements), and in the finishing process of textile fibers [3]. Chitosan is commercially available from many suppliers in various grades of purity, molecular weight, and degree of deacetylation. The degree of deacetylation is one of the most important chemical characteristics as it reported to influence the physicochemical properties and the performance of chitosan in many of its applications. Chitosan versatility depends mainly on the chemically reactive amino groups.

The degree of deacetylation of chitosan ranges from 56% to 99%, depending on the crustacean species and the preparation method. Various methods have been reported for the determination of the degree of deacetylation of chitosan. These included ninhydrin test, linear potentiometric titration, infrared spectroscopy, near-infrared spectroscopy, nuclear magnetic resonance spectroscopy, hydrogen bromide titrimetry, infrared spectroscopy, elemental analysis, colloidal titration, circular dichroism, ultraviolet spectroscopy, pyrolysis-gas chromatography, gel permeation chromatography and thermal analysis, acid hydrolysis, and X-ray diffraction methods and first derivative UV-spectrophotometry [4-6]. Chitosan could be also assayed colorimetrically using Cibacron brilliant red 3B-A [7,8].

All the above mentioned methods employed for the evaluation of chitosan slightly vary when measuring the number of free amino groups in the structure (deacetylation degree, DD). Obviously, the DD values are highly dependent on the analytical methods employed [9, 10]. Hence, we propose that the analytical method used for the evaluation of chitosan products would also consider the functional capacity of the matrix. This approach is easily perceived when a reference matrix is taken into account.

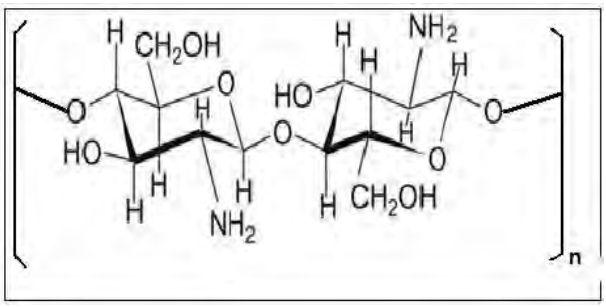

Figure 1. Structure of Chitosan unit.

Colorimetric assays are often developed as simple and sensitive practical procedures to rapidly evaluate drug quality in rapid and inexpensive protocol. Chitosan possesses a free amino group that acts as a reactive binding site for anionic dyes such as bromocresol purple to produce a color-bound complex. Therefore, our objective is to develop and evaluate a colorimetric technique to measure the functional capacity, which relates to deacetylation degree, so as to quantitatively assess these products in pharmaceutical preparations.

2. Methods—Experimental Data

2.1. Reagents and Apparatus

All reagents, hydrochloric acid, pyridine, acetic anhydride and sodium hydroxide, were of analytical-reagent grade, distilled or deionized water (DI) was used to prepare all aqueous solutions. Pharmaceutical-grade chitosan was used, bromocresol purple Indicator is a product of Reidel-DeHaen Ag, Seelze-Hannover, sodium bicarbonate, and sodium hydroxide from Sigma-Aldrich (St. Louis, MO, USA); Microgranular pre-swollen DEAE-32 Cellulose, Whatman, Springfield Mil, Madison, Kent, England.

2.2. Apparatus

Shimadzu UV 1601PC, UV/VIS double beam spectrophotometer (Kyoto, Japan) was used and equipped with 1 cm quartz cells and connected to IBM compatible computer. The software was UVPC personal spectroscopy software version 3.7 (Shimadzu). The spectral width applied was set at 2 nm.

2.3. Sample Preparation

The colorimetric methods were evaluated in terms of linearity, precision, and accuracy by using different pharmaceutical batches of raw material compounds. Accurately weighed quantities of three commercially available (1-60 mgs) chitosan powder were introduced into small sintered funnel or filtration tubes. The chitosan sample were soaked with 0.2 ml of water allow swelling of the polymer matrix.

2.4. Bromocresol Purple Dye Solution

Dye solution is prepared by dissolving 100 mg of bromocresol purple in 5 mL of ethanol.

2.5. Diethyl Amino Cellulose (DEA-32)

Diethylamino cellulose ion-exchanger was used as a functional reference to relate the chitosan performance. DEAE cellulose was selected because of its structural resemblance to chitosan. Accurately weighed quantities (10-80 mgs) of DEAE cellulose ion exchanger were treated the same procedure like chitosan samples.

2.4. Preparation of Acetylated Chitosan

200 mgs from each chitosan samples were suspended in 0.5 ml of dry and distilled pyridine. 2 ml of acetic anhydride were added and stirred for 4 hours at room temperature then kept in dark for overnight. The reaction mixture is then quenched with cold water and the product, acetylated chitosan, was filtered off, washed with DI followed by ethanol and dried in an oven at 60˚C for 15 minutes.

2.5. Colorimetric Assay

Bromocresol purple was used for the colorimetric assay and prepared at a concentration of 20 mg/mL in water. For all chitosan samples (weights from 1mg and up to 50 mgs of chitosan or their equivalent amounts) were accurately weighed. The chitosan samples were weighed either directly into small sintered glass funnels, or in Pasteur pipettes (disposable pipettes) packed at the bottom with glass wool. Secure the porosity of the filter pad, especially when glass wool, to carefully hold and do not allow passage of any of the loaded chitosan powder. The powdered sample in each tube was then wetted with 0.2 mL of DI water and allowed to soak for 15 minutes to allow possible swelling of the matrix. Approximately 0.3 mL of the dye solution is slowly passed through the sintered funnels. Each tube is then loaded with 0.2 ml of the dye solution. Excess dye solution is drained out and excess dye was washed out with 0.5 mL of DI followed by 95% ethanol till complete removal of all color in the wash solution. The tube packed with chitosan-dye complex is then contained in clean 20 mL volumetric flasks. The chitosan-bound dye was then stripped off the bed by 20 ml of 1N HCl solution and completed to volume. The acid solution is filtered through a 0.45 μ membrane filter. Five milliliter aliquots were withdrawn from each sample concentration into a separate 50 m volumetric flask and

completed to volume with 1N sodium hydroxide solution. The developed blue color for each sample concentration is used for absorbance measurement at 589 nm.

2.6. Calibration Graphs

5 mL aliquots from the liberated sample solutions were transferred into 50 mL volumetric flasks. The reaction flasks are completed to volume with 1N NaOH and the solutions were measured spectrophotometrically at the λmax of 589 nm and the recorded absorbances for different samples of each sample were used to construct calibration graphs (**Figure 2**).

3. Results

The product from acetylating chitosan was treated with the dye solution the same way as described for chitosan. Although the acetylated chitosan matrix have acquired a red color once wetted with bromocresol purple, yet, the acidic solution used to drive out the adsorbed dye did not release any noticeable color intensity. Moreover, when the collected acidic wash solution was treated with sodium hydroxide and the measured at the same wavelength, such solutions did not record any appreciable absorbance readings. This finding illustrates that the presence of the free amino groups are essential for the working-efficiency of chitosan as an ion-exchanger. All chitosan samples, however, have produced abstracted appreciable quantities of the dye and released considerable color intensities upon acidification. The sensitivity of color-measurement is further enhanced by shifting the pH to the alkaline side with sodium hydroxide. The quantities of the dye freed from the chitosan-dye complex are then proportional to the quantities of chitosan used and hence calibration graphs were constructed. The good linearity and slope of the calibration graphs for the different chitosan batches indicate the efficient and strong sensitivity of the chitosan polymer in binding acidic compounds. Alternatively, when DEAE cellulose was treated with the dye solution, it showed a better linearity and a superior capacity. This data suggests that DEAE cellulose retains better functional characteristics that observed with chitosan polymers (**Figure 3**).

4. Discussion

The high value of the correlation coefficient and the intercept value were used to evaluate the linearity of the calibration curves. Regression analysis of these plots using the method of least squares had produced correlation coefficients (r) equal to 0.9904-0.998 indicating a good linearity (**Figure 2**). The sensitivity of the method to different batches is evident from the slope and intercepts values in the calibration curves. Moreover, the intercept and slope values of DEAE-cellulose in comparison to those obtained with chitosan products tip off the analyst to the performance properties, efficiency and capacity of such polymers as anionic exchangers relative to a different match of known operational parameters. The reported methods for the evaluation of chitosan products target measuring the deacetylation degree (DD) to reflect the quantity of free amino group on the chitosan matrix relative to the fully acylated chitosan (chitin). However, those methods do not gauge the factual capacity or working efficiency of the polymer. Accordingly, it has been viewed as more sensible to compare chitosan products as "functional" rather than chemical operators. Synthetic ion-exchangers of known chemistry, capacity

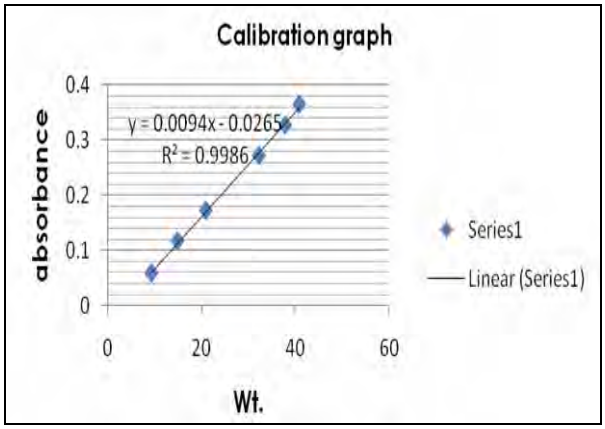

Figure 2 Calibration curve for chitosan.

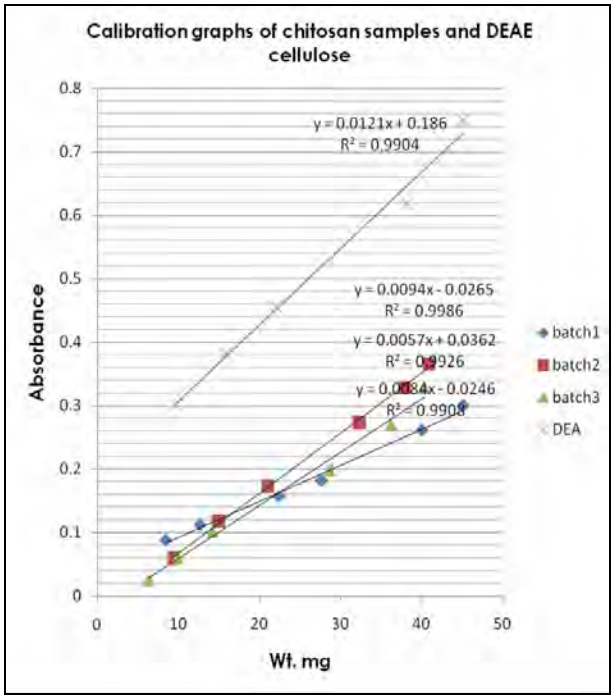

Figure 3 Comparison of chitosan samples and DEAE cellulose.

and performance, like DEAE cellulose, can pose as a "yardstick" reference chemical to weigh against the efficiency of similar compounds. The applied method is also valuable as a routine tool for the quantitative analysis of very small amounts of chitosan products while depending on the selective ion-exchange capacity of the polymer. The observed linearity and sensitivity of the methods promotes its friendly application in routine analysis of such polymers.

5. Conclusions

Simple, quick and inexpensive colorimetric assays serve as convenient means to rapidly and straightforwardly assess product quality in a cost-efficient transaction. The reaction of chitosan with anionic dyes has instantly produced stable and colored adducts. This has triggered developing anionic dyes like bromocresol purple as an analytical reagent for assessing the quality of chitosan. Anionic dyes such as bromocreaol purple and bromocresol green form colored dye-matrix complexes with chitosan to produce a colored product. The dye-binding method produces a colored product which shed and equivalent amount of dye which is linearly proportional to chitosan quantity. Colorimetric tests are rapid and easy to perform. The reagents and equipment for colorimetric tests are inexpensive, environmentally safe, and are ideal for use in non-very well-equipped labs.

6. References

[1] M. N. V. R. Kumar, "A Review of Chitin and Chitosan Applications," *Reactive and Functional Polymers*, Vol. 46, No. 1, 2000, pp. 1-27.

[2] G. A. F. Roberts, "Thirty Years of Progress in Chitin and Chitosan," *Progress on Chemistry and Application of Chitin*, Vol. 13, 2008.

[3] S.-O. Fernandez-Kim, "Physicochemical and Functional Properties of Crawfish Chitosan as Affected by Different Processing Protocols," M. S. Dissertation, Seoul National University, Seoul, 2004.

[4] N. I. Larionova, D. K. Zubaerova, D. T. Guranda, M. A. Pechyonkin and N.G. Balabushevich, "Colorimetric Assay of Chitosan in Presence of Proteins and Polyelectrolytes by Using *O*-Phthalaldehyde," *Carbohydrate Polymers*, Vol. 75, No. 4, 2009, pp. 724-727.

[5] J. J. Park, "Development of Biomems Device and Package for a Spatially Programmable Biomolecule Assembly," Ph.D. Dissertation, Faculty of the Graduate School of the University of Maryland, College Park, 2006.

[6] K. van de Velde and P. Kiekens, "Structure Analysis and Degree of Substitution of Chitin, Chitosan and Dibutyryl Chitin by FT-IR spectroscopy and Solid State ^{13}C NMR," *Carbohydrate Polymers*, Vol. 58, No. 4, 1998, p. 409.

[7] R. A. A. Muzzarelli, "Colorimetric Determination of Chitosan," *Analytical Biochemistry*, No. 260, 1998, pp. 255-257.

[8] C. Wischke and H. Borchert, "Increased Sensitivity of Chitosan Determination by a Dye Binding Method," *Carbohydrate Research*, Vol. 341, No. 18, 2006, pp. 2978-2979.

[9] T. A. Khan, K. K.Peh and H. S. Ch'ng, "Reporting Degree of Deacetylation Values of Chitosan: The Influence of Analytical Methods," *Journal of Pharmacy & Pharmaceutical Sciences*, Vol. 5, No. 3, 2002, pp. 205-212.

[10] K. M. Picker-Freyer and D. Brink, "Evaluation of Powder and Tableting Properties of Chitosan," *AAPS Pharmaceutical Science and Technology*, Vol. 7, No. 3, 2006.

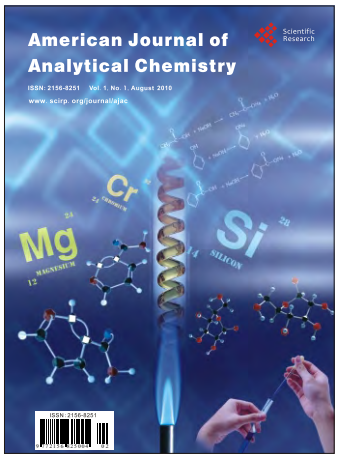

American Journal of Analytical Chemistry

ISSN Print: 2156-8251 ISSN Online: 2156-8278
http://www.scirp.org/journal/ajac/

American Journal of Analytical Chemistry is a peer reviewed international journal dedicated to the latest advancement of analytical chemistry. The goal of this journal is to keep a record of the state-of-the-art research and to promote study, research and improvement within its various specialties. With an open access publication model of this journal, all interested readers around the world can freely access articles online. Now we sincerely invite you to submit your research manuscript to AJAC.

Editorial Board

Subject Coverage

The American Journal of Analytical Chemistry publishes original papers including but not limited to the following fields:

Chromatography and Electrophoresis	Crystallography
Crystallography	Mass Spectrometry
Microscopy	Spectrophotometry and Colorimetry
Spectroscopy	

We are also interested in short papers (letters) that clearly address a specific problem, and short survey or position papers that sketch the results or problems on a specific topic. Authors of selected short papers would be invited to write a regular paper on the same topic for future issues of the AJAC.

Notes for Intending Authors

Submitted papers should not have been previously published nor be currently under consideration for publication elsewhere. Paper submission will be handled electronically through the website. All papers are refereed through a peer review process. For more details about the submissions, please access the website.

Website and E-Mail

http://www.scirp.org/journal/ajac E-mail: ajac@scirp.org

American Journal of Analytical Chemistry, **2010, 1, 41-94**
Published Online August 2010 in SciRes (http://www.SciRP.org/journal/ajac/).

TABLE OF CONTENTS

Volume 1 Number 2 **August 2010**

